Examining the Asynchronous Behaviour of the Upernavik Isstrøm in Northwest Greenland

by

Kelsey Voss

A Thesis submitted to the Faculty of Graduate Studies of

The University of Manitoba

In partial fulfillment of the requirements of the degree of

MASTER OF SCIENCE

Department of Environment and Geography

University of Manitoba

Winnipeg

ABSTRACT

The Upernavik Isstrøm, located in northwest Greenland, consists of five marine-terminating glaciers (referred to as U0 to U4, north to south) that have all been responding asynchronously to climate change. All five outlets share similar oceanic, atmospheric, and dynamic influences as they are geographically close, yet contrasting ice-flow behaviour was observed between outlets. This thesis presents a detailed analysis of the varying ice dynamics by updating the observational record of Upernavik's outlets with recently derived satellite data, examining the role of floating ice tongues by evaluating a variety of proxies for floating ice, and modelling the drivers of ice-flow speed at the two fastest outlets, U1 and U2, with a recent flowline model, Icepack. We found recent patterns in floatation for U1 and U2 that indicated both outlets have new floating ice tongues that persisted through 2021. We evaluated four proxies of floating termini, including tabular iceberg calving, plume polynyas, hydrostatic elevation, and slope, and found only hydrostatic elevation and slope to be reliable proxies. While we initially hypothesized that floating ice tongues drove the acceleration of U1 and U2, our measured velocity data and modelled ice-flow sensitivity to changes in basal slipperiness, shear margin strength, thinning, and terminus retreat, showed ice-flow was realistically explained by changes in basal slipperiness. Icepack was capable of handling this complex case study and the simplified model provided great context regarding the forcings acting on Upernavik's outlets. This strongly supports that U1 and U2 are seasonally and inter-annually controlled by subglacial hydrology. While the timing and magnitude of observed changes in thinning and retreat varies between outlets, all outlets displayed behaviour characteristic of glaciers controlled by meltwater

availability at the bed. These results emphasize the importance of including subglacial hydrology in future studies of Upernavik and other marine-terminating glaciers to improve our understanding of how climate change may affect Greenland in the future.

ACKNOWLEDGEMENTS

I would like to express my utmost gratitude to both my co-advisors, Dr Karen Alley and Dr. Dorthe Dahl-Jensen, who helped me tremendously throughout this project. It was very difficult navigating the remote world of research during COVID-19, but I was met with encouragement and patience the entire way. Their support, guidance, and dedication were truly remarkable and it is with my deepest thanks to them for helping me through my graduate program. I consider myself lucky to have such wonderful mentors.

I would like to thank my amazing committee members, both Dr. Jens Ehn and Dr. Juliana Marson for providing experienced insight to my project and guidance along the way. I am thankful for their oceanography background and the special topics ocean course I took with Dr. Jens Ehn, which provided me with sufficient knowledge in my study area. A deeply extended thank you to Dr. David Lilien, whose immense modelling knowledge enabled us to add incredible detail to our study with our ice-flow model. As someone with little background in modelling, his patience allowed me to grow and improve and end this program with a better understanding of glaciology.

This work was supported by funding from the Natural Sciences and Engineering Research Council of Canada (NSERC) grants: the Canada Excellence Research Chair CERC-2018-00002 and the Discovery Grant RGPIN-2021-02910. Additional financial support from the University of Manitoba Graduate Fellowship (UMGF) made this study possible. I am very grateful for the intricate network of funding provided to me and this study as well as the community of support that the Centre for Earth Observation Science (CEOS) has provided me.

DEDICATION

To my loving sister for her continuous emotional support and encouragement, my supportive father, for his unwavering support and dedication for women in STEM, and my partner, for his uplifting presence.

To my dear mom, whose intelligent, tenacious, and strong memory kept me going through tough times.

TABLE OF CONTENTS

ABSTRACT ..... ***ii***

ACKNOWLEDGEMENTS ..... ***iv***

DEDICATION ..... ***v***

CHAPTER 1.0: INTRODUCTION ***1***

1.1 Research Objective 3
1.2 Thesis Structure 6
References 6

CHAPTER 2.0 LITERATURE BACKGROUND ***10***

2.1 Glacier Physics 10
2.2 The Greenland Ice Sheet 15
2.3 Baffin Bay and Greenland Fjords 17
2.4 Marine-Terminating Glaciers and Floating Ice Tongues 19
2.4 The Upernavik Isstrøm 25
2.5 Conclusion 31
References 34

CHAPTER 3.0 The Role of Terminus Conditions in the Ice-Flow Speed of the Upernavik Isstrøm in Northwest Greenland ***43***

ABSTRACT **43**

3.1 INTRODUCTION **44**

3.2 METHODS **48**

3.2.1 Terminus and Bed Observations 48
3.2.2 Velocity 50
3.2.3 Evidence for Floating Ice 51
3.2.4 Numerical Flowline Model 54

3.3 RESULTS **59**

3.3.1 Terminus Position and Retreat 61
3.3.2 Velocities 63
3.3.3 Calving Behaviour 70
3.3.4 Hydrostatic Analysis 71
3.3.5 Elevation and Bed Topography 73
3.3.6 Evidence of Plume Polynyas 76
3.3.7 Ice Flow Model 77

3.4 DISCUSSION **81**

3.4.1 Floating Ice Tongue Evidence and Methods 81
3.4.2 Causes of Complex Ice-Flow Changes at Upernavik's Outlets 82
3.4.3 Likely Future Changes at Upernavik's Outlets 87

3.5 CONCLUSION 87

ACKNOWLEDGEMENTS 89

References 90

CHAPTER 4.0: SUMMARY AND CONCLUSIONS 99

4.1 Summary of Changes at Upernavik's Five Outlets from 2000-2021 99
4.2 Error Analysis and Limitations 107
4.3 Future Recommendations and Considerations 111
References 112

CHAPTER 5.0 APPENDICES 116

5.1 Appendix A: Additional Hydrostatic Figures 116
5.2 Appendix B: Subglacial Drainage and Tabular Iceberg Images 122
5.3 Appendix C: Modelling Figures.....126

LIST OF FIGURES

CHAPTER 1.0

Figure 1.1: The Upernavik Isstrøm outlets……3

CHAPTER 3.0

Figure 3.1: Upernavik Outlets and Flowlines……60
Figure 3.2: Upernavik Terminus Positions……61
Figure 3.3: Upernavik Flowline Summer Velocities……63
Figure 3.4: Upernavik Seasonal Velocities……...65
Figure 3.5: Terminus Velocity Comparison at Upernavik.……69
Figure 3.6: Upernavik Hydrostatic Profiles. ……71
Figure 3.7: Upernavik Bed and Ice Elevation Profiles. ……..73
Figure 3.8: U1 model inputs and ice-flow speeds. ……77
Figure 3.9: U2 model inputs and ice-flow speeds. ……79

CHAPTER 4.0

Figure 4.2: Upernavik's Asynchronous Results……..…105

APPENDIX A

Figure 5.1: U0 2011 Hydrostatic Profile..……116
Figure 5.2: U0 2013 Hydrostatic Profile…..……116
Figure 5.3: U1 2010 Hydrostatic Profile.……117
Figure 5.4: U1 2011 Hydrostatic Profile.……..…117
Figure 5.4: U1 2012 Hydrostatic Profile.……..…118
Figure 5.5: U3 2010 Hydrostatic Profile.……..…118
Figure 5.6: U3 2011 Hydrostatic Profile…..……119
Figure 5.7: U3 2012 Hydrostatic Profile.……..…119
Figure 5.8: U3 2013 Hydrostatic Profile.……..…120
Figure 5.9: U3 2015 Hydrostatic Profile.……..…120
Figure 5.10: U4 2013 Hydrostatic Profile.……..…121

APPENDIX B

Figure 5.1: U0 drainage event example.……..…122
Figure 5.2: U2 drainage event example.……..…123
Figure 5.3: U2 lake drainage event.……...124
Figure 5.4: Tabular Icebergs and Plume Polynyas.……..125

APPENDIX C

Figure 5.1: U1 2014 modelled velocity and C_{side} sensitivity……126
Figure 5.2: U2 2015 modelled velocity and C_{side} sensitivity……127
Figure 5.3: U2 2018 modelled velocity and C_{side} sensitivity……128

CHAPTER 1.0: INTRODUCTION

In the face of climate change, the increasing retreat and acceleration of marine-terminating glaciers in Greenland is an escalating concern. Between 1992 and 2018, the Greenland Ice Sheet contributed a 10.8 mm global sea-level rise as a result of surface melting, ice discharge, and submarine melt (Shepherd and others, 2020). Ice dynamics at marine-terminating glaciers comprise an increasing percentage of mass loss (Mouginot and others, 2019), making it essential to study the dynamics of marine-terminating glaciers and to identify the regions most sensitive to ocean-driven change. The northwest margin of Greenland has recently played a significant role in mass loss as the measured estimate of global sea-level rise by Mouginot and others (2019) from 1972 to 2018 was 4.4 mm, with a 64% increase in ice discharge after 2008 (Enderlin and others, 2014). Enderlin and others (2014) estimate this northwest contribution to global sea-level rise could reach 33 mm by 2100.

Dynamic mass loss occurring from marine-terminating glaciers is a consequence of patterns of thinning, retreat, and acceleration (Moon and others, 2015; Nick and others, 2009). Both oceanic and atmospheric forcings play a role in the acceleration of marine-terminating glaciers. Subglacial drainage as a result of increased atmosphere temperatures and surface melting can lubricate the glacial bed and cause acceleration (Fried and others, 2015; Slater and others, 2019; Straneo and Cedenese, 2015), although this acceleration is sometimes short-lived on seasonal timescales (Zwally and others, 2002; Moon and others, 2014). Warming ocean temperatures and the intrusion of warm, salty Atlantic Water can also cause acceleration and mass loss when fjord water mixes with subglacial drainage and initiates turbid plumes that melt the calving

front (Moon and Joughin, 2008; Khan and others, 2010; Enderlin and Howat, 2013; Straneo and Heimbach, 2013; Straneo and Cedenese, 2015). Glaciers can develop floating ice tongues, which are longitudinal floating ice extensions of the terminus, that may be highly sensitive to changes in ocean temperatures and submarine melt, as well as stresses applied from the rest of the glacier (Enderlin and Howat, 2013; Khan and others, 2010; Wood and others, 2021). The changing conditions of floating ice tongues can cause increased retreat and acceleration (Moon and Joughin, 2008; Nick and others, 2009).

The role of climate forcings as drivers for mass loss, as well as local controls such as bed geometry, are frequently debated in glacier retreat and acceleration. The Upernavik Isstrøm, a rapidly retreating and accelerating ice stream in northwest Greenland, comprises five glaciers terminating in a shared fjord (Figure 1.1). Varying patterns of retreat and acceleration, as well as changing terminus conditions, were observed over the past two decades, resulting in asynchronous outlet behaviour (Khan and others, 2013; Larsen and others, 2016). The last complete remote sensing analysis was concluded in 2013 (Larsen and others, 2016), and much work remains to be done on understanding the controls on the fluctuating ice speeds. Investigating the glacier dynamics of Upernavik is necessary to assess its role in Greenland's mass loss as well as its response to climate change.

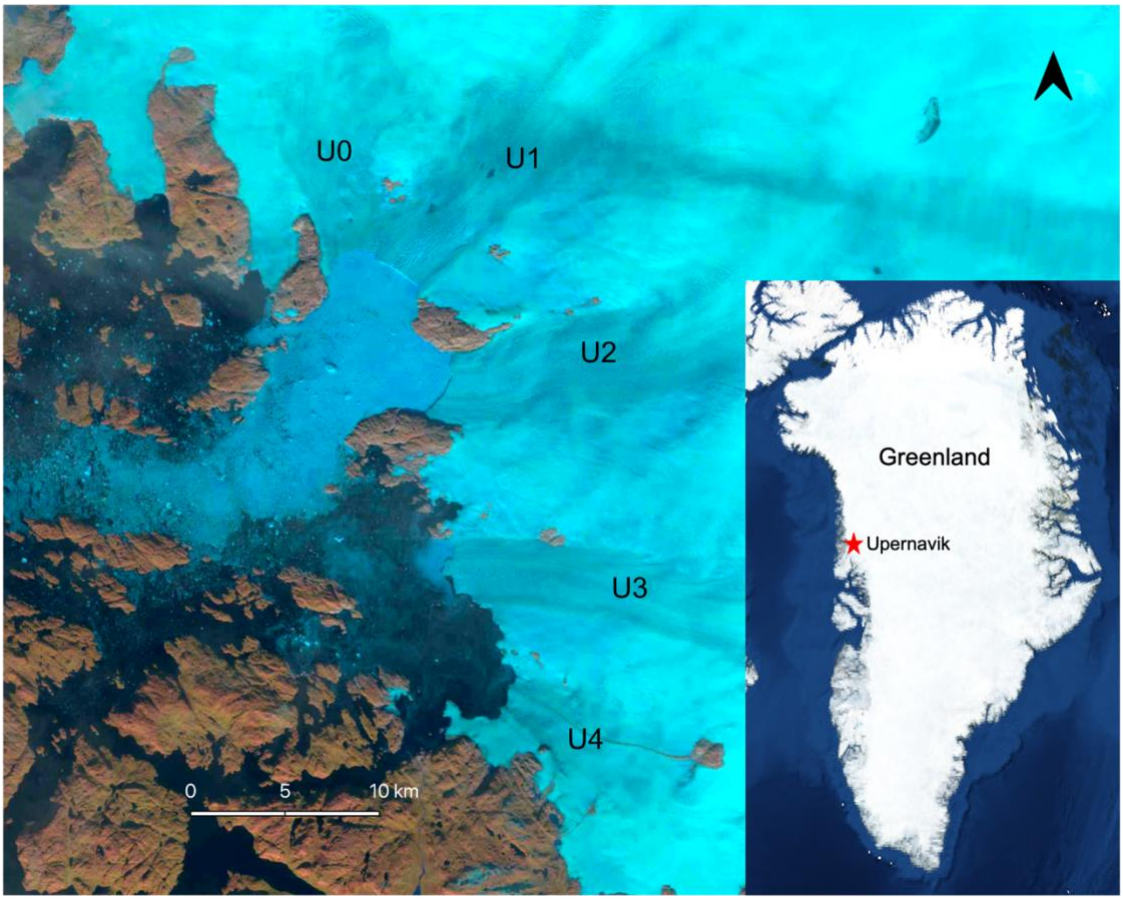

Figure 1.1: The Upernavik Isstrøm outlets. U0 to U4 from north to south, visualized using a Landsat 7 image from September 4th, 2002, courtesy of the U.S. Geological Survey.

1.1 Research Objective

As much of the Upernavik Isstrøm's fluctuating velocities and response to climate change after 2013 is undocumented, an updated analysis of each outlet, including the relatively unstudied fifth outlet to the north, is needed to examine the dynamic, atmospheric, and oceanic influences in the northwest region. Contrasting behaviors between outlets, coupled with rapid and complex velocity changes, make Upernavik an optimal location to examine ice dynamics, bed topography, and the impacts of atmospheric and oceanic forcings.

In this thesis, we will focus on updating the current understanding of all five outlets of the Upernavik Isstrøm by incorporating recent airborne and satellite data. We will build off Larsen and others (2016) to analyze the asynchronous behaviour of each outlet and to create a thorough and updated timeline of the varying responses of each glacier from 2000 to 2021. Hovmöller We will assess terminus conditions that may relate to ice flow: that the loss of the U1 floating ice tongue drove its acceleration in 2007, U2 had a floating ice tongue through 2013 and was accelerating, and that U3 may still be near floatation, while U0 and U4 are grounded. We will track the presence of plume polynyas at the glacier termini as a partial indicator of subglacial hydrologic activity. We will also assess the ocean sensitivity of each outlet by examining the timeline of the presence of floating ice tongues for the outlets and whether this can be related to fjord research done by Andresen and (2014) and Muilwijk and others (2022). Our goal is to assess linkages between significant acceleration, terminus retreat, and dynamically induced thinning with atmospheric and oceanic influences from 2000 to 2021.

We will specifically assess the controls of ice flow by examining the changing terminus conditions of floating ice tongues, bed topography, and basal and lateral friction forces. We will explore our central hypothesis that changes in floating ice tongues dominantly control changes in ice flow at Upernavik. This hypothesis is grounded in the results and conclusions from previous studies of Upernavik as well as evidence from many other marine-terminating glaciers in Greenland, such as Jakobshavn Isbræ (Joughin and others, 2004; Thomas, 2004; Howat and others, 2005, 2008), that the break-up of large floating ice tongues caused significant ice-flow

acceleration. As we investigate the role of floating ice tongues, we will also explore multiple methods used as proxies for floating ice-tongue presence. We will test our central hypothesis against our observations and measured velocities for all Upernavik outlets as well as using a numerical ice-flow model, Icepack, to quantitatively constrain the dynamic controls on ice velocity at the two outlets with major floatation observed, U1 and U2 (Shapero and others 2021). We will also explore the utility of the model and compare our results to recent simulations of Upernavik in higher-order models. Taken together, our analysis of Upernavik will provide a thorough and updated foundation of knowledge for future research in this area.

Below, we summarize our main objectives of this thesis:

1) Examine the asynchronous behaviour of the Upernavik Isstrøm by updating observations with modern remote sensing data;
2) Investigate which outlets have floating ice tongues and when by testing a variety of proxies for floating ice;
3) Explore our hypothesis that ice-velocity fluctuations can be explained by changing conditions of floating ice tongues by comparing velocity data to available proxies for floating ice tongues;
4) Investigate additional factors that may play a role in ice flow changes, including bed topography, basal drag, and lateral shear margins;
5) Test the capability of a new flowline model application, Icepack, for understanding the dynamics of Upernavik's two largest outlets; and

6) Provide a detailed foundation and framework that future studies can use to further explore the Upernavik Isstrøm and other large marine-terminating glaciers.

1.2 Thesis Structure

The structure of this thesis by chapter is as follows. Chapter 2: We provide an overview of relevant past literature related to Greenland and the fjord and ocean dynamics along western Greenland in Baffin Bay. Then we give a brief background of glacier physics, an overview of marine-terminating glacier dynamics in Greenland, and review previous studies on the Upernavik Isstrøm. Chapter 3: We present an article on the controls on ice flow of the Upernavik Isstrøm; at the time of writing this thesis, the manuscript in Chapter 3 is being prepared for submission to the Annals of Glaciology for peer-review. Chapter 4: We present a summary of our findings of the asynchronous behavior for each outlet, and discuss study limitations, future implications, future recommendations, and the main conclusions of this thesis.

References

Andresen, C. S., Kjeldsen, K. K., Harden, B., Nørgaard-Pedersen, N., & Kjær, K. H. (2014). Outlet glacier dynamics and bathymetry at Upernavik Isstrøm and Upernavik Isfjord, north-west Greenland. *GEUS Bulletin*, *31*, 79-82.

Enderlin, E. M., Howat, I. M., & Vieli, A. (2013). High sensitivity of tidewater outlet glacier dynamics to shape. *The Cryosphere*, *7*(3), 1007-1015.

Enderlin, E. M., Howat, I. M., Jeong, S., Noh, M. J., Van Angelen, J. H., & Van Den Broeke, M. R. (2014). An improved mass budget for the Greenland ice sheet. *Geophysical Research Letters*, *41*(3), 866-872.

Fried, M. J., Catania, G. A., Bartholomaus, T. C., Duncan, D., Davis, M., Stearns, L. A., ... & Sutherland, D. (2015). Distributed subglacial discharge drives significant submarine melt at a Greenland tidewater glacier. *Geophysical Research Letters*, *42*(21), 9328-9336.

Howat, I. M., Joughin, I., Tulaczyk, S., & Gogineni, S. (2005). Rapid retreat and acceleration of Helheim Glacier, east Greenland. *Geophysical Research Letters*, *32*(22).

Howat, I. M., Joughin, I., Fahnestock, M., Smith, B. E., & Scambos, T. A. (2008). Synchronous retreat and acceleration of southeast Greenland outlet glaciers 2000–06: ice dynamics and coupling to climate. *Journal of Glaciology*, *54*(187), 646-660.

Joughin, I., Tulaczyk, S., MacAYEAL, D. R., & Engelhardt, H. (2004). Melting and freezing beneath the Ross ice streams, Antarctica. *Journal of Glaciology*, *50*(168), 96-108.

Khan, S. A., Kjaer, K. H., Korsgaard, N. J., Wahr, J., Joughin, I. R., Timm, L. H., ... & Babonis, G. (2013). Recurring dynamically induced thinning during 1985 to 2010 on Upernavik Isstrøm, West Greenland. *Journal of Geophysical Research: Earth Surface*, *118*(1), 111-121.

Larsen, S. H., Khan, S. A., Ahlstrøm, A. P., Hvidberg, C. S., Willis, M. J., & Andersen, S. B. (2016). Increased mass loss and asynchronous behavior of marine-terminating outlet glaciers at Upernavik Isstrøm, NW Greenland. *Journal of Geophysical Research: Earth Surface*, *121*(2), 241-256.

Moon, T., & Joughin, I. (2008). Changes in ice front position on Greenland's outlet glaciers from 1992 to 2007. *Journal of Geophysical Research: Earth Surface*, *113*(F2).

Moon, T., Joughin, I., Smith, B., Van Den Broeke, M. R., Van De Berg, W. J., Noël, B., & Usher, M. (2014). Distinct patterns of seasonal Greenland glacier velocity. *Geophysical research letters*, *41*(20), 7209-7216.

Moon, T., Joughin, I., & Smith, B. (2015). Seasonal to multiyear variability of glacier surface velocity, terminus position, and sea ice/ice mélange in northwest Greenland. *Journal of Geophysical Research: Earth Surface*, *120*(5), 818-833.

Mouginot, J., Rignot, E., Bjørk, A. A., Van den Broeke, M., Millan, R., Morlighem, M., ... & Wood, M. (2019). Forty-six years of Greenland Ice Sheet mass balance from 1972 to 2018. *Proceedings of the national academy of sciences*, *116*(19), 9239-9244.

Muilwijk, M., Straneo, F., Slater, D. A., Smedsrud, L. H., Holte, J., Wood, M., ... & Harden, B. (2022). Export of Ice Sheet Meltwater from Upernavik Fjord, West Greenland. *Journal of Physical Oceanography*, *52*(3), 363-382.

Nick, F. M., Vieli, A., Howat, I. M., & Joughin, I. (2009). Large-scale changes in Greenland outlet glacier dynamics triggered at the terminus. *Nature Geoscience*, *2*(2), 110-114.

Shapero, D. R., Badgeley, J. A., Hoffman, A. O., & Joughin, I. R. (2021). icepack: A new glacier flow modeling package in Python, version 1.0. *Geoscientific Model Development*, *14*(7), 4593-4616.

Shepherd, A., Ivins, E., Rignot, E., Smith, B., Van Den Broeke, M., Velicogna, I., ... & Wuite, J. (2020). Mass balance of the

Straneo, F., & Heimbach, P. (2013). North Atlantic warming and the retreat of Greenland's outlet glaciers. *Nature*, *504*(7478), 36-43.

Straneo, F., & Cenedese, C. (2015). The dynamics of Greenland's glacial fjords and their role in climate. *Annual review of marine science*, *7*, 89-112.

Thomas, R. H. (2004). Force-perturbation analysis of recent thinning and acceleration of Jakobshavn Isbræ, Greenland. *Journal of Glaciology*, *50*(168), 57-66.

Wood, M., Rignot, E., Fenty, I., An, L., Bjørk, A., van den Broeke, M., ... & Zhang, H. (2021). Ocean forcing drives glacier retreat in Greenland. *Science advances*, *7*(1), eaba7282.

Zwally, H. J., Abdalati, W., Herring, T., Larson, K., Saba, J., & Steffen, K. (2002). Surface melt-induced acceleration of Greenland ice-sheet flow. *Science*, *297*(5579), 218-222.

CHAPTER 2.0 LITERATURE BACKGROUND

2.1 Glacier Physics

Glacier physics play an important role in the processes that will be discussed regarding marine-terminating glaciers and their relationship with the Greenland Ice Sheet. In this section, we review the most relevant aspects of glacier physics to the following study on Upernavik. We start by reviewing the most important mass balance components related to Greenland and Upernavik, and then discuss the mechanisms of ice flow, including the driving and resistive forces, as well as subglacial hydrology. The mass loss of the Greenland Ice Sheet can be split into two major processes: surface mass balance and ice discharge from marine-terminating glaciers, both of which are influenced by the ocean and atmosphere (Khan and others, 2015; Mouginot and others, 2019).

2.1.1 Surface Mass Balance

Greenland's surface mass balance is controlled by the balance between surface accumulation, primarily in the form of snow or rain, and surface mass loss through melt driven by warm atmospheric temperatures (Cuffey and Paterson, 2010). The difference between accumulation and ablation processes determines the direction and rate of surface mass change of glaciers and ice sheets, and a negative mass balance invites concern for the future of these ice stores and the sea-level contributions delivered to the ocean by outlet glaciers (Khan and others, 2015). Accumulation surplus needs to be compensated by ablation over multiple years for the surface mass balance to be in steady state (Paterson, 2000; Jiskoot, 2011). Surface mass balance over time is often

estimated using regional climate models, but this is challenging due to the spatially and temporally varying nature of snow and rain (Ettema and others, 2009; Khan and others, 2015).

2.1.2 Ice Dynamics and Calving

Ice discharge from marine-terminating glaciers is induced by ice dynamics, the response of glaciers to external or internal ice-flow drivers (Jiskoot, 2011). Calving can vary greatly and adjust to changes in ice flow (Cuffey and Paterson, 2010). Calving is the release of ice from the glacier front as a result of crevasse formation in response to stress (Benn and others, 2007). New or old crevasses extend enough to cut off ice blocks at the terminus (Benn and others, 2007). Calving is locally controlled by the stress conditions required for fractures to propagate enough to release the ice, controls on the rate of and extent of these fractures, as well as the orientation of the ice blocks calved, making a universal calving model incredibly challenging (Benn and others, 2007). For floating glaciers, longitudinal stretching of shelves can drive crevassing and facilitate calving (Cuffey and Paterson, 2010). The fjord geometry also controls the shelf stretching, where retreat or advance into a wider fjord can induce lateral stretching across the shelf, yet this is often more localized to the side margins (Cuffey and Paterson, 2010). Stretching produces parallel fractures to the ice front from longitudinal tensional stresses that produce large full-thickness icebergs (Joughin and others, 2008; Cuffey and Paterson, 2010). While the process of calving is due to fracturing, calving rates are largely controlled by ice flow processes distributing ice to the calving margin (Alley and others, in press). Calving plays an important role in mass loss from ice sheets and glaciers (both grounded and floating) but is poorly represented in ice-sheet

and glacier models (Benn and others, 2007). As such, accurately including calving in models is important for predicting mass loss and sea-level rise.

The calving rate can be controlled by the ice mélange. Recent research suggests that rigid sea ice and ice mélange at a glacier terminus can suppress calving and allow the glacier terminus to advance (Joughin and others, 2008, Amundson and others, 2010, Howat and others, 2010). For example, Moon (2015) studied 16 northwest Greenland outlets between 2009 and 2014 and found that the glaciers with rigid ice mélange were associated with terminus advance compared to glaciers with open water at the calving front. The presence of rigid mélange can apply back stress on the glacier terminus which can affect the calving rate (Slater and others, 2019). This is important when considering the factors controlling ice discharge.

2.1.3 Ice Flow, Driving and Resistive Stresses

Ice flows due to three main mechanisms: plastic deformation, basal sliding, and bed deformation (Cuffey and Paterson, 2010). Plastic deformation involves two major equations: the conservation of linear momentum and the conservation of mass for incompressible ice, as described by the Stokes Equation (Rückamp and others, 2022). Plastic or internal deformation is when ice creeps from ice crystal movement; ice behaves as a nonlinear viscous material (Cuffey and Paterson, 2010). Ice rheology, the relationship between the stress, in which the ice crystals exert the stress or internal force on one another due to an external force, and the strain rate, how quickly the ice deforms in response to stress, is difficult to constrain. Glacial ice is a non-Newtonian fluid and the constitutive relation used in the Stokes Equation is typically represented by

Glen's flow law, derived by Glen (1955). In steady-state creep, where $\dot{\varepsilon}$ is the strain-rate tensor, Glen's flow law is defined in Equation 1 as:

(1)

$$\dot{\varepsilon} = A\tau^n$$

where *A* is a temperature dependent rate-factor (fluidity), $\boldsymbol{\tau}$ is the stress tensor, *n* is the flow law exponent which is usually ≈ 3 (Glen, 1995; Jiskoot, 2011; Shapero and others, 2021).

Basal sliding is directly affected by the meltwater availability at the bed. An efficient drainage system that reduces meltwater will reduce basal sliding whereas sufficient meltwater availability and high-water pressure will separate the ice from the bed and increase basal sliding (Cuffey and Paterson, 2010). Basal sliding can affect seasonal velocity fluctuations as surface melting increases through the spring until mid-summer (Cuffey and Paterson, 2010). Bed deformation results in ice flow when the non-frozen bed sediments are sufficiently filled with meltwater in the pore space to overcome grain resistance (Cuffey and Paterson, 2010).

The parameters affecting ice flow can change as climatic conditions evolve or through natural variability. The gravitational driving force is determined by the ice thickness, slope, and density (Jiskoot, 2011). Resistive stresses include basal and lateral drag along the bed and shear margins and dynamic resistance due to longitudinal stress (Jiskoot, 2011). Basal drag depends on ice thickness and temperature, which affects the water pressure at the bed, and the bed topography whereas the strength of lateral shear margins depends on the contact area with perimeter topography and the glacier's centre ice thickness (Jiskoot, 2011). Both shear

and plug flow (uniform horizontal velocity as a result of basal sliding) can occur at marine-terminating glaciers, though floating ice tongues or lightly grounded ice experiences only plug flow (Jiskoot, 2011). Adjustments in driving and resistive stresses, resulting from, for example, changes in the surface mass balance, increased surface melting resulting in changes in subglacial hydrology, and large calving events like the disintegration of a floating ice tongue, can all have significant long-term effects on glacier velocity (Jiskoot, 2011). Floating ice has no basal shear stress on the glacier, but resistive stress comes from the sidewalls of the shelf as they are usually constrained by local topography; the loss of ice buttressing can impact the force balance and thus cause velocity adjustments (Jiskoot, 2011).

2.1.4 Subglacial Hydrology

Though difficult to study due to the inaccessibility of the glacier bed, glaciers have extensive networks of subglacial meltwater films, cavities, and channels. Warmer summer temperatures lead to increased surface melting (Zwally and others, 2002). Temperate glaciers, which are at the freezing point throughout, allow for enough pore spaces and the development of conduits for meltwater to percolate to the bed (Cuffey and Paterson, 2010). Primary water sources are from surface glacier melt or runoff from adjacent terrain, which collect in supraglacial lakes or drain directly into moulins, which transport the meltwater to the bed of the glacier (Zwally and others, 2002; Cuffey and Paterson, 2010). Pressure melting can occur at the glacier bed, which has even been observed at glaciers with little measured surface melt (Cuffey and Paterson, 2010). For drainage to occur, basal water pressure must match the overburden pressure, driving water through passages that can form efficient drainage channels, eventually reducing

the water pressure and meltwater availability (Cuffey and Patterson, 2010). The efficiency of water flow at the bed determines basal sliding and in turn, allows for seasonal and interannual velocity patterns as a response to atmospheric forcing (Zwally and others, 2002). The ice base can be at the pressure melting point all year, but particularly in the summer, increased pressure at the ice-bed interface from excess meltwater can decouple the ice from the bed and cause summer acceleration (Zwally and others, 2002). Near the end of the melt season, when meltwater is reduced at the bed, the effect on acceleration decreases (Zwally and others, 2002).

2.2 The Greenland Ice Sheet

It is important to study Greenland ice dynamics because of the influence of climate change on the Greenland Ice Sheet (GIS) and the limitations in understanding the processes involved with ice loss and sea-level rise. Mass loss from the GIS quadrupled from 1992 to 2011 and led to about a 7.5 mm rise in global sea level, accounting for one quarter of the rate of global sea-level rise during this time period (Church and others, 2011; Enderlin and others, 2014). Later estimates suggested about a 10.8 mm rise in sea level from an approximate total of 3902 billion tonnes of ice-loss from 1992 to 2018, peaking between 2007 and 2012 (Shepherd and others, 2020). Greenland's mass loss is mainly due to increased surface melt and the dynamic retreat and speedup of approximately 300 marine-terminating Greenland glaciers (Enderlin and others, 2014; Slater and others, 2019). Of these outlets, only 15 glaciers accounted for 77% of extreme mass loss since 2000, with four alone accounting for 50%, meaning individual outlets in Greenland may have a large role in a future with sea-level rise (Enderlin and others, 2014).

Along most of the western margin of the GIS, ice flows seaward at approximately 100 m $year^{-1}$ with surface melt rates around 2.5 m $year^{-1}$ (Joughin and others, 2008). Ice also moves through faster ice streams and terminates as marine-terminating outlets in western Greenland with speeds that can range from 200 to 12000 m $year^{-1}$ (Joughin and others, 2008). Ice discharge has been increasing by approximately 3 Gt a^{-2} in the west and northwest since 2000, with projections of global sea-level rise contribution reaching an additional 33 mm by 2100 (Enderlin and others, 2014). The majority of global sea-level contribution from 1972 to 2018 was seen in the northwest from marine-terminating glaciers, accounting for about a 4.4 mm rise (Mouginot and others, 2019). Northwestern Greenland, where there are approximately 80 marine-terminating glaciers, accounted for the 64% increase in discharge after 2008 (Moon and Joughin, 2008; Enderlin and others, 2014). The Upernavik Isstrøm accounted for the largest change in the northwest (Mouginot and others, 2019). Multiple studies show a low contribution rate of ice discharge from the northwest prior to 2005, with a sudden increase in discharge moving up the northwest coast after this time (Khan and others, 2010; Enderlin and others, 2014).

Acceleration of marine-terminating glaciers in northwest Greenland has been attributed to dynamic changes at the terminus, including increased submarine melting of floating ice tongues and submerged calving faces in contact with increased ocean heat transport in Greenland fjords (Khan and others, 2010; Enderlin and Howat, 2013). The influence of glacial hydrology and terminus retreat on ice flow velocity is still poorly understood, especially in this region. Some synchronous marine-terminating glacier retreat has been seen across Greenland during 2000 to 2006, which coincided with a

1.1˚C increase in mean summer air surface temperature, but increasing warm Atlantic Water has also been noted as a primary driver in mass-loss across ice-ocean margins in Greenland (Moon and Joughin, 2008; Straneo and Cedenese, 2015).

2.3 Baffin Bay and Greenland Fjords

Atlantic Water (AW) circulating around Greenland has likely been the main driver of the retreat and acceleration of marine-terminating glaciers since the mid 1990's (Wood and others, 2021). Warming of the deeper AW into the 2000's occurred from the fluctuation of heat content in the North Atlantic Subpolar Gyre during a transition in the North Atlantic Oscillation (Gillard and others, 2020; Wood and others, 2021). As the North Atlantic Subpolar Gyre expanded, it increased heat fluxes along the Greenland coast, part of which were transferred by the West Greenland Current as it carries both cold, relatively fresh Polar Water (PW) and warm, salty AW northward into Baffin Bay (Gillard and others, 2020; Wood and others, 2021). Warming and cooling trends of heat fluxes of the North Atlantic Subpolar Gyre into West Greenland roughly occur on a decadal scale (Wood and others, 2021). In the 2010's, the ocean thermal forcing has cooled compared to the 2000's, but remains higher than the 1990's (Wood and others, 2021).

Greenland has large and deep fjords that tend to have deep sills and deeply grounded glaciers (Straneo and Cedenese, 2015). The morphology of these fjords is important for understanding the reach of ocean circulation toward Greenland's ice-ocean margin. Both dense AW and less dense PW circulate along western Greenland's continental shelf at the mouth of the fjords as a part of the continental shelf-driven circulation that enters the water dynamics of the fjord (Straneo and Cedenese, 2015).

Deepened troughs along the shelf and deep fjords allow warmer AW to reach western Greenland as a part of fjord circulation (Chauché and others, 2014; Straneo and Cedenese, 2015). The presence of sills greatly affects the transfer of AW to Greenland's outlets (Chauché and others, 2014).

Fjord circulation is mainly influenced by tides, the buoyancy forcing from tidewater glaciers and icebergs, surface fluxes, local winds, and continental shelf circulation exchange at the mouth of the fjord (Straneo and Cedenese, 2015). Denser AW enters the fjord from the shelf when it occurs above the depth of sills at fjord mouths (Straneo and Cedenese, 2015). As the water travels to the glacier, buoyancy circulation takes place, where AW meets the glacier base and interacts with fresh subglacial meltwater at distinct injection points, causing buoyant and turbulent plumes to rise along the glacier face (Chauché and others, 2014; Straneo and others, 2014). These plumes mix with the fresher PW that is then carried out of the fjord (Figure 2) as part of an overturning process (Straneo and others, 2014).

The West Greenland Current has been found to transfer AW at depths greater than 400 m around the coast of southern Greenland into Arctic waters, where it then enters western Greenland's fjords (Chauché and others, 2014). About 50% of mass loss from 74 deep outlet glaciers across Greenland from 1992 to 2017 has been attributed to the influence of AW (Wood and others, 2021). Northwest marine-terminating glacier retreat has specifically been attributed to AW, with the most retreat of 28% (contributing to Greenland's mass loss through ice discharge) compared to other regions during this same period (Wood and others, 2021). This is likely from the ocean thermal forcing rising between +2˚C and 3˚C during a period of warmer ocean temperatures from 1998

to 2007 in the northwest (Morlighem and others, 2019; Wood and others, 2021). Many floating ice tongues and ice shelves collapsed in the central-west and northwest regions during this period, including Jakobshavn Isbræ from AW intrusion undercutting the terminus ice (Wood and others, 2021). Even during an ocean warming pause from 2008 to the end of the study by Wood and others (2021) in 2017, when the ocean thermal forcing decreased by about 1.5˚C in the northwest, net ice discharge still increased and floating extension glaciers in deep fjords made up 22% of grounded ice retreat from undercutting.

There is a severe knowledge gap around the ice-ocean interface because of the presence of floating ice tongues or sea ice and mélange coverage (Straneo and others, 2012). However, AW that can access the ice front is likely to affect the melt rate of the glacier (Chauché and others, 2014). For floating ice tongues, the accessibility of AW is dependent on the morphology of the floating extension and the bed geometry and fjord bathymetry (Wood and others, 2021). Small floating ice tongues or temporary floating ice tongues that sit on a shallow ridge may be less susceptible to undercutting from AW than a large floating extension in deeper water that allows direct contact of AW (Wood and others, 2021).

2.4 Marine-Terminating Glaciers and Floating Ice Tongues

Greenland's extensive network of marine-terminating glaciers play a large role in linking changes to the GIS with climate change, especially when evaluating the role of the ocean in mass-loss. Many of these outlets experienced a greater than 100% increase in ice velocity around the turn of the 21st century (Moon and others, 2012).

There are several processes involved with marine-terminating glacier flow and

retreat, including terminus thinning or reaching floatation, changes in back stress at the terminus, increased calving, retreat into deeper water, and subglacial drainage (Moon and others, 2015; Nick and others, 2009). Though difficult to study, subglacial drainage can cause rapid changes to ice flow, but it may not be a primary driver in terminus retreat at the ice-ocean interface for all glaciers as it is highly variable and seasonal (Straneo and Cedenese, 2015; Fried and others, 2015; Slater and others, 2019).

Marine-terminating glaciers adjust very rapidly to changes in the boundary conditions at the terminus (Nick and others, 2009). Dynamic adjustments usually begin at the calving front and then propagate upstream (Nick and others, 2009). When terminus retreat occurs, this changes the along-flow resistive stress and boundary conditions, which can lead to an increase in velocity and thinning that propagates up-glacier (Moon and others, 2015; Nick and others, 2009). There is often a positive feedback between glacier thinning and retreat (Nick and others, 2009). As the glacier terminus retreats over a pinning point into deeper water, ice speed and discharge then increase, which can in turn lead to further thinning and retreat (Moon and others, 2015; Nick and others, 2009). A calving model assessment by Nick and others (2010) evaluated episodic retreats related to the depth of the glacier trough. For Jakobshavn Isbræ, a reduction in discharge and calving rate was seen when the terminus reached shallow water compared to when it retreated into deeper water (Nick and others, 2010).

Glaciers also react to changes in resistive stresses such as the impacts of changes in floating ice tongues, which buttress the terminus (Moon and others, 2015; Nick and others, 2009). Changing conditions of floating ice tongues at the glacier terminus can cause initial glacier retreat (Moon and Joughin, 2008; Nick and others,

2009). Once the ice tongue thins to the point of collapse, the loss of ice buttressing, often coupled with retreating into deeper water, can cause further retreat and increased terminus velocity (Moon and Joughin, 2008; Nick and others, 2009). At Jakobshavn Isbræ, the loss of resistive back-stress from the loss of its floating ice tongue was argued as the driver for its acceleration (Joughin and others, 2004; Thomas, 2004). A flow model for Jakobshavn Isbræ demonstrated the glacier dynamics relied on the feedback between calving, terminus retreat, and loss of ice buttressing (Vieli and Nick, 2011). Floating ice tongues are likely more sensitive than grounded ice fronts to changes in the ocean thermal forcing because of the higher surface area in contact with the ocean (Straneo and others, 2013). Dynamic thinning near the terminus then causes velocities to propagate up-glacier and allows for destabilization of the near-terminus ice (Moon and Joughin, 2008; Nick and others, 2009). This type of retreat behaviour, along with the positive feedback between thinning and retreat, has been seen across multiple outlets in Greenland, including Jakobshavn Isbræ, Helheim Glacier, and Kangerdlugssuaq Glacier (Holland and others, 2008; Moon and others, 2015). There are currently only a handful of floating ice tongues that are still present in northern Greenland (Slater and others, 2019).

Research on analyzing Antarctic ice shelves can be used for constraining the presence and absence of floating ice tongues at Greenland marine-terminating glaciers by investigating slope-break at the grounding line (Bindschadler and others, 2011; Enderlin and Howat, 2013; Li and others, 2022). Inflection points appear in the ice surface slope of ice shelves where the slope changes rapidly at the grounding zone (Bindschadler and others, 2011; Li and others, 2022). This is often analyzed in

Antarctica to identify the approximate grounding line and where the ice transitions to floating (Bindschadler and others, 2011; Li and others, 2022). Determining the grounding line of ice is important for estimating the contact extent the ocean has under floating ice (Bindschadler and others, 2011). The ice elevations along the ice shelves can also be used to determine the hydrostatic line for the ice to determine the extent of free-floating ice along the ice shelf (Bindschadler and others, 2011). Enderlin and Howat (2013) used distinct slope-break to identify grounding line positions and changes in longitudinal strain rates to indicate floatation for several marine-terminating glaciers in Greenland.

Tabular icebergs are also widely used in Antarctica and Greenland as evidence for ice shelves and floating ice tongues (Jacobs and others, 1986; Melton and others, 2022). Calving behaviour is dependent on a glacier's floatation, as evidenced when unexpected ungrounding of an Alaskan glacier led to a change from irregular low-volume icebergs to large flow-perpendicular icebergs characteristic of ice shelves (Walter and others, 2010). Floating ice tongues commonly produce large tabular icebergs that remain floating upright away from the terminus (Melton and others, 2022). Glaciers with a grounding zone close to floatation over a sufficient distance can also produce tabular icebergs that remain upright (Melton and others, 2022). At Jakobshavn Isbræ, tabular icebergs were calved all year when the glacier had a floating ice tongue and when tabular icebergs were no longer being produced in the summer, this indicated the glacier was only calving grounded or nearly grounded ice (Amundson and others, 2010). Similarly at Helheim Glacier in eastern Greenland, tabular icebergs were calved from the floating ice tongue and remained upright (Melton and others, 2022).

Subglacial drainage in Greenland also plays a large role in terminus retreat and is often evidenced by plume polynyas at the calving front. Greenland has an extensive subglacial hydrology network, forming channels that follow ice flow routes and drain at the toes of land-terminating and marine-terminating glaciers (Fried and others, 2015). When water reaches the glacier bed, particularly in the spring and summer months during warmer air temperatures, this can increase basal lubrication and water pressure, which can affect the sliding rate of the glacier, causing acceleration, thinning, and retreat (Fried and others, 2015; Moon and others, 2015). Rather than release of back-stress from the modelled break up of 79N glacier's ice tongue, increased basal slipperiness caused realistic ice-flow changes (Rankmann and others, 2017). Mini surges have been seen at the Ryder Glacier in northern Greenland that were likely due to short-lived increased basal water pressure from the sudden drainage of supraglacial lakes upstream (Joughin and others, 1996; Joughin and others, 2008). However, thick Greenland ice and fjord conditions make it extremely difficult to study subglacial drainage patterns, channel locations, and the morphology of the terminus face (Fried and others, 2015; Straneo and Cedenese, 2015). These are all important factors when understanding the impacts of glacier drainage, as the morphology of the terminus can greatly influence the effect that subglacial water has on terminus retreat (Fried and others, 2015).

Though subglacial drainage may not be the main driver of large-scale glacier retreat in Greenland, for glaciers that have substantial drainage networks, plume formation can be an important control on terminus retreat, depending on the heat and salt budgets (Fried and others, 2015; Slater and others, 2019). Subglacial drainage can

initiate dynamic responses in marine-terminating glaciers by affecting the calving rate and causing undercutting when fresh meltwater mixes with fjord water and creates a buoyant and turbid plume (Chauché and others, 2014; Slater and others, 2019; Wood and others, 2021). Patterns of the filling and drainage of supraglacial lakes was also seen at Helheim Glacier, where drainage appeared at the glacier terminus as a plume-polynya (Melton and others, 2022).

Enderlin and Howat (2013) found that 85% of mass-loss from floating ice tongues was caused by submarine melting, including subaqueous melting from Atlantic Water intrusion as well as turbid plume formations melting the ice face (Holland and others, 2008; Rignot and others, 2010; Truffer and Motyka, 2016). While plume polynyas can be used to determine if subglacial drainage systems are present, their appearance when there are floating ice tongues is less certain for Greenland. For Helheim Glacier, it has been suggested that plume polynyas only appeared when the glacier front was partially or fully grounded (Melton and others, 2022). It is suggested that plume polynyas and calving occurrence are proxies for the grounding state of Helheim Glacier (Melton and others, 2022). Both tabular icebergs and plume-polynyas may only be able to occur simultaneously if the glacier is both partially grounded and floating in different sections along the terminus (Melton and others, 2022). Oppositely in Antarctica, plume-polynyas do develop at the edge of ice shelves, as long durations can carve channels into the floating sections that originate at the grounding line (Alley and others, 2019). Though it is difficult to observe, analyzing subglacial drainage at marine-terminating glaciers is important for understanding the floating state of the terminus and how this relates to glacier dynamics. It is also important for understanding meltwater availability

at the bed basal drag. Increased melting at the bed from increased water pressure under thick glaciers can facilitate glacier sliding (Iken and others, 1981).

2.5 The Upernavik Isstrøm

The Upernavik Isstrøm has five distinct outlets; previous literature has focused on the southernmost four. The three main central trunks of Upernavik are U1, U2, and U3 (numbered from north to south) with the smaller outlets U0 and U4 in the north and the south, respectively (Figure 1.1). The four commonly studied outlets (U1-U4) of the Upernavik Isstrøm have undergone multiple periods of acceleration and retreat during the satellite record. Khan and others (2013) found that ice dynamics caused 79% of total ice mass loss of Upernavik between 1985 and 2010. An ice sheet system model from 1995 to 2012 by Haubner and others (2018) found ice mass loss from changes in terminus position was due to thinning and acceleration. Two distinct periods of increased terminus retreat during the late 1990's and from 2005 to 2009 were likely due to dynamically induced thinning from increases in air and ocean temperatures (Khan and others, 2013; Andresen and others, 2014; Larsen and others, 2016). From 2005 to 2010, Upernavik lost a total mass of 53.4 ± 12.8 Gt (Khan and others, 2013). The sea-level equivalent that drained from U1 accounted for an increase of approximately 141 Gt/yr from 1996 to 2013 and U2 accounted for an increase of approximately 73 Gt yr^{-1} from 1993 to 2018 (Mouginot and others, 2019).

Of the outlets, U1 has experienced the largest changes over the last two decades. U1 began to accelerate around 2005 to 2006 until 2011 and retreated about 5 km from 2005 to 2008 compared to 1 km during 2000 to 2005 (Khan and others, 2013; Larsen and others, 2016). Velocities increased by over 50% (roughly 2000 m $year^{-1}$) between

2006 and 2008 (Khan and others, 2013; Larsen and others, 2016). Velocities stabilized around 2008 to 2010, with a deceleration of 15% between 2009 and 2010, but then reached a maximum of 5000 m $year^{-1}$ in 2011 before reaching stabilization at a high velocity after 2011 (Khan and others, 2013; Larsen and others, 2016).

U1 likely had a floating ice tongue from around 1985 until 2007, when it disintegrated during the accelerated retreat period (Larsen and others, 2016). Enderlin and Howat (2013) found significant change in slope around where U1 is believed to be grounded between 2001 and 2007 that indicated floatation. While other studies, such as McFadden and others (2011), suggested that a slightly sloping surface of the 3 km long ice tongue meant that the outlet was not freely floating, Larsen and others (2016) suggested that the higher surface slope was due to lateral friction in the narrow trough. The release of back stress and decreased flow resistance from the disintegration of the floating ice tongue around 2007 is likely what caused further acceleration, retreat, and dynamic thinning (Khan and others, 2013; Larsen and others, 2016). Dynamic thinning exceeded 100 m for U1 and U4 during this period, which, along with glacier speedup, is consistent with other outlets along the northwest (Khan and others, 2013).

The second-most variable outlet of the ice stream, U2, had a relatively stable calving front from 1985 to 2010, with acceleration beginning in 2009 through to the end of detailed outlet research done in 2013 (Khan and others, 2013; Larsen and others, 2016). Velocities increased after 2008 by 50% (Larsen and others, 2016). During this period, the surface ice elevation of U2 showed a long 2-3 km horizontal section at the terminus at buoyancy of a likely floating ice tongue about 2.5 km in length (Larsen and others, 2016). Larsen and others (2016) used tabular icebergs to determine the

presence of floating termini for Upernavik. Landsat 7 images collected in 2009 and 2010 also showed large-scale tabular icebergs calving from U2, indicating a floating ice tongue was likely present during this time (Larsen and others, 2016). Based on available literature, it is unclear when U2 first reached floatation.

U3 also had a relatively stable calving front from 1985 to 2010, though it is the longest outlet with approximately 142 km of bed below sea level (Khan and others, 2013; Larsen et al., 2016). Velocities declined slightly between 2000 and 2013, and it showed some seasonal variability associated with meltwater runoff (Moon and others, 2014; Larsen and others, 2016). This outlet has been categorized as being seasonally controlled by having meltwater lubricating the bed from 2009 to 2013 and later as forming an efficient drainage channel that reduced meltwater at the bed and increased basal drag (Moon and others, 2014; Vijay and others, 2019, 2021). Though the base is relatively horizontal and the terminus is likely grounded with very little retreat seen, the first 5 km of the outlet had ice thicknesses within 100 m of floatation based on observations between 2000 and 2013 (Larsen and others, 2016).

While U4, the southernmost outlet, has experienced little dynamic change in the 21st century, it has very distinct properties compared to the northern outlets. U4 experienced much of its retreat (3 km) from 1985 to 1991 and 1996 to 2000 before entering a period of stability during 2000 to 2010, with more than 100 m of dynamically induced thinning also seen up until 2002 (Khan and others, 2013). This opposite timing compared to U1-U3 and its deceleration from 1992 to 2013 is more comparable to changes occurring in southeast Greenland (Khan and others, 2013; Larsen and others, 2016). Only a short period of a 30-40% increase in ice flow speed near the terminus

during 2009 to 2010 was seen for U4 (Larsen and others, 2016). U4 also has seasonal variability between a late spring increase and late summer decrease lower than winter velocities, indicative of an extensive subglacial drainage system during the melt season (Larsen and others, 2016). Variations between the U1-U3 outlets and U4 may be due to differences in fjord geometry at the glacier calving fronts (Larsen and others, 2016).

A recent article by Downs and Johnson (2022) conducted numerical model simulations on ocean-driven retreat and the force balance of glaciers at the ice-ocean interface. Downs and Johnson (2022) used the Upernavik Isstrøm for their investigation with the hypothesis that rapidly retreating glaciers are less sensitive to perturbations in basal drag than glaciers that are not rapidly retreating. Floating ice tongues are sensitive to subaqueous melting of the glacier front as well as turbulent plumes that create heat exchange, both of which contribute to submarine melt rates (Holland and others, 2008; Rignot and others, 2010; Truffer and Motyka, 2016). Bed geometry and submarine melt have been suspected as drivers for changes in glacier dynamics at Upernavik by Larsen and others (2016). Model results by Downs and Johnson (2022) indicated that Upernavik glaciers were sensitive to perturbations in basal drag over their entire range of subaqueous melt rates, rejecting the initial hypothesis. Basal drag played a role no matter how fast the glaciers were flowing (Downs and Johnson, 2022). They also found that there is an inverse relationship for sensitivity to changes between subaqueous melt and basal drag (Downs and Johnson, 2022). Another finding was that basal drag perturbations caused acceleration and thinning upstream whereas subaqueous melt more locally affected the terminus (Downs and Johnson, 2022).

Bathymetric data are sparse across Greenland, but Andresen and others (2014) provided the first detailed look at the bathymetry of the Upernavik Fjord, which is approximately 80 km long and 5-7 km wide. While most of the fjord is over 900 m deep, the depth near the head of the fjord varies as it reaches the outlets, and a combination of local observations and some bathymetric data near the head suggest a range in water depth from 600 to 700 m (Andresen and others, 2014). Water depths near the termini of U1-U3 are particularly difficult to measure as they are covered by icebergs and ice mélange throughout the year. The water depth offshore of the terminus of U4 is approximately 200 m (Andresen and others, 2014). The terminus of U4 has a grounding line depth of 100 m, while U1-U3 have an estimated grounding line depth of anywhere from 400 to 700 m (Andresen and others, 2014; Morlighem and others, 2014). This was updated by Larsen and others (2016), who estimated that the calving front at U1 was about 1 km thick, U2 was 250 m thick when it had a floating ice tongue, and U3 was 500 m thick.

Oceanographic measurements were made in 2013 by Andresen and others (2014) to determine the presence of AW in the fjord. Fjord waters showed distinct stratification, with a 2˚C warm, fresher surface layer about 50 m thick, followed by a 50 to 150 m cold (0.5˚C to 1.5˚C) PW layer, then a dense and salty bottom layer that warms from 1˚C to 3˚C and is characteristic of AW. Sediment cores also indicated subsurface warm water entrainment near the outlets below 250 m (Vermassen and others, 2019). Bathymetry data and the hydrographic data in the fjord indicate that there is no shallow sill near the mouth of the fjord, meaning that AW can access the head of the fjord and all outlets except for U4 (Andresen and others, 2014).

A new study by Muilwijk and others (2022) released summer hydrographic profiles from 2013 to 2019 for the Upernavik Fjord and shelf area that confirms the presence of AW in the fjord. In the shelf area, profiles showed a warm (1.7˚C to 2.9˚C) and salty AW layer below 300 m with the warmest core around 400 m, which is overlain by cooler (0˚C to 2˚C) and fresher PW (Muilwijk and others, 2022). Below 500 m, the waters are slightly cooler (Muilwijk and others, 2022). Fjord profiles showed nearly identical AW properties as the shelf to a 450 m depth while the AW below this depth is uniform and does not cool like the bottom shelf water (Muilwijk and others, 2022). This may indicate a sill is present at 450 m between the shelf and the fjord which may be shallower than other estimates (Muilwijk and others, 2022). However, there is a relatively clear consensus that AW is able to flow unmodified into the fjord above 450 m by both Andresen and others (2014) and Muilwijk and others (2022). Throughout the time period, there was slight cooling and freshening of the AW mass in the fjord, with a total maximum temperature decrease of 1˚C, which is consistent with the ocean cooling period noted by other studies in Baffin Bay (Muilwijk and others, 2022).

During the distinct retreat periods for Upernavik, accelerated retreat for the northern outlets was likely from increased ocean temperatures, while dynamic thinning of U4, since it is not in contact with AW, is likely from increased air temperatures that may have increased subglacial discharge and higher submarine melt rates (Andresen and others, 2014). However, terminus retreat at Upernavik also occurred during periods when AW was reduced and cooler, which may indicate that ocean warming is not the only control on glacier acceleration and retreat in Upernavik (Vermassen and others, 2019).

2.5 Conclusion

Greenland has an extensive network of marine-terminating glaciers that contribute to ice-sheet mass-loss (Enderlin and others, 2014; Slater and others, 2019). The dominant margin contributing to Greenland's mass-loss is the northwest, where rapid changes in glacier retreat and acceleration have been attributed to ocean warming in Baffin Bay (Moon and Joughin, 2008; Khan and others, 2010; Enderlin and Howat, 2013; Straneo and Cedenese, 2015; Mouginot and others, 2019). The West Greenland Current carries warm, salty Atlantic Water along the continental shelf of Greenland and deep fjord systems allow for the transfer of Atlantic Water to reach the calving front of many deeply-grounded or floating glaciers (Chauché and others, 2014; Straneo and Cedenese, 2015; Gillard and others, 2020; Wood and others, 2021).

Some of these outlets have developed large floating ice tongues, which are more susceptible to ocean forcing due to the intrusion of Atlantic Water, which contributes to high submarine melt rates through turbulent and subaqueous melting, and can cause the disintegration of floating ice tongues due to intense thinning (Nick and others, 2009; Moon and others, 2015; Straneo and others, 2015). The resulting loss of resistive back-stress from the loss of a floating ice tongue can cause significant glacier acceleration, which has been argued as a driver at multiple outlets across Greenland, including Jakobshavn Isbræ (Joughin and others, 2004; Thomas, 2004; Howat and others, 2005, 2008; Joughin and others, 2008; Nick and others, 2009; Moon and others 2015). Rigid ice melange can also apply back stress on the terminus and hinder calving (Joughin and others, 2008; Amundson and others, 2010; Howat and others, 2010; Moon, 2015; Slater and others, 2019). Several methods have been presented for identifying a

floating ice tongue, including slope break, tabular icebergs, and plume polynyas (Jacobs and others, 1986; Amundson and others, 2010; Bindschadler and others, 2011; Enderlin and Howat, 2013; Li and others, 2022; Melton and others, 2022). Other factors also play a role in acceleration.

Additional controls of acceleration are also important. Bed and fjord geometry can aid in acceleration if a glacier retreats into a deeper or wider trough and the depth as well as depth of the bed, which determines the contact of Atlantic Water at the ice-front (Nick and others, 2009; Moon and others, 2015). Subglacial drainage, which can be driven by warming atmospheric temperatures, can lubricate the bed and reduce basal drag, allowing for seasonal speed ups (Moon and others, 2014; Straneo and Cedenese, 2015; Fried and others, 2015; Slater and others, 2019). On the other hand, channelization can efficiently outflow meltwater enough to reduce lubrication at the glacier bed and slow velocities (Moon and others, 2014). Weakened shear margins from thinning or increased water content can also cause acceleration (Van Der Veen and others, 2011).

At Upernavik, multiple periods of acceleration and retreat were found during intense atmosphere and ocean warming periods along western Greenland, particularly in the late 1990's and between 2005 and 2009 (Khan and others, 2013; Andresen and others, 2014; Larsen and others, 2016). Most of Upernavik's mass-loss contribution has been due to dynamic thinning, mainly from U1 and U2, both of which reside in a deep part of the fjord in contact with Atlantic Water (Khan and others, 2013; Andresen and others, 2014; Larsen and others, 2016; Mouginot and others, 2019; Vermassen and others, 2019; Muilwijk and others, 2022). Acceleration of U1 was attributed to the loss of

back-stress when its ice tongue disintegrated around 2007 (Khan and others, 2013; Larsen and others, 2016). U2 experienced retreat and acceleration through 2013 with a floating ice tongue present (Khan and others, 2013; Larsen and others 2016). Strong seasonal variation observed at U3 and U4, which reside in the shallow part of the fjord, is primarily controlled by meltwater (Moon and others, 2015; Larsen and others, 2016). Upernavik's outlets are sensitive to changes in basal friction, indicating subglacial hydrology plays an important role in the changes seen at all glaciers (Downs and Johnson, 2022).

References

Alley, K. E., Scambos, T. A., Alley, R. B., & Holschuh, N. (2019). Troughs developed in ice-stream shear margins precondition ice shelves for ocean-driven breakup. *Science advances*, *5*(10), eaax2215.

Alley, RB, Cuffey, KM, Bassis, JN, Alley, KE, Wang, S, Parizek, BR, Anandakrishnan, S, Christianson, K and DeConto, RM (In press, 2023). Iceberg Calving: Regimes and Transitions. *Annual Review of Earth and Planetary Sciences*, **51.**

Amundson, J. M., Fahnestock, M., Truffer, M., Brown, J., Lüthi, M. P., & Motyka, R. J. (2010). Ice mélange dynamics and implications for terminus stability, Jakobshavn Isbræ, Greenland. *Journal of Geophysical Research: Earth Surface*, *115*(F1).

Andresen, C. S., Kjeldsen, K. K., Harden, B., Nørgaard-Pedersen, N., & Kjær, K. H. (2014). Outlet glacier dynamics and bathymetry at Upernavik Isstrøm and Upernavik Isfjord, north-west Greenland. *GEUS Bulletin*, *31*, 79-82.

Benn, D. I., Warren, C. R., & Mottram, R. H. (2007). Calving processes and the dynamics of calving glaciers. *Earth-Science Reviews*, *82*(3-4), 143-179.

Bindschadler, R., Choi, H., Wichlacz, A., Bingham, R., Bohlander, J., Brunt, K., ... & Young, N. (2011). Getting around Antarctica: new high-resolution mappings of the grounded and freely-floating boundaries of the Antarctic ice sheet created for the International Polar Year. *The Cryosphere*, *5*(3), 569-588.

Blatter, H. (1995). Velocity and stress fields in grounded glaciers: a simple algorithm for including deviatoric stress gradients. *Journal of Glaciology*, *41*(138), 333-344.

Chauché, N., Hubbard, A., Gascard, J. C., Box, J. E., Bates, R., Koppes, M., ... & Patton, H. (2014). Ice–ocean interaction and calving front morphology at two west Greenland tidewater outlet glaciers. *The Cryosphere*, *8*(4), 1457-1468.

Church, J. A., Gregory, J. M., White, N. J., Platten, S. M., & Mitrovica, J. X. (2011). Understanding and projecting sea level change. *Oceanography*, *24*(2), 130-143.

Cuffey, K. M., & Paterson, W. S. B. (2010). *The physics of glaciers*. Academic Press.

Downs, J., & Johnson, J. V. (2022). A rapidly retreating, marine-terminating glacier's modeled response to perturbations in basal traction. *Journal of Glaciology*, 1-10.

Enderlin, E. M., Howat, I. M., Jeong, S., Noh, M. J., Van Angelen, J. H., & Van Den Broeke, M. R. (2014). An improved mass budget for the Greenland ice sheet. *Geophysical Research Letters*, *41*(3), 866-872.

Fried, M. J., Catania, G. A., Bartholomaus, T. C., Duncan, D., Davis, M., Stearns, L. A., ... & Sutherland, D. (2015). Distributed subglacial discharge drives significant submarine melt at a Greenland tidewater glacier. *Geophysical Research Letters*, *42*(21), 9328-9336.

Gillard, L. C., Hu, X., Myers, P. G., Ribergaard, M. H., & Lee, C. M. (2020). Drivers for Atlantic-origin waters abutting Greenland. *The Cryosphere*, *14*(8), 2729-2753.

Glen, J. W. (1955). The creep of polycrystalline ice. *Proceedings of the Royal Society of London. Series A. Mathematical and Physical Sciences*, *228*(1175), 519-538.

Glen, J. W. (1958). The flow law of ice: A discussion of the assumptions made in glacier theory, their experimental foundations and consequences. *IASH Publ*, *47*(171), e183.

Haubner, K., Box, J. E., Schlegel, N. J., Larour, E. Y., Morlighem, M., Solgaard, A. M., ... & Kjær, K. H. (2018). Simulating ice thickness and velocity evolution of Upernavik Isstrøm 1849–2012 by forcing prescribed terminus positions in ISSM. *The Cryosphere*, *12*(4), 1511-1522.

Holland, D. M., Thomas, R. H., De Young, B., Ribergaard, M. H., & Lyberth, B. (2008). Acceleration of Jakobshavn Isbræ triggered by warm subsurface ocean waters. *Nature geoscience*, *1*(10), 659-664.

Howat, I. M., Joughin, I., Tulaczyk, S., & Gogineni, S. (2005). Rapid retreat and acceleration of Helheim Glacier, east Greenland. *Geophysical Research Letters*, *32*(22).

Howat, I. M., Joughin, I., Fahnestock, M., Smith, B. E., & Scambos, T. A. (2008). Synchronous retreat and acceleration of southeast Greenland outlet glaciers 2000–06: ice dynamics and coupling to climate. *Journal of Glaciology*, *54*(187), 646-660.

Howat, I. M., Box, J. E., Ahn, Y., Herrington, A., & McFADDEN, E. M. (2010). Seasonal variability in the dynamics of marine-terminating outlet glaciers in Greenland. *Journal of Glaciology*, *56*(198), 601-613.

Iken, A. (1981). The effect of the subglacial water pressure on the sliding velocity of a glacier in an idealized numerical model. *Journal of Glaciology*, *27*(97), 407-421.

Jacobs, S. S., Macayeal, D. R., & Ardai, J. L. (1986). The recent advance of the Ross Ice Shelf Antarctica. *Journal of Glaciology*, *32*(112), 464-474.

Jiskoot, H. (2011). Dynamics of glaciers. *physical Research*, *92*(B9), 9083-9100.

Joughin, I., Tulaczyk, S., Fahnestock, M., & Kwok, R. (1996). A mini-surge on the Ryder Glacier, Greenland, observed by satellite radar interferometry. *Science*, *274*(5285), 228-230.

Joughin, I., Tulaczyk, S., Fahnestock, M., & Kwok, R. (1996). A mini-surge on the Ryder Glacier, Greenland, observed by satellite radar interferometry. *Science*, *274*(5285), 228-230.

Joughin, I., Tulaczyk, S., MacAYEAL, D. R., & Engelhardt, H. (2004). Melting and freezing beneath the Ross ice streams, Antarctica. *Journal of Glaciology*, *50*(168), 96-108.

Joughin, Ian, Sarah B. Das, Matt A. King, Ben E. Smith, Ian M. Howat, and Twila Moon. "Seasonal speedup along the western flank of the Greenland Ice Sheet." *Science* 320, no. 5877 (2008): 781-783.

Khan, S. A., Wahr, J., Bevis, M., Velicogna, I., & Kendrick, E. (2010). Spread of ice mass loss into northwest Greenland observed by GRACE and GPS. *Geophysical Research Letters*, *37*(6).

Khan, S. A., Kjaer, K. H., Korsgaard, N. J., Wahr, J., Joughin, I. R., Timm, L. H., ... & Babonis, G. (2013). Recurring dynamically induced thinning during 1985 to 2010 on Upernavik Isstrøm, West Greenland. *Journal of Geophysical Research: Earth Surface*, *118*(1), 111-121.

Khan, S. A., Aschwanden, A., Bjørk, A. A., Wahr, J., Kjeldsen, K. K., & Kjær, K. H. (2015). Greenland ice sheet mass balance: a review. *Reports on progress in physics*, *78*(4), 046801.

Larsen, S. H., Khan, S. A., Ahlstrøm, A. P., Hvidberg, C. S., Willis, M. J., & Andersen, S. B. (2016). Increased mass loss and asynchronous behavior of marine-terminating outlet glaciers at Upernavik Isstrøm, NW Greenland. *Journal of Geophysical Research: Earth Surface*, *121*(2), 241-256.

Li, T., Dawson, G. J., Chuter, S. J., & Bamber, J. L. (2022). A high-resolution Antarctic grounding zone product from ICESat-2 laser altimetry. *Earth System Science Data*, *14*(2), 535-557.

Melton, S. M., Alley, R. B., Anandakrishnan, S., Parizek, B. R., Shahin, M. G., Stearns, L. A., ... & Finnegan, D. C. (2022). Meltwater drainage and iceberg calving observed in high-spatiotemporal resolution at Helheim Glacier, Greenland. *Journal of Glaciology*, 1-17.

Moon, T., & Joughin, I. (2008). Changes in ice front position on Greenland's outlet glaciers from 1992 to 2007. *Journal of Geophysical Research: Earth Surface*, *113*(F2).

Moon, T., Joughin, I., Smith, B., & Howat, I. (2012). 21st-century evolution of Greenland outlet glacier velocities. *Science*, *336*(6081), 576-578.

Moon, T., Joughin, I., Smith, B., Van Den Broeke, M. R., Van De Berg, W. J., Noël, B., & Usher, M. (2014). Distinct patterns of seasonal Greenland glacier velocity. *Geophysical research letters*, *41*(20), 7209-7216.

Moon, T., Joughin, I., & Smith, B. (2015). Seasonal to multiyear variability of glacier surface velocity, terminus position, and sea ice/ice mélange in northwest Greenland. *Journal of Geophysical Research: Earth Surface*, *120*(5), 818-833.

Morlighem, M. et al. 2021, updated 2021. *IceBridge BedMachine Greenland, Version 4*. [Indicate subset used]. Boulder, Colorado USA. NASA National Snow and Ice Data Center Distributed Active Archive Center. doi: https://doi.org/10.5067/VLJ5YXKCNGXO.

Mouginot, J., Rignot, E., Bjørk, A. A., Van den Broeke, M., Millan, R., Morlighem, M., ... & Wood, M. (2019). Forty-six years of Greenland Ice Sheet mass balance from 1972 to 2018. *Proceedings of the national academy of sciences*, *116*(19), 9239-9244.

Muilwijk, M., Straneo, F., Slater, D. A., Smedsrud, L. H., Holte, J., Wood, M., ... & Harden, B. (2022). Export of Ice Sheet Meltwater from Upernavik Fjord, West Greenland. *Journal of Physical Oceanography*, *52*(3), 363-382.

Nick, F. M., Vieli, A., Howat, I. M., & Joughin, I. (2009). Large-scale changes in Greenland outlet glacier dynamics triggered at the terminus. *Nature Geoscience*, *2*(2), 110-114.

Nye, J. F. (1957). The distribution of stress and velocity in glaciers and ice-sheets. *Proceedings of the Royal Society of London. Series A. Mathematical and Physical Sciences*, *239*(1216), 113-133.

Paterson, W. S. B. (2000). *Physics of glaciers*. Butterworth-Heinemann.

Pattyn, F. (2003). A new three-dimensional higher-order thermomechanical ice sheet model: Basic sensitivity, ice stream development, and ice flow across subglacial lakes. *Journal of Geophysical Research: Solid Earth*, *108*(B8).

Rignot, E., Koppes, M., & Velicogna, I. (2010). Rapid submarine melting of the calving faces of West Greenland glaciers. *Nature Geoscience*, *3*(3), 187-191.

Rückamp, M., Kleiner, T., & Humbert, A. (2022). Comparison of ice dynamics using full-Stokes and Blatter–Pattyn approximation: application to the Northeast Greenland Ice Stream. *The Cryosphere*, *16*(5), 1675-1696.

Shapero, D. R., Badgeley, J. A., Hoffman, A. O., & Joughin, I. R. (2021). icepack: A new glacier flow modeling package in Python, version 1.0. *Geoscientific Model Development*, *14*(7), 4593-4616.

Shepherd, A., Ivins, E., Rignot, E., Smith, B., Van Den Broeke, M., Velicogna, I., ... & Wuite, J. (2020). Mass balance of the Greenland Ice Sheet from 1992 to 2018. *Nature*, *579*(7798), 233-239.

Slater, D. A., Straneo, F., Felikson, D., Little, C. M., Goelzer, H., Fettweis, X., & Holte, J. (2019). Estimating Greenland tidewater glacier retreat driven by submarine melting. *The Cryosphere*, *13*(9), 2489-2509.

Straneo, F., Sutherland, D. A., Holland, D., Gladish, C., Hamilton, G. S., Johnson, H. L., ... & Koppes, M. (2012). Characteristics of ocean waters reaching Greenland's glaciers. *Annals of Glaciology*, *53*(60), 202-210.

Straneo, F., & Heimbach, P. (2013). North Atlantic warming and the retreat of Greenland's outlet glaciers. *Nature*, *504*(7478), 36-43.

Straneo, F., & Cenedese, C. (2015). The dynamics of Greenland's glacial fjords and their role in climate. *Annual review of marine science*, *7*, 89-112.

Thomas, R. H. (2004). Force-perturbation analysis of recent thinning and acceleration of Jakobshavn Isbræ, Greenland. *Journal of Glaciology*, *50*(168), 57-66.

Truffer, M., & Motyka, R. J. (2016). Where glaciers meet water: Subaqueous melt and its relevance to glaciers in various settings. *Reviews of Geophysics*, *54*(1), 220-239.

Van Der Veen, C. J., Plummer, J. C., & Stearns, L. A. (2011). Controls on the recent speed-up of Jakobshavn Isbræ, West Greenland. *Journal of Glaciology*, *57*(204), 770-782.

Vermassen, F., Andreasen, N., Wangner, D. J., Thibault, N., Seidenkrantz, M. S., Jackson, R., ... & Andresen, C. S. (2019). A reconstruction of warm-water inflow to Upernavik Isstrøm since 1925 CE and its relation to glacier retreat. *Climate of the Past*, *15*(3), 1171-1186.

Vieli, A., & Nick, F. M. (2011). Understanding and modelling rapid dynamic changes of tidewater outlet glaciers: issues and implications. *Surveys in geophysics*, *32*(4), 437-458.

Vijay, S., Khan, S. A., Kusk, A., Solgaard, A. M., Moon, T., & Bjørk, A. A. (2019). Resolving seasonal ice velocity of 45 Greenlandic glaciers with very high temporal details. *Geophysical Research Letters*, *46*(3), 1485-1495.

Vijay, S., King, M. D., Howat, I. M., Solgaard, A. M., Khan, S. A., & Noël, B. (2021). Greenland ice-sheet wide glacier classification based on two distinct seasonal ice velocity behaviors. *Journal of Glaciology*, *67*(266), 1241-1248.

Wood, M., Rignot, E., Fenty, I., An, L., Bjørk, A., van den Broeke, M., ... & Zhang, H. (2021). Ocean forcing drives glacier retreat in Greenland. *Science advances*, *7*(1), eaba7282.

Zwally, H. J., Abdalati, W., Herring, T., Larson, K., Saba, J., & Steffen, K. (2002). Surface melt-induced acceleration of Greenland ice-sheet flow. *Science*, *297*(5579), 218-222.

CHAPTER 3.0 The Role of Terminus Conditions in the Ice-Flow Speed of the Upernavik Isstrøm in Northwest Greenland

Authors: Kelsey Voss, Karen Alley, David Lilien, Dorthe Dahl-Jensen

Affiliations: The Centre for Earth Observation Science; The Clayton H. Riddell Faculty of Environment, Earth, and Resources; The University of Manitoba

This paper is to be submitted to the Annals of Glaciology. The extensive work done on this paper represents the core of my thesis. As the first author, I was primarily responsible for the remote sensing analysis, with the aid of Dr. Karen Alley and Dr. Dorthe Dahl-Jensen, and the modelling work, with the aid of Dr. David Lilien. Dr. David Lilien was responsible for the model set-up, including all inversions, while I was responsible for incorporating our data into the model simulations and executing the model.

ABSTRACT

The five outlets of Upernavik Isstrøm have experienced complex and contrasting ice-flow-speed changes over the last two decades. The Upernavik Isstrøm is located in northwest Greenland, where the most mass loss from ice dynamics and highest contribution to sea-level rise from Greenland has been measured, making it an important case study for investigating controls on ice flow. We present a detailed remote sensing analysis of the ice dynamics at Upernavik's outlets from 2000 to 2021, and explore the capability of a new flowline model, Icepack, to evaluate physical forcings controlling the ice-flow changes. Previous research suggested floating ice tongues are an important ice-flow control. We constrained floating ice tongues and found they were

not consistent with observed patterns of acceleration. The modelled sensitivity of Upernavik's ice flow to basal slipperiness was the most physically and spatially accurate, rather than changes in shear margin strength, thinning, or terminus retreat. The simplified flowline model, Icepack, successfully captured complex ice dynamics over multiple simulated years. Our results provide a strong indication that speed fluctuations at Upernavik's outlets are seasonally and inter-annually controlled by subglacial hydrology.

3.1 INTRODUCTION

In a warming climate, Greenland's marine-terminating glaciers have undergone significant changes in ice flow. Northwest Greenland has lost mass as a result of recent changes in glacier dynamics, where the highest retreats in Greenland (contributing to mass loss through ice discharge) of 28% were measured from 1992 to 2017 (Wood and others, 2021). This region has most of Greenland's deep-water outlet glaciers, and from 1972 to 2018 it contributed 4.4 mm to global sea-level rise, the highest contribution out of any region in Greenland (Mouginot and others, 2019; Wood and others, 2021). Ice dynamics in the northwest contributed to 86% of its total mass loss compared to surface mass balance, with the percentage increasing every decade from 1998 to 2018 (Joughin and others, 2018). Controls on ice flow acceleration have been linked to several processes, including thinning of floating ice tongues, retreat into deeper or wider glacier troughs, and subglacial drainage (Moon and others, 2015; Nick and others, 2009). Subglacial drainage due to warmer air temperatures and surface melting can lubricate the glacier bed and also cause short-term acceleration, thinning, and retreat (e.g. Zwally and others, 2002; Fried and others, 2015; Straneo and others, 2015).

However, the changing conditions of a floating ice tongue have been identified to significantly influence velocities at the terminus that then propagate upstream (Moon and Joughin, 2008; Nick and others, 2009). This has been argued as a driver for the acceleration of other large glaciers in Greenland, including Jakobshavn Isbræ (Thomas, 2004; Joughin and others, 2004; Vieli and Nick, 2011).

One of the largest and fastest-retreating ice streams in northwest Greenland is the Upernavik Isstrøm. Model results by Haubner and others (2018) between 1995 and 2012 showed glacier acceleration at Upernavik was responsible for 80% of its mass loss. The Upernavik Isstrøm has five marine-terminating glaciers, several of which have contributed significantly to Greenland's ice-mass loss. We will refer to the five distinct outlets as U0 to U4 (Figure 3.1), from north to south, although previous literature has focused on the southernmost four. The two northern outlets with the most significant velocities and retreat, U1 and U2, accounted for an increase in sea-level equivalent drainage of approximately 141 Gt yr^{-1} from 1996 to 2013 for U1 and 73 Gt yr^{-1} from 1993 to 2018 for U2 (Mouginot and others, 2019).

The Upernavik Isstrøm is important not just due to its size, but also because it has experienced complex and contrasting behaviours in velocity between its individual outlets. There are observed periods of deceleration at the southern outlets while acceleration occurred at the northern outlets. Between 2005 and 2006 compared to 2000 and 2001, U1 increased in ice flow by over 50% (Khan and others, 2013). Between 2006 and 2008, glacier velocities increased by 50-60% at U1 and between 2008 and 2013, U2 velocities also increased by 50% (Larsen and others, 2016). The average regional speed in the northwest, based on its fast-flowing marine-terminating

glaciers, increased by just 18% between 2005 and 2010 (Moon, 2012), demonstrating the outlying magnitude of Upernavik's acceleration and the need to investigate its ice flow. There have also been periods of ice-flow slow-downs, such as the deceleration of U1 by 15% (1000 m $year^{-1}$) between 2009 and 2010 (Larsen and others, 2016). There is debate over the controls on the non-uniform ice-flow fluctuations of the Upernavik Isstrøm. Acceleration at these two northern outlets may be driven by several processes, including the depth of the fjord at each outlet, allowing warm Atlantic Water to access the glaciers and cause acceleration and retreat (Andresen and others, 2014) and the calving fronts retreating into deeper water (Larsen and others, 2016),

The northern outlets reside in a deeper region of the fjord compared to the southern outlets and are likely in contact with warmer Atlantic Water at depths varying between 250 and 450 m, which may explain some velocity fluctuations (Andresen and others, 2014; Vermassen and others, 2019; Muilwijk and others, 2022). Recent measurements in the Upernavik Fjord suggest the warmest core lies around 400 m (Muilwijk and others, 2022). The glaciers with deep ice fronts in contact with Atlantic Water are suggested to be more susceptible to ocean forcing and thus more sensitive at the ice-ocean boundary (Rignot and others, 2010; Chauché and others, 2014; Wood and others, 2021). However, acceleration at Upernavik also occurred during periods when Atlantic Water was not as warm, meaning it may not be the only control responsible for changes in ice flow (Vermassen and others, 2019).

The loss of the floating ice tongue at U1 is also proposed as a possible reason for its acceleration (Khan and others, 2013; Larsen and others, 2016). The acceleration of Jakobshavn Isbræ is attributed to the loss of ice buttressing from the disintegration of

its long floating ice tongue (Joughin and others, 2004; Thomas, 2004; Holland and others, 2008; Vieli and Nick, 2011). Slower or stable velocities are observed when Greenland glaciers terminate with floating ice tongues, including Jakobshavn Isbræ (Nick and others, 2010; Moon, 2012). U1 and U2, in the northern part of the fjord with the most acceleration measured, are the only two outlets with evidence of floating ice tongues (Enderlin and Howat, 2013; Khan and others, 2013; Larsen and others, 2016).

Changes at the glacier terminus can alter resistive stresses along the glacier bed and fjord walls that can also influence velocities (Pfeffer, 2007; Howat and others, 2005, 2008). The acceleration of Jakobshavn is debated to be due to weakened shear-margins rather than solely from the loss of back-stress from the break up of its floating ice tongue (Van Der Veen and others, 2011). Joughin and others (2012) suggested that basal water pressure may have driven acceleration along with the change in ice buttressing. At the Nioghalvfjerdsfjorden (79N) glacier in northeastern Greenland, rather than the loss of its 76 km ice tongue or weakened shear margins, basal slipperiness produced realistic seasonal velocities in a numerical ice flow model (Rathmann and others, 2017). Recent Ice-Sheet and Sea-Level System Model simulations by Downs and Johnson (2022) investigated Upernavik's sensitivity to perturbations in basal drag and submarine melt rates to investigate mass loss. They found that rapidly retreating marine-terminating glaciers are sensitive to perturbations in basal drag (Downs and Johnson, 2022). Changes in meltwater at the bed was found to be an important factor in ice dynamics at Upernavik, not just ocean interactions at the terminus (Downs and Johnson, 2022).

In this study, we investigate the hypothesis that the changing conditions of floating ice tongues are the main driver of significant terminus acceleration at Upernavik over time. Our most interesting target is the recently accelerating outlet U2, as the most recent study by Larsen and others (2016) indicated a floating ice tongue present at the end of their record in 2013. We use remote sensing data to update the responses of all outlets since 2013 to assess major changes over our time period from 2000 to 2021. We find significant changes in velocities since 2013, making it even more important to understand what factors may be driving acceleration. We use tabular icebergs, plume-polynyas, and slope-break patterns to constrain when there floating ice tongues exist at each of Upernavik's outlets. We observe and analyze retreat, calving type, subglacial drainage, elevation profiles and thinning. We then compare the observational data with velocity data to test our hypothesis that velocity fluctuations can be explained by the changing conditions of floating ice tongues. We also explore the role of bed geometry and the stress balances that control ice flow using the new software package Icepack. This is done using a numerical flowline model that incorporates bed topography, basal drag, and shear margins acting on U1 and U2 for datasets from time periods with and without evidence of floatation.

3.2 METHODS

3.2.1 Terminus and Bed Observations

We first updated the observational record at Upernavik from 2000 to 2021 using airborne and satellite data. Ice front positions and observed retreat, evidence of subglacial drainage patterns, bed topography, and near-terminus bathymetry were all

examined. This was done to evaluate what has changed since the last detailed research conducted in 2013.

Landsat 7 and 8, courtesy of the U.S. Geological Survey, provided a detailed record of visual change up to 2021, as well as supplement terminus positions in recent years. The Programme for Monitoring of the Greenland Ice Sheet (PROMICE) provided terminus position outlines for all outlets that were derived from Landsat, Aster, and Sentinel-2 from 1999 to 2019 (Andersen and others, 2019). We supplemented the existing PROMICE record by digitizing the terminus positions for all outlets per year from 2019 to 2021, using the same method as PROMICE. The end of the melt season was determined by PROMICE as most retreated position of the glacier from July and November (Andersen and others, 2019).

While it is difficult to gather evidence about specific subglacial patterns using satellite imagery, some information on channelization and drainage events can be gleaned by tracking plume polynyas. Plume polynyas are open-water areas that form when subglacial channels release buoyant meltwater that rises to the glacier front (Melton and others, 2022). We manually inspected all available and cloudless Landsat 7 and 8 imagery from 2000 to 2021 and developed a record of all the occasions where plume polynyas were visible.

We used NASA's Operation Icebridge BedMachine Greenland, Version 4 (Morlighem and others, 2020) as an estimate to evaluate the depth of the fjord near each outlet and the bed topography of each outlet so we could assess the water bodies in contact with the ice front and what future retreat may look like in each glacier's trough.

3.2.2 Velocity

We used a variety of ice flow data available at Upernavik to investigate the timing and magnitude of acceleration. We used ITS_LIVE, a velocity dataset updated through 2021, which is generated using the feature-tracking program auto-RIFT and provided by the NASA MEaSUREs ITS_LIVE project (Gardner and others, 2019). Landsat 7 and 8 images were used to compile velocity data across Greenland from 1985 to 2018 to create velocity mosaics and image-pair velocities (Gardner and others, 2019). Though ITS_LIVE mosaics were not available for our analysis past 2018, we extracted and averaged ITS_LIVE data along our points from the Global Glacier Velocity Point Data Access (Gardner and others, 2022). We also used GoLIVE velocity pair which extended our velocity analysis to 2021 for analysis involving flowlines. GoLIVE was generated from pairs of Landsat 8 panchromatic images from 2013 to 2021 (Scambos and others, 2016). Data were generated for GoLIVE using an image correlation algorithm that produces grids of ice displacement referenced to in-image rock outcrops, slow moving ice, and/or geo-positioning (Scambos and others, 2016). GoLIVE image pairs from four Landsat path/rows covering the Upernavik region were interpolated onto a common grid and stacked. A mosaiced product for each summer season was created by taking the mean of each pixel stack. Annual ITS_LIVE velocities are available at a 240 m resolution while GoLIVE velocities are available at a 300 m resolution. As they are derived using panchromatic optical imagery, which is only available during months with sufficient sunlight due to Upernavik's latitude, we used these data as an estimate of summer velocities. Error provided by the ITS_LIVE dataset was used in our velocity diagrams.

NASA's MEaSUREs project also offers a Greenland Ice Sheet Velocity Map for winter velocities using InSAR speckle tracking data (Joughin and others, 2011). This is available sporadically across the time period of interest with 200 m and 500 m resolutions (Joughin and others, 2011). Each winter velocity year available is derived from varying sources, including RADARSAT-1, ALOS, TerraSAR-X/TanDEM-X, and Sentinel-1A and Sentinel-1B (Joughin and others, 2011). The winter velocities are derived from the fall of one year to the early spring of the next. Error was used from the MEaSUREs dataset in our velocity diagrams.

3.2.3 Evidence for Floating Ice

In order to test our hypothesis on the relationship between ice flow and the changing conditions of floating ice tongues, we needed a variety of evidence to assess the presence of floating ice. We used a multi-dataset approach that relied on identifying tabular icebergs throughout the entire time period, more extensive integration of ice elevations and thicknesses in a hydrostatic analysis for floating ice, and ArcticDEM elevations to identify slope-break and horizontally-sloped floating ice at the terminus. Our analysis focused on the largest outlets, U1 and U2, where floating ice tongues have been observed during two periods in the 2000's and the 2010's.

The first method we used to constrain floating ice tongues were observations of tabular icebergs throughout the full Landsat record. Marine-terminating glaciers in deep fjords can produce tabular icebergs, which are considered evidence of (near) floatation because full-thickness tabular bergs can only separate and remain upright from a terminus if the ice is sufficiently thin (Joughin and others, 2008; Amundson and others, 2010, Kehrl and others, 2017; Melton and others, 2022). Larsen and others (2016)

identified tabular icebergs being produced from U3 not necessarily from floatation but due to its long horizontal slope and shallow bed topography. Though tabular icebergs were tracked by Larsen and others (2016) from 2009 to 2010 for U2 for its floating ice tongue, we looked for tabular icebergs and evident changes in calving behaviour and type throughout the entire time period and for all outlets in order to provide supporting evidence indicating that floating ice tongues were present.

The second method we used to constrain floating ice tongues is the hydrostatic analysis for floating ice, which had shown to be a reliable method in many settings (e.g. Bentley and others, 2022; Wild and others, 2022). When IceBridge thickness data were available, we conducted a hydrostatic elevation analysis to identify floating termini. For this, we used a simple version of the hydrostatic equation below in Equation 1 (e.g. Jenkins and Doake, 1991)

(1)

$$Z_s = \left(1 - \frac{\rho_i}{\rho_w}\right) H$$

where ρ_i is the density of ice, ρ_w is the density of seawater, H is the ice thickness (derived from radar data as described in the next paragraph), and Z_s is the hydrostatic elevation. As the terminus of Upernavik's outlets lie in the ablation zone, we assumed the entire thickness is solid glacial ice. We assumed ρ_i to be 917 kg m^{-3}, and the ρ_w to be 1026 kg m^{-3}. Comparison between Z_s and the actual surface elevation indicated if the ice at the terminus of each outlet was at or near floatation. We used this equation to determine if and when the glacier had a floating ice tongue.

We constructed a record of ice thicknesses from 2010 to 2017 for each outlet using a mixture of data products from NASA's Operation IceBridge's Multichannel Coherent Radar Depth Sounder (MCoRDS). The MCoRDS L2 Ice Thickness Version 2 dataset contains pre-processed data in roughly flow-parallel IceBridge flightlines along Upernavik, but temporal and spatial coverage of all outlets was limited due to minimal flightlines (Paden and others, 2010). The year 2013 is the only year that covered all outlets. The MCoRDS L1B Geolocated Radar Echo Strength Profiles Version 1 dataset was used to fill in gaps (Paden and others, 2014). We used the L1B and L2 data to take our own echogram data picks when the MCoRDS dataset could not complete ice thicknesses, particularly near the terminus, by manually selecting the strongest reflector representing the ice bottom. We obtained hydrostatic thickness results for U0 in 2011 and 2013. U1 had five seeable IceBridge flightlines available in 2010, 2011, 2012, 2013, 2014. Two IceBridge flightlines with good coverage were available for U2, in 2013 and 2017. We were able to obtain hydrostatic data for six flightlines available for U3 in 2010, 2011, 2012, 2013, 2015, and 2017. U4 only had one IceBridge flightline available, in 2013.

The third method we used to constrain the presence and absence of floating ice tongues was a detailed elevation analysis using ArcticDEM. Though there are multiple sources of ice surface elevations for Upernavik, the most recent edition of ArcticDEM provided detailed elevation data for each outlet over the recent years (Porter, Claire, and others, 2022). ArcticDEM is constructed from in-track and cross-track ~0.5 m resolution imagery from the Maxar constellation of optical imaging satellites (Porter and others, 2018). It is mainly generated from panchromatic bands from WorldView-1,

WorldView-2, and WorldView-3, with some data generated from the GeoEye-1 satellite sensor (Porter, Claire, and others, 2022). ArcticDEM includes 2 m resolution strips from 2010 to 2021 (Porter, Claire, and others, 2022). We measured error by using rock outcrop elevation points near the glacier termini from the ArcticDEM high resolution mosaic and calculating the mean squared difference from all the overlying elevation strips. Adding a high-resolution dataset like ArcticDEM to our analysis greatly improved our understanding of vertical change at Upernavik. Slope break near the terminus of glaciers has been used as evidence of the grounding line, where ice past that point is likely floating (Bindschadler and others, 2011; Enderlin and Howat, 2013; Li and others, 2022). We used ArcticDEM to analyze slope change and also used the elevations to investigate thinning rates for each outlet. Thinning rates from ArcticDEM were calculated from year to year and also from 2011 to 2021 to compare between glaciers as U1 and U0 have very sparse and incomplete 2010 data. This helped us put together patterns of thinning and retreat for each outlet and how this tied into outlets with floating ice tongues.

3.2.4 Numerical Flowline Model

For our final analysis, we used a two-dimensional ice-flow model to help us understand how the presence of floating ice tongues, bed properties, and stress forces relate to ice flow. We chose to examine the two largest outlets, which both experienced changes in ice-tongue presence and had varying trends in acceleration. We ran diagnostic simulations in multiple years for both U1 and U2 to assess the role of the tongue and the other factors in ice flow, including basal drag and sidewall drag. We first established reasonable parameters for basal drag using an inverse model on the

earliest elevation and hydrostatic dataset available for each U1 and U2, and then asked whether those same parameters can reproduce the observed velocities along our 75 km flowlines in later years. Through this comparison, and through a series of experiments altering the basal drag and sidewall drag coefficients, we were able to infer some of the important controls on Upernavik's dynamics.

We ran our model using the open-source, finite-element model Icepack (Shapero and others, 2021). Icepack has a lower barrier to entry than many other open-source ice-flow models while still allowing the user to solve a higher-order approximation to ice flow (Blatter, 1995; Pattyn, 2003). It runs on the finite-element library Firedrake using a language embedded into Python, which abstracts much of the numerics and reduces the input to specifying the weak form of the equation to be solved (Shapero and others, 2021). We used Icepack's hybrid flow solver (i.e. the Blatter-Pattyn higher order equations), which allows for both shear and plug flow modes, characteristic of marine-terminating glaciers (Shapero and others, 2021). The model uses terrain-following coordinates with one vertical layer; despite this low resolution, the model is still able to resolve realistic vertical variations in velocity by using fourth-order Gauss-Legendre trial and test functions in the vertical.

We ran simulations on flowlines for U1 and U2, derived from ITS_LIVE mosaics averaged from 2000 to 2018. We extracted ArcticDEM surface elevations for the years of interest for our model runs and BedMachine Greenland bed topography along the flowline (Morlighem and others, 2021; Porter, Claire, and others, 2022). The ice thickness was calculated by subtracting the bed from the elevation. For years with floatation, we determined where the likely ice bottom was compared to the bedrock by

using a reverse hydrostatic calculation. We used the hydrostatic ice bottom rather than the bed elevation for the thickness calculation whenever the ice bottom was shallower than the bed. This was mostly applicable for U2 in 2013, when the ice tongue was significantly thinner near its collapse.

We sourced temperature data to be incorporated in the model to determine the fluidity rate factor A in Glen's flow law, which is a function of temperature and melt fraction (Shapero and others, 2021). Annual mean surface temperature was obtained from HIRHAM from 1980 to 2014 (Langen and others, 2015). We assumed the reanalysis value at the surface varied linearly to the pressure melting temperature at the bed in order to estimate the basal temperature. We solved for the pressure melting temperature through Equation 2 by Aschwanden (2010):

(2)

$$T_m = T_{tp} + \gamma_p(\rho g H - p_{tp})$$

where triple point temperature and pressure, T_m and p_{tp} were 273.16 K and 611.73 kPa. The Clausius-Clapeyron constant, γ_p, we used for pure ice was $7.42 \bullet 10^{-5}$ K kPa^{-1}. The density of ice, ρ, at Upernavik is 917 kg m^{-3} and H is our calculated ice thickness.

We required a basal boundary condition, an inflow condition, and an outflow condition. At the inflow, we fixed the horizontal velocity to match the surface velocity for all depths. At the outflow, we applied hydrostatic back-pressure on the calving front, which is zero above sea level and linearly increases below it (Shapero and others, 2021). For the basal boundary condition, we inferred the basal drag using a three-dimensional model also implemented in Icepack using the Blatter-Pattyn equations

using standard glaciological inverse methods (e.g. MacAyeal and others, 1993). This inversion covered the entire Upernavik catchment with 300 m horizontal resolution. The model was solved on a single vertical layer with second-order Gauss-Legendre trial and test functions. The surface and bed were extracted from Bedmachine (Morlighem and others, 2021). The inversion sought to minimize the RMS misfit between the modeled velocity and the MEAsUREs multiyear velocity product (Joughin and others, 2018). The optimization was done using the Rapid Optimization Library (Ridzal and others, 2017), a part of the Trilinos library. The inversion used Tikhonov regularization, with strength determined using an L-curve analysis (Calvetti and others, 2000). The inversion results were extracted along our flowlines and included in the model parameters. It was necessary to use this nested model approach (boundary condition for the 2d model extracted from a 3d one) due to limitations in the available data; imperfect coverage of the elevation and velocity products prevented simulating all outlets in all years. The basal drag coefficient (C_{base}) was used in the initialization and following model runs.

Our initialization model runs (2011 for U1 and 2013 for U2) were used to establish a working model for both outlets with our inversion products and measured flowline data. These data alone did not output an accurate velocity, which we attributed to the lack of sidewall drag. These outlets flow through confined fjords, where sidewall drag may be a significant component of the force balance (Gagliardini and others, 2010). To account for this effect, we performed inversions along each flowline to infer the drag needed to reproduce the observed velocities. We conducted the sidewall drag inversion only along our flowlines for the initial model years: 2011 for U1 and 2013 for U2 following Icepack's friction definitions (Shapero and others, 2021). The sidewall drag

inversion used the domain, physics, and boundary conditions described above, but added an additional friction term in Equation 3.

(3)

$$\tau_s = -\frac{m}{m+1} H C_{side} \|u\|^{1/m-1} u$$

where $\boldsymbol{\tau}_s$ is deviatoric stress, *m* is the friction exponent (taken to be 3), C_{side} is the sidewall drag coefficient which is the square of our inversion output, and *u* is the modelled velocity. This term mimics nonlinear Weertman sliding. The inversion procedure sought to optimize C_{side} to minimize the misfit between the modeled and observed velocities. Essentially, our model output for the U1 2011 and U2 2013 runs was our sidewall drag inversion velocity output. The initialization was successful for both outlets.

We solved the model diagnostically and our model output produced an estimate of the surface velocity to compare to the measured velocity data along the flowline for each model run. The following model runs based on the best available data and the most interesting changes are as follows:

- U1 2011: with no evidence of floatation
- U1 2014: with evidence of re-floatation
- U2 2013: with evidence of floating ice tongue
- U2 2015: with no evidence of floatation; retreat
- U2 2018: with evidence of re-floatation; thinning

We also tested the response of the model to a dynamic geometry as the model dimensions adjusted to the retreat of U2 between 2013 and 2015. We explored the

surface velocity sensitivity in each model simulation to varying basal and sidewall drag coefficients as well as retreat, thinning, and bed topography.

3.3 RESULTS

The majority of our data and results were extracted along our outlet flowlines (Figure 3.1) to estimate bed topography and near-terminus bathymetry, elevation, and ice flow. We used ~30 km long flowlines for the three central and long trunks, U1, U2, and U3, and ~15 km for the smaller U0 and U4. The flowlines were generated using stacked ITS_LIVE mosaics from 2000 to 2018 (Gardner and others, 2019). We first present our ice-flow results followed by observations at the glacier termini, our floating ice tongue evidence along with bed topography and thinning, subglacial drainage evidence, and our model results.

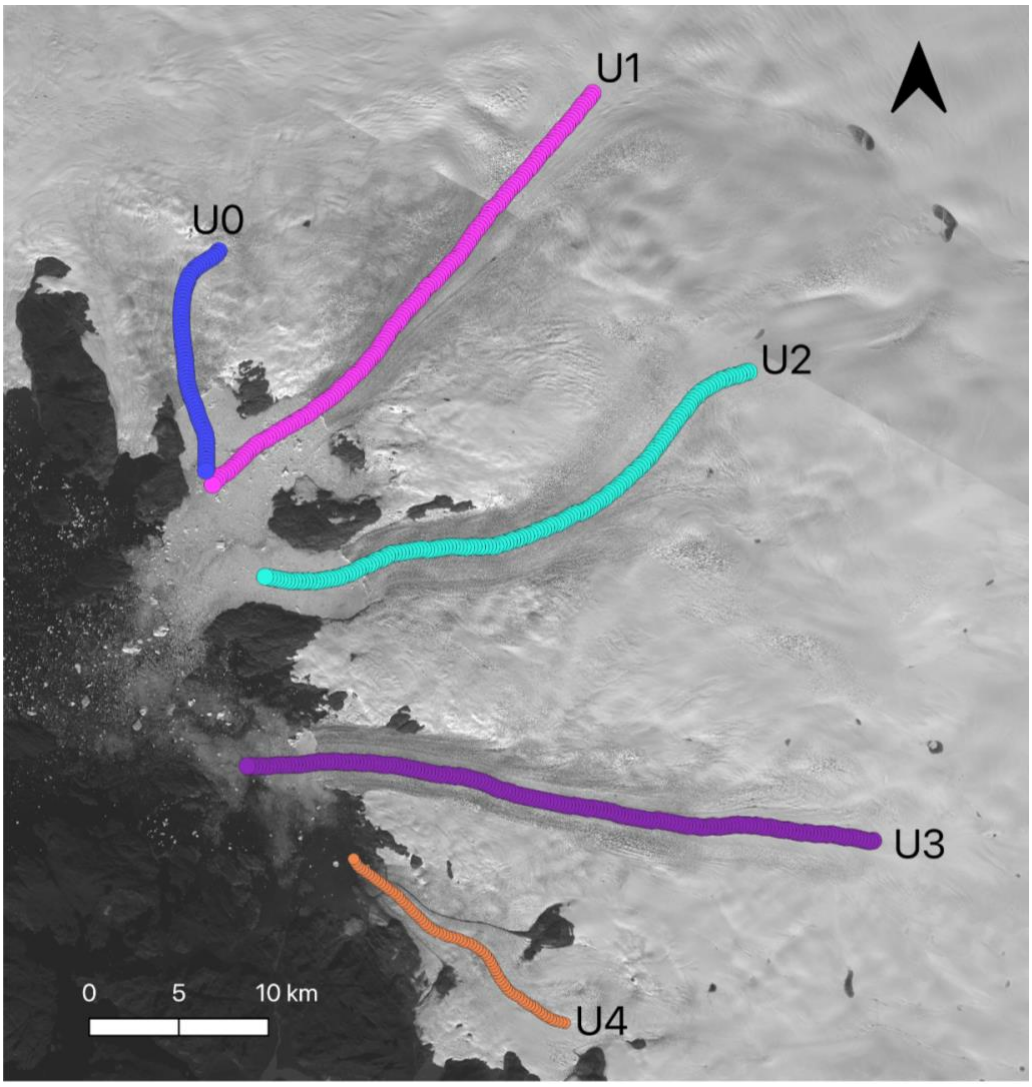

Figure 3.1: Upernavik Outlets and Flowlines. Upernavik outlet flowlines obtained from averaged ITS_LIVE (Gardner and others, 2019) velocities from 2000 to 2018, positioned over top a Landsat 8 image from September 2, 2021, courtesy of the U.S. Geological Survey.

3.3.1 Terminus Position and Retreat

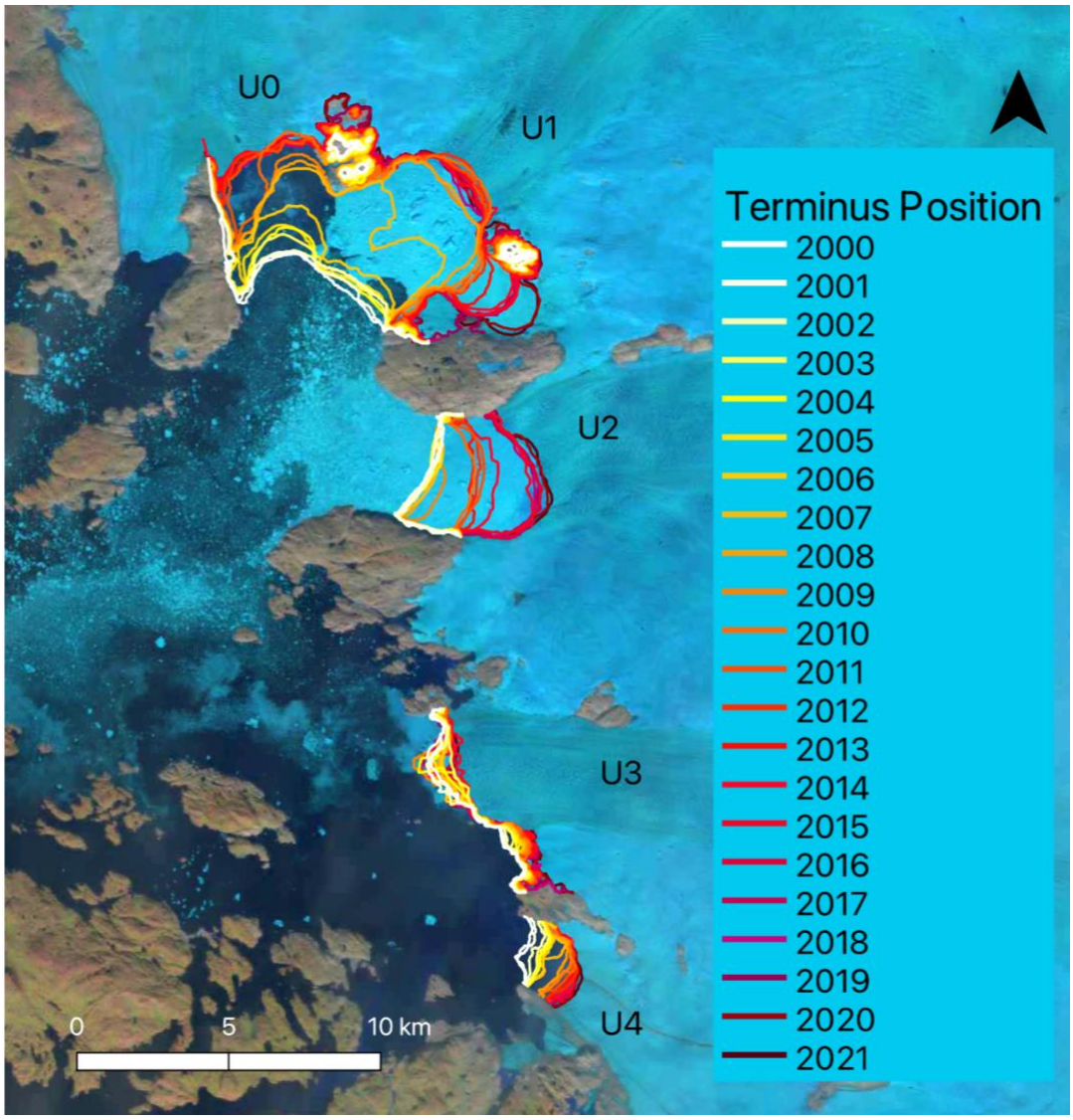

Figure 3.2: Upernavik Terminus Positions. The change in terminus position for Upernavik's outlets from 2000 to 2019 using data from PROMICE (Andersen and others, 2019) and our own 2020 and 2021 polylines over a Landsat 7 image from August 1, 2021, courtesy of the U.S. Geological Survey.

The data showed large terminus retreat for U0, U1, and U2 over 2 km throughout the time period. Figure 3.2 shows the change in ice front positions at each outlet. U0 and U1 shared a terminus until 2007 when they separated into two narrower troughs during the extensive retreat of U1. The retreat at U1 was approximately 5.5 km from

2000 to 2008, with most of the retreat occurring from 2006 to 2008. U1 then reached a relatively stable calving front with fluctuations seen within 1 km up to 2021. U0 retreated by about 2.5 km as it separated during this same period and then retreated an additional 1 km until reaching its stable calving front in 2011. This was a significant amount of retreat for this smaller outlet. U2 experienced its first significant retreat later, retreating 1 km from 2009 to 2010, then remained relatively stable until it retreated by approximately 2 km from 2013 to 2015 before reaching a stable calving line again through 2019. The outlet has been gradually retreating into a wider section of the trough. Both 2020 and 2021 showed further retreat. U4 and U3 experienced less retreat than the northern outlets. U3 experienced the smallest retreat, mostly with its center extension fluctuating in the same 1.5 km throughout the time period, where most calving occurred. The retreat at U4 measured 1.5 km from 2000 to 2008, with most of its fast retreat of 0.7 km measured between 2006 and 2008, similar to U1. From 2000 to 2021, U4 retreated a total of ~2 km, which was significant for its size in comparison to U1 and U2.

3.3.2 Velocities

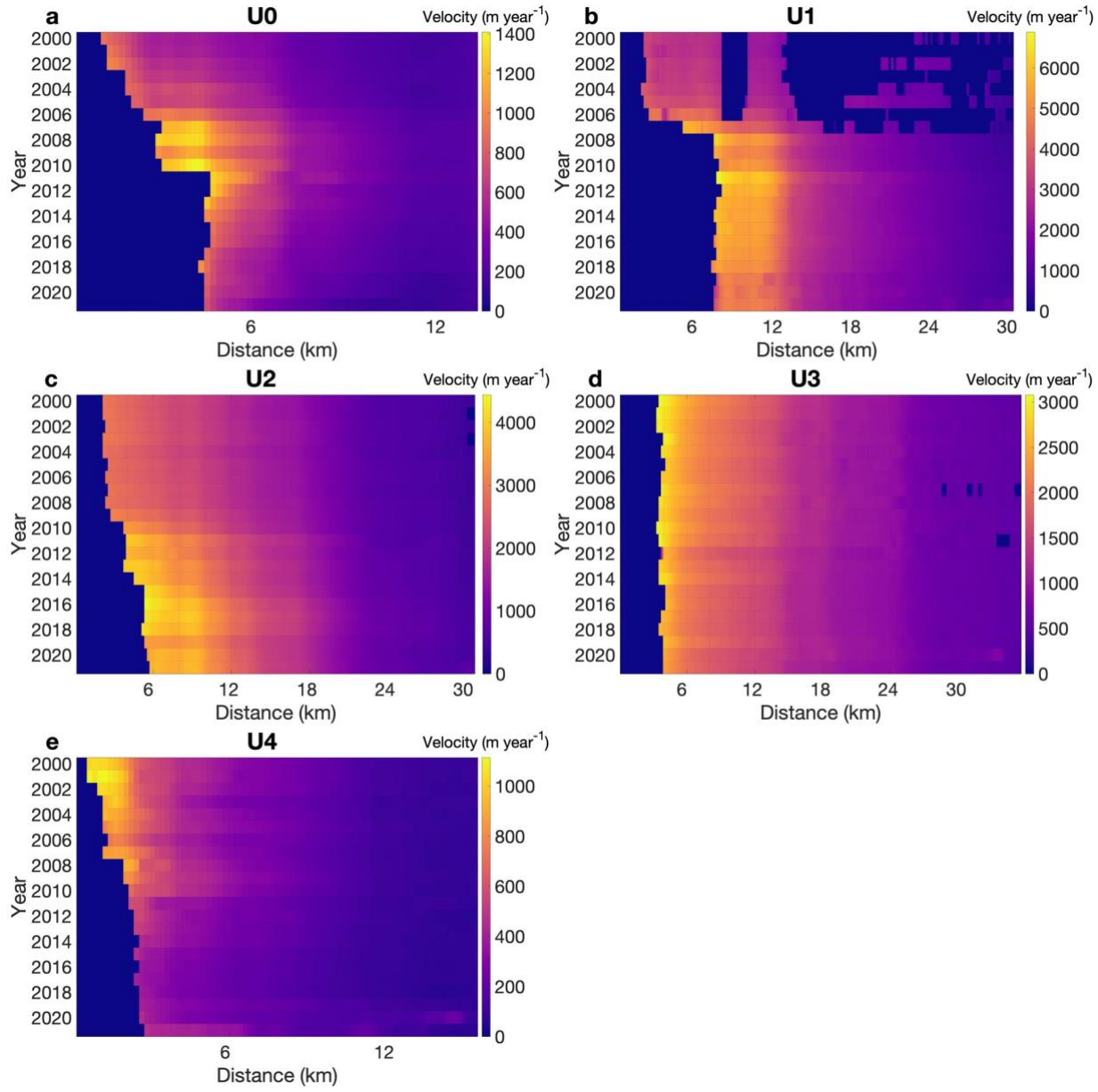

Figure 3.3: Upernavik Flowline Summer Velocities. (a-e) Hovmöller summer velocity diagrams from 2000 to 2021 for U0-U4, respectively. Velocity scales vary between outlets. All velocity data from 2000 to 2018 are from ITS_LIVE velocity mosaics and from 2019 to 2021 the data are from stacked GoLIVE velocity geotiffs (Gardner and others, 2019; Scambos and others, 2016).

We used Hovmöller velocity diagrams (Figure 3.3) to track full flowline velocity changes as well as terminus retreat. Figure 3.3.a shows that following the first period of retreat, the terminus of U0 accelerated between 2007 and 2010. Ice-flow acceleration during this time also propagated upstream in the flowline. U0 retreated immediately after this acceleration and the velocities slowed down. At U1, acceleration started in 2006, just preceding a rapid retreat (Figure 3.3.b). High velocities were maintained throughout the remainder of the record, with slight deceleration following 2010, while the terminus remained in a relatively consistent position. Figure 3.3.c shows three periods of retreat that occurred at U2. Initial retreat occurred between 2008 and 2011 and was immediately followed by acceleration. The second period of retreat from 2013 to 2015 occurred while the glacier was accelerating and was immediately followed by further acceleration through 2018. Deceleration occurred in 2019 at the time of a third period of retreat. Following 2019, ice-flow has been increasing again. The terminus of U3 remained in a relatively consistent position throughout the record, with multi-annual fluctuations. Ice-flow at the terminus was higher in the 2000's than in the 2010's and many short periods of acceleration and deceleration occurred (Figure 3.3.d). The highest acceleration at U4 occurred at the beginning of the record between 2000 and 2001 (Figure 3.3.e). Immediately following this, the glacier decelerated while the terminus steadily retreated. A brief period of advance in 2007 before retreat to 2008 coincides with a short period of acceleration from 2007 to 2008.

Figure 3.4 shows the specific timing and magnitude of significant changes in summer and winter velocities. We selected four points along each glacier flowline for analysis: a point near the terminus (accounting for terminus retreat), and points in the

lower (LM), middle (UM), and upper thirds of the flowline. ITS_LIVE data represent summer velocities and MEaSUREs data represent winter velocities (Joughin and others, 2011; Gardner and others, 2019, Gardner and others, 2022). We included evidence of floatation (discussed in section 3.3.4) in the plots of U1, U2, and U3.

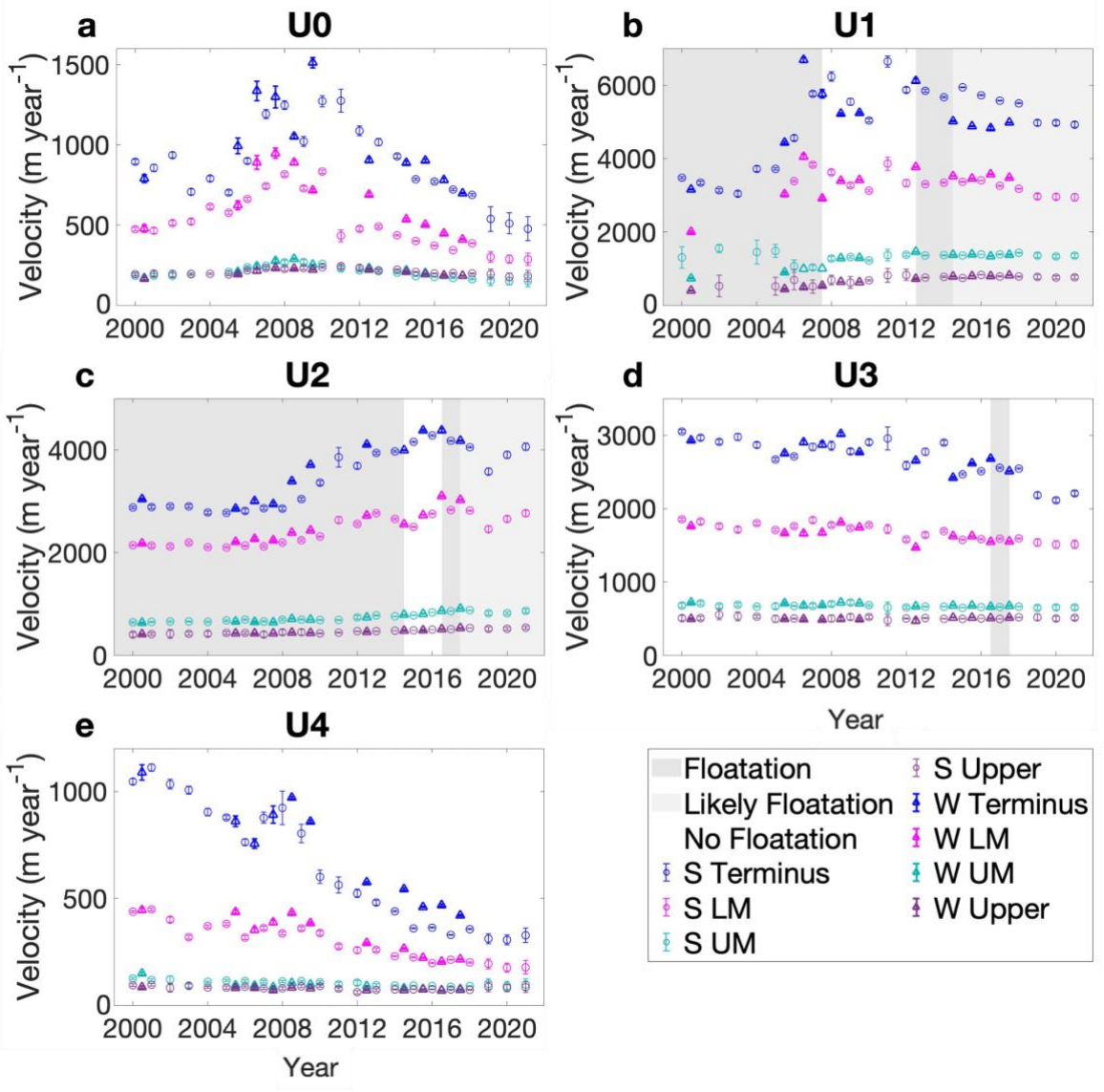

Figure 3.4: Upernavik Seasonal Velocities. (a-e) Seasonal velocity from 2000 to 2021 for U0-U4, with evidence of floatation provided for U1, U2, and U3. The four points along each glacier were selected by identifying the terminus and end flowline point (upper-glacier) and selecting the lower-middle (LM) and upper-middle (UM) points evenly spaced in between. S and W indicate summer velocities derived from ITS_LIVE data and winter velocities derived

from MEaSUREs data (Joughin and others, 2011; Gardner and others, 2019). Concrete evidence for floatation is determined by available hydrostatic data, calving behaviour, and previous studies. Likely floatation is evidenced by elevation profiles. No floatation is evidenced by elevation profiles, calving behaviour, and/or when hydrostatic data shows no floatation.

The terminus and lower reaches of U0 both accelerated after 2005, leading to two distinct terminus summer velocity peaks in 2008 of 1248 m year^{-1} and 2011 of 1276 m year^{-1} (Figure 3.4.a). Following 2011, velocities declined until 2021 to 478 m year^{-1}. U0 experienced seasonal changes from the lower glacier to the terminus such as 2000-01, when winter terminus velocities were lower in 2000-01 by 105 m year^{-1} compared to terminus velocities in the summer of 2000. Once acceleration began after 2005, winter velocities were significantly higher than summer velocities in both the lower glacier and terminus. During acceleration, the winter terminus velocities were higher with a peak to 1337 m year^{-1} in 2006-2007 and 1512 m year^{-1} in 2009-2010. Seasonal variation lessened towards a final summer terminus velocity in 2021 of 478 m year^{-1}.

Though there are less data available for U1 in the early 2000's, terminus velocities declined until 2003, as seen in Figure 3.4.b. The terminus and lower reaches of U1 showed a pattern with two distinct velocity peaks: one in 2008 reaching 6240 m year^{-1} at the terminus, and one in 2011 reaching 6649 m year^{-1}. This pattern was seen to some extent at the middle glacier point, but did not propagate upstream to the upper glacier. From 2013 onwards, there was evidence of deceleration aside from a short summer increase at the terminus in 2015. Seasonal fluctuation patterns towards the terminus of the glacier were evident during specific times. During acceleration between 2003 and 2013, there was a high 2006-07 winter velocity peak of 6689 m year^{-1}, 2124 m year^{-1} higher than the summer terminus velocity in 2006. Since 2013 when the glacier

was likely floating again, winter terminus velocities were significantly lower than the summer terminus velocities, such as 2015-16 when the winter terminus velocity was 1060 m year^{-1} lower than the summer terminus velocity in 2015.

From 2000 to 2008, Figure 3.4.c shows summer terminus velocities at U2 have been relatively steady within 130 m year to year. Acceleration occurred between 2008 and 2011 in the terminus and lower-glacier, leading to a summer terminus velocity peak in 2011 of 3856 m year^{-1}. After a slight decline following 2011 and during the time of the loss of its floating ice tongue, U2 summer terminus velocities continued to increase from 3939 m year^{-1} in 2013 to 4158 m year^{-1} in 2015. The terminus increased past 2015 to a summer velocity peak in 2016 of 4284 m year^{-1}. When U2 was at floatation again in 2017, we measured the start of rapid decline of the lower and terminus glacier velocities to a summer terminus velocity low in 2019 of 3581 m year^{-1}. Since this time, velocities have rapidly increased again, with the last measured summer terminus velocity in 2021 at 4063 m year^{-1}, almost as high as the peak in 2016. Velocities in the upper glacier points have also steadily risen over time. Seasonal differences were not as high as U0 and U1 over the entire record, however, between 2008 and 2011, the winter terminus velocities were up to 671 m year^{-1} higher.

While U3 has been steadily declining in terminus and lower-glacier velocities over the last two decades. There has been a variety of inter-annual fluctuations with 2-to-6-year increases followed by short and sharp 1–2-year decreases (Figure 3.4.d). For example, between 2005 and 2011, summer terminus velocities increased by 286 m year^{-1} while velocities between 2011 and 2012 decreased by 370 m year^{-1}. When floatation was seen at U3 in 2017, velocities were at the peak during an increasing

period before a major decline to 2020 was measured. The summer terminus velocity in 2000 was 3051 m year^{-1} while the summer terminus velocity in 2021 was 2207 m year^{-1}. Seasonal variation was relatively minimal, though winter terminus velocities tended to be higher than summer terminus velocities during increasing periods, opposite of the lower glacier.

Figure 3.4.e shows U4 terminus velocities have significantly slowed down over the record. Summer terminus velocities peaked in 2001 at 1111 m year^{-1} to the lowest velocity measured in 2020 at 306 m year^{-1}. However, the summer terminus velocity reached a peak in 2008 of 923 m year^{-1} from 763 m year^{-1} in 2006. Lower glacier velocities also increased to a peak in 2008. Sharp decline followed, with the summer terminus velocity in 2010 measuring at 601 m year^{-1}. From 2008 onwards, winter velocities at the terminus were higher than summer velocities. The winter terminus velocity in 2008-09 peaked higher than the 2008 summer terminus velocity at 971 m year^{-1}. Between 2014 and 2018, winter terminus velocities were higher by a difference of up to 105 m year^{-1} between 2016 and 2016-17. Upper glacier velocities have remained stable with little seasonal variation.

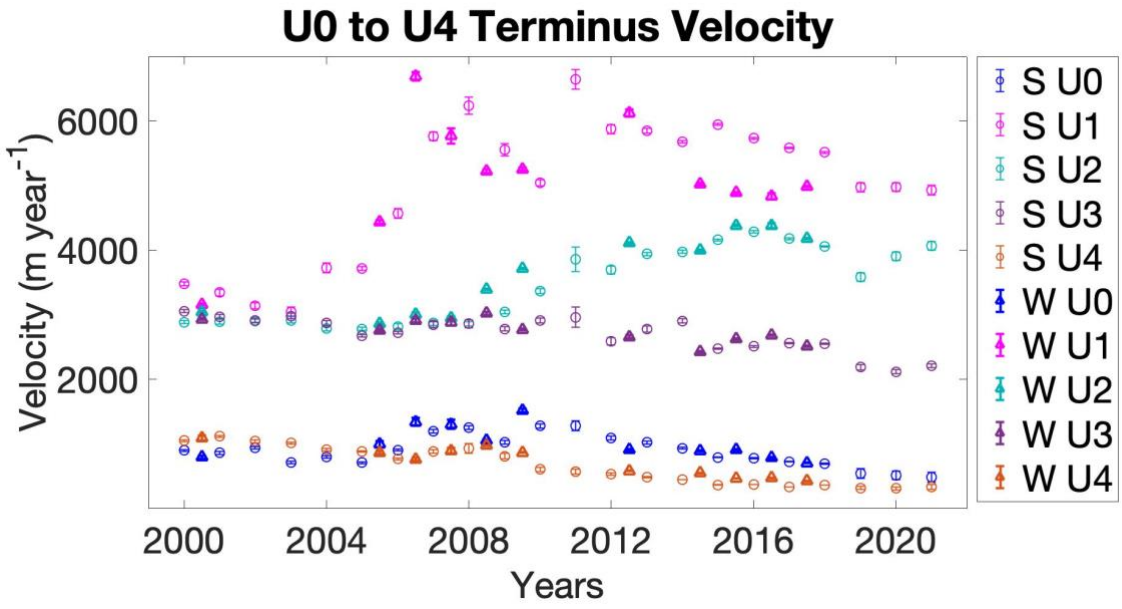

Figure 3.5: Terminus Velocity Comparison at Upernavik. A comparative seasonal terminus velocity plot of U0 to U4 showing ITS_LIVE summer (S) and MEaSUREs winter (W) ice velocities from 2000 to 2021 (Gardner and others, 2019; Joughin and others, 2011).

All five outlets showed important consistencies in terms of periods of acceleration, yet there were distinct periods of diverging behaviour. A comparison of seasonal velocities at the terminus points for each glacier is presented in Figure 3.5. U0 and U1 showed similar velocity patterns in the 2000s, with decreasing trends in the early 2000s followed by acceleration until 2008. There were two distinct summer peaks in velocities in 2008 and 2011 for both outlets. Winter velocity peaks occurred earlier in 2006-07 for U0 and U1, along with a later winter peak in 2009-10 for U0. U0, U1, U2, and U3 all had significantly higher winter velocities in 2006-07 compared to 2006. Velocities at these two outlets continued to decline after 2011. All five outlets had a velocity peak in 2008, though U2 reached this velocity high in 2007 and had a similar high velocity in 2008. U2, U3, and U4 all had higher measured winter velocities over the time period, while U0 and U1 experienced more fluctuating seasonal velocities and

recently much lower winter velocities than summer velocities at U1. U0, U1, and U2 all had summer velocity peaks in 2011, though U2 continued to increase to a peak in 2016, similar to one increasing period for U3 from 2015 to 2017. However, while U2 and U3 matched in terminus velocities in the early 2000's, U3 overall continued to decline after 2008. U2 is the only outlet to continue increasing most of the time through the 2010's. Recently, U2 was also the only outlet to undergo acceleration. While all outlets experienced simultaneous periods of acceleration, the majority of trends varied greatly between outlets.

3.3.3 Calving Behaviour

Significant transitions in calving behaviour from tabular to non-tabular calving were seen for U1 and U2. U1 produced large tabular icebergs, typically from 0.5 to 2.5 km long, until the end of summer in 2007 when Khan and others (2013) and Larsen and others (2016) estimated its floating extension fully broke up. U1 then transitioned to primarily non-tabular calving. U2 also produced large tabular icebergs, around the same length as U1, from 2000 to the end of summer in 2014 (Appendix B: Figure 5.4) and then transitioned to infrequent non-tabular calving. U3 produced tabular icebergs throughout the entire time period from 2000 to 2021, suggesting that it has been near or at floatation for the last two decades (Appendix B: Figure 5.4). U0 and U4 did not produce any tabular icebergs and experienced minimal calving.

3.3.4 Hydrostatic Analysis

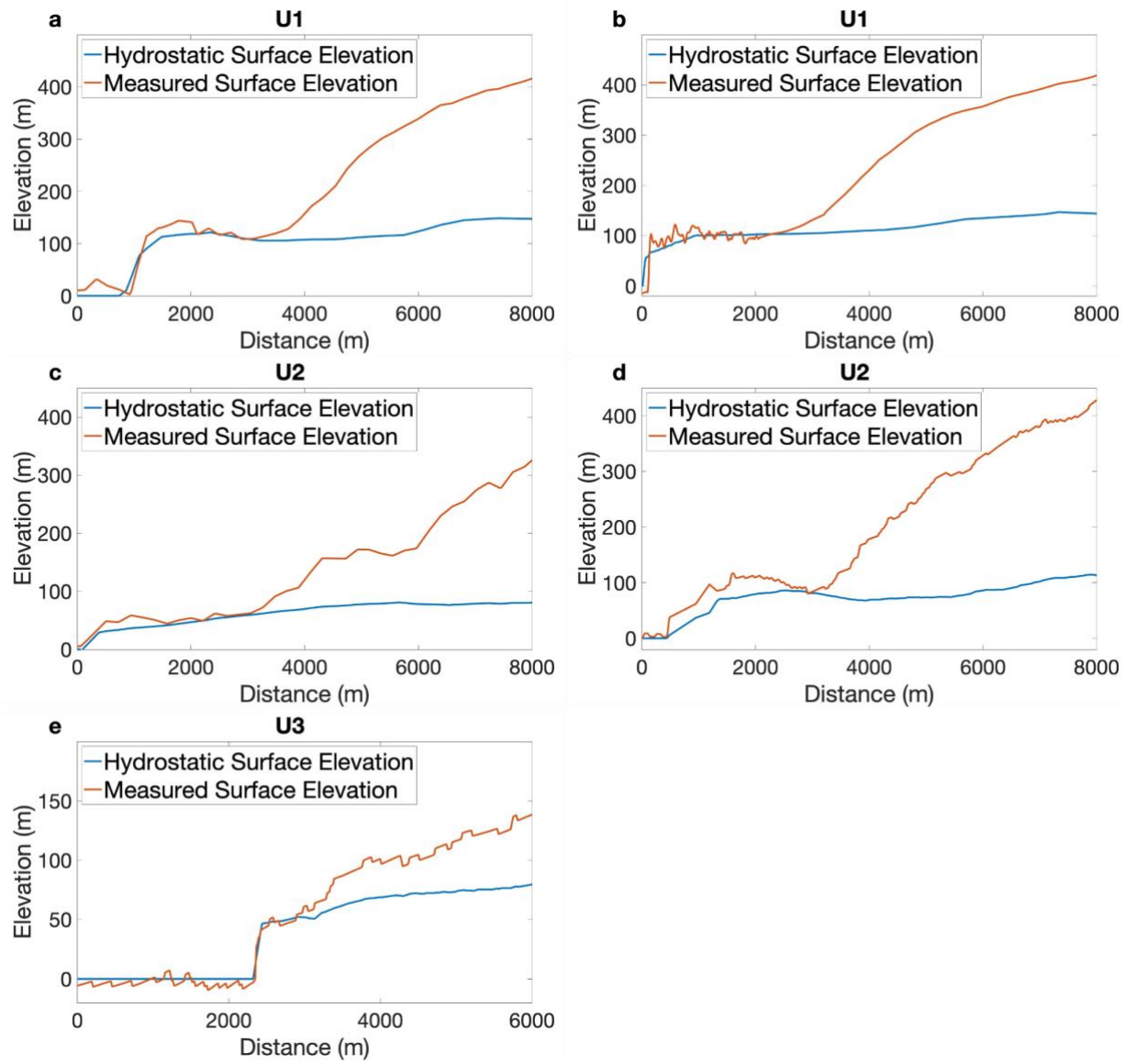

Figure 3.6: Upernavik Hydrostatic Profiles. (a) U1 hydrostatic elevation compared to the actual elevation in 20130418. (b) U1 hydrostatic elevation compared to the actual elevation in 20140426. (c) U2 hydrostatic elevation compared to the actual elevation in 20130418. (d) U2 hydrostatic elevation compared to the actual elevation in 20170410. (e) U3 hydrostatic elevation compared to the actual elevation in 20170410. The hydrostatic elevation, calculated using the hydrostatic equilibrium equation with MCoRDS data (Paden and others, 2010, Paden and others, 2014).

Figure 3.6 displays the five flightlines that showed evidence of floatation along some portion near the terminus, where the hydrostatic surface height calculated based

on ice thickness matches the observed surface height. Though hydrostatic elevation lines in 2010, 2011, and 2012 did not show floatation (Appendix A: Figure 5.3-5.5), U1 reached floatation in our profiles in both 2013 and 2014 (Figure 3.6.a, 3.6.b). There were higher terminus elevations past the slope-break towards the ocean in 2013 compared to the more horizontal slope in 2014, suggesting that the terminus may have been partially floating and partially pinned to the bed. Our hydrostatic results for U2 showed floatation in both 2013 and 2017 (Figure 3.6.c, 3.6.d). In 2013, there was a long floating extension of the terminus below 100 m in elevation that was mostly at hydrostatic elevation or very close. This disappeared by 2017 and the new slope-break is thinned to hydrostatic elevation. U3 was not at the hydrostatic elevation in any profiles (Appendix A: Figure 5.6-5.9) until the last observation in 2017, when the terminus was near or at floatation (Figure 3.6.e). U0 and U4 did not have evidence of floatation in any available year (Appendix A: Figure 5.1, 5.2, 5.10).

3.3.5 Elevation and Bed Topography

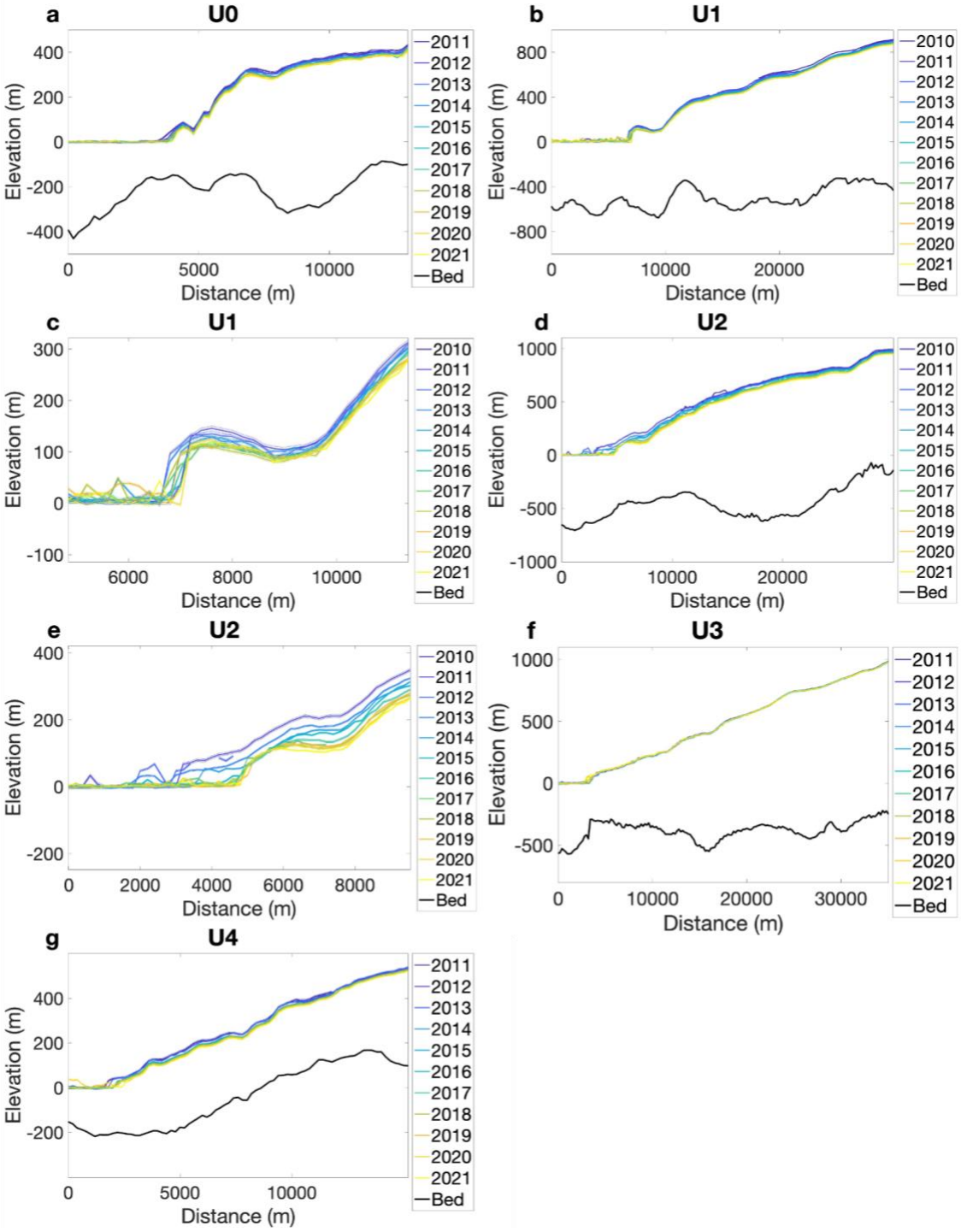

Figure 3.7: Upernavik Bed and Ice Elevation Profiles. (a) U0 bed and ice elevation profile from 2011 to 2021. (b) U1 bed and ice elevation profile from 2010 to 2021. (c) U1 terminus close up of the bed and ice elevation profile from 2010 to 2021. (d) U2 bed and ice elevation

profile from 2010 to 2021. (e) U2 terminus close up of the bed and ice elevation profile from 2010 to 2021. (f) U3 bed and ice elevation profile from 2011 to 2021. (g) U4 bed and ice elevation profile from 2011 to 2021. Data are obtained from BedMachine and ArcticDEM from 2011 to 2021 (Porter, Claire, and others, 2022). Error was calculated for ArcticDEM and upper and lower bounds are included in this plot.

Figure 3.7.a shows a likely pinned terminus of U0 residing in a shallow bed of 150 m, but it is evident that when U0 extended further into the fjord in the 2000's attached to U1, its bed was deeper up to 367 m. Further inland, the bed elevation is deeper again and the entire flowline is below sea level. U0 had a measured thinning rate from 2011 to 2021 of 5.43 m year^{-1}. The maximum thinning along the flowline was 54.27 m at the terminus at 0.4 km of the 9.4 km glacier section used to calculate the loss. Most thinning occurred between 2011 and 2013 in our elevation record.

The U1 entire bed is below sea-level and the bed is relatively deep with most of its bed depth around 500 m (Figure 3.7.b). The current bed depth of the U1 terminus is 576 m, but it has yet to retreat into the deepest part of the flowline upstream, which reaches a bed depth of 676 m. U1's surface elevation sloped downwards steadily towards the coast before reaching a break in slope that is present throughout the record (Figure 3.7.c), and likely indicated the persistent presence of a floating ice tongue, with the exception of the period between 2008 and 2012 when the terminus was likely grounded and pinned. U1 thinned steadily throughout the observational period, with a thinning rate from 2011 to 2021 of 3.03 m year^{-1}. The maximum thinning along the flowline was 46.23 m in the lower-middle glacier at 4.2 km of the 23 km glacier section.

The terminus of U2 has a shallower bed depth of 455 m (Figure 3.7.d). However, in the past, U2 did reside in a deeper bed of up to 645 m. Past this shallow topography further inland, the bed reached depths of 621 m and the entire flowline has bed depths

below sea-level. The glacier also has a steep sloping bed and ice elevation in the upper glacier region. Figure 3.7.e shows the floating section of U2 until it thins and fully disintegrates after 2014. In years since then, the higher elevation terminus than the previous floating ice tongue continued to thin drastically again and we observed it eventually reach a horizontal slope with a well-defined slope-break from 2017 onwards. U2 had a thinning rate from 2011 to 2021 of 5.99 m year^{-1}. The maximum thinning was 103.16 m in the lower glacier at 4.6 km of the 27.2 km glacier section. High thinning occurred between 2013 and 2018.

A steep underwater cliff in the fjord is located in front of the U3 terminus, where the glacier has a bed depth of 302 m (Figure 3.7.f). The entire flowline is below sea-level. The shape of the terminus changed over time but has mostly been gradually sloping. U3 experienced almost no thinning, with accumulation seen in recent years. The maximum thinning was 7.61 m in the lower-glacier at 11.8 km of the 32.2 km glacier section.

The grounded terminus bed depth of U4 is 212 m and only about half of the flowline has a bed below sea level (Figure 3.7.g). A shallow sill was measured in front of the terminus with depths closer to 100 m. This outlet has thin ice thicknesses compared to the northern four outlets but high thinning. U4 had a measured thinning rate from 2011 to 2021 of 2.62 m year^{-1}. The maximum thinning was 44.46 m at the terminus at 0.6 km of the 13.4 km glacier section (including the first upper 3.2 km of missing data).

3.3.6 Evidence of Plume Polynyas

Distinct plumes were visible at the terminus of U0 through U3 in many years between June and August. We were limited by the lack of mélange at the terminus of U4 to identify plume polynyas. U0 through U3 all appear to have sporadic subglacial hydrologic outflow patterns, with no clear patterns in plume-polynya appearance other than clustering around the mid to late 2000's and the mid 2010's.

The most plume polynyas were seen at U0, with a total count of appearances in Landsat imagery of 33 across our entire record, most appearing at the terminus centre. Very few plume polynyas were observed at U1; only four with one in 2002, one in 2014, and two in 2016 (likely the same plume) in the middle to south area of the terminus. 11 plume polynyas were observed across the glacier front for U2 from 2005 to 2016 in clusters (Appendix B: Figure 5.4), one being a large outburst. The second-most spotted plume polynyas were at U3, with 21 observed from 2000 to 2021 but most seen from 2014 to 2021, specifically in the north (Appendix B: Figure 5.4). Ten plume polynyas and muddy water outflows were observed at U4, most occurring in recent years since 2014.

U0 and U2 both experienced large subglacial drainage events, including a shared significant drainage event in the same two-week duration in late June and early July of 2010 (Appendix B: Figure 5.1-5.3). Large outbursts were seen as larger-than-average plume polynyas, often spanning across the terminus (Appendix B: Figure 5.1, 5.2). However, U0 experienced multiple other drainage events spanning from 2009 to 2016. We did not find U0 to have any large supraglacial lakes upstream, only one or two small lakes that may have drained. On the other hand, U2, which has the largest

upstream lakes (~3 km in length) for this ice stream, which drained during the 2010 event (Appendix B: Figure 5.3).

3.3.7 Ice Flow Model

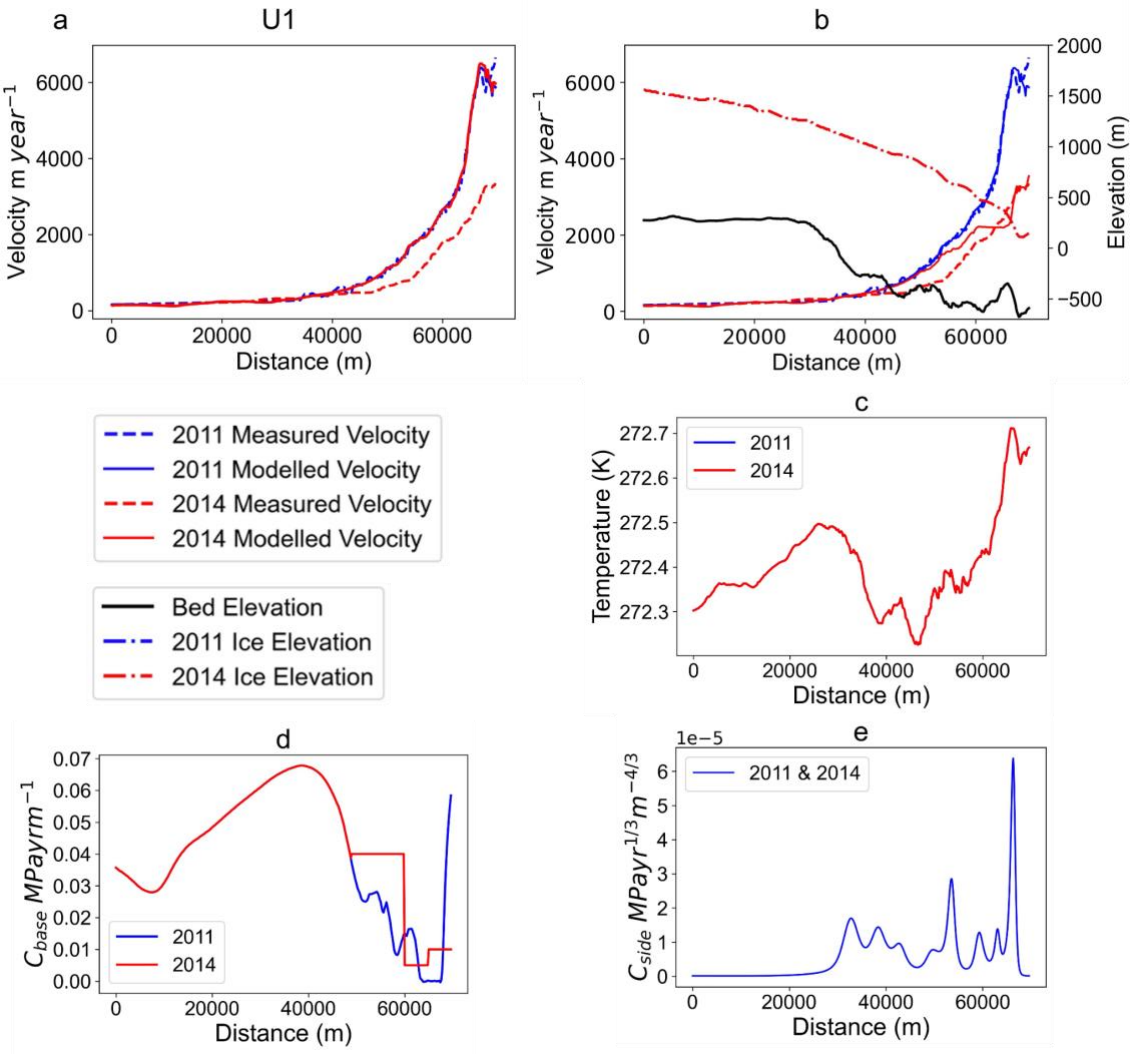

Figure 3.8: U1 model inputs and ice-flow speeds. (a) U1 measured and modelled velocity using the same drag inputs (C_{base}, C_{side}) over time. (b) U1 measured and modelled velocity in 2011 and 2014 using modified basal drag coefficient, along with ice surface elevation and bed depth. (c) U1 basal temperature in 2011 and 2014. (d) U1 basal drag inversion output (C_{base}) in 2011 and manipulated drag in 2014. (e) U1 sidewall drag inversion output (C_{side}) used in both model runs. The flowline at 0 m is the measured upper-glacier and as the flowline approaches 75000 m, this is the terminus section of the glacier.

Using the inferred basal and sidewall drag, modelled velocities closely matched observations at initialization (2011 for U1 and 2013 for U2). U1 velocities in 2011 increased towards the terminus, but slowed at a point near the terminus where the outlet interacts with a shallow ridge in the bed. From the basal drag coefficient result in 2011, low friction was observed over this bed peak and high friction at the terminus. The sidewall drag inversion likely corrected for this at the terminus. Our sidewall drag inversion for U2 in 2013 corrected for zero basal drag near the terminus to output an accurate velocity.

For the following model year at U1, when the measured velocity is lower, we investigated if changes in driving stress alone (based on a new surface elevation), combined with non-changing basal and sidewall drag coefficients, could explain the ice-flow output in 2014. The resulting ice-flow output matched the higher velocity from the initial 2011 model run more than the measured velocity in 2014. Little thinning and retreat occurred over the 3-year span, indicating the driving stress as a result of changing ice thickness cannot explain the lower measured velocity in 2014. It is therefore likely that a change in either sidewall drag, basal slipperiness, or both is responsible for the observed velocity decrease. To address the lack of resistance on the ice-flow in our 2014 run, we first assessed the ice-flow sensitivity to changes in the sidewall drag coefficient (Appendix C: Figure 5.1). The sidewall drag would have to increase significantly over the 3-year timespan, with little thinning and retreat, in order to decrease the output ice-flow velocity. Therefore, we investigated the surface velocity sensitivity to the basal drag coefficient by experimenting with the replacement of slipperiness highs and lows with constant values. The surface velocity responded more

sensitively to changes in slipperiness than sidewall drag, and changes in the basal drag coefficient beneath small areas affected the ice-flow upstream. In 2014, modifying the basal drag coefficient in the lower-glacier and terminus was required to decrease the terminus velocities. This included eliminating zero-friction before the terminus and greatly reducing the terminus friction.

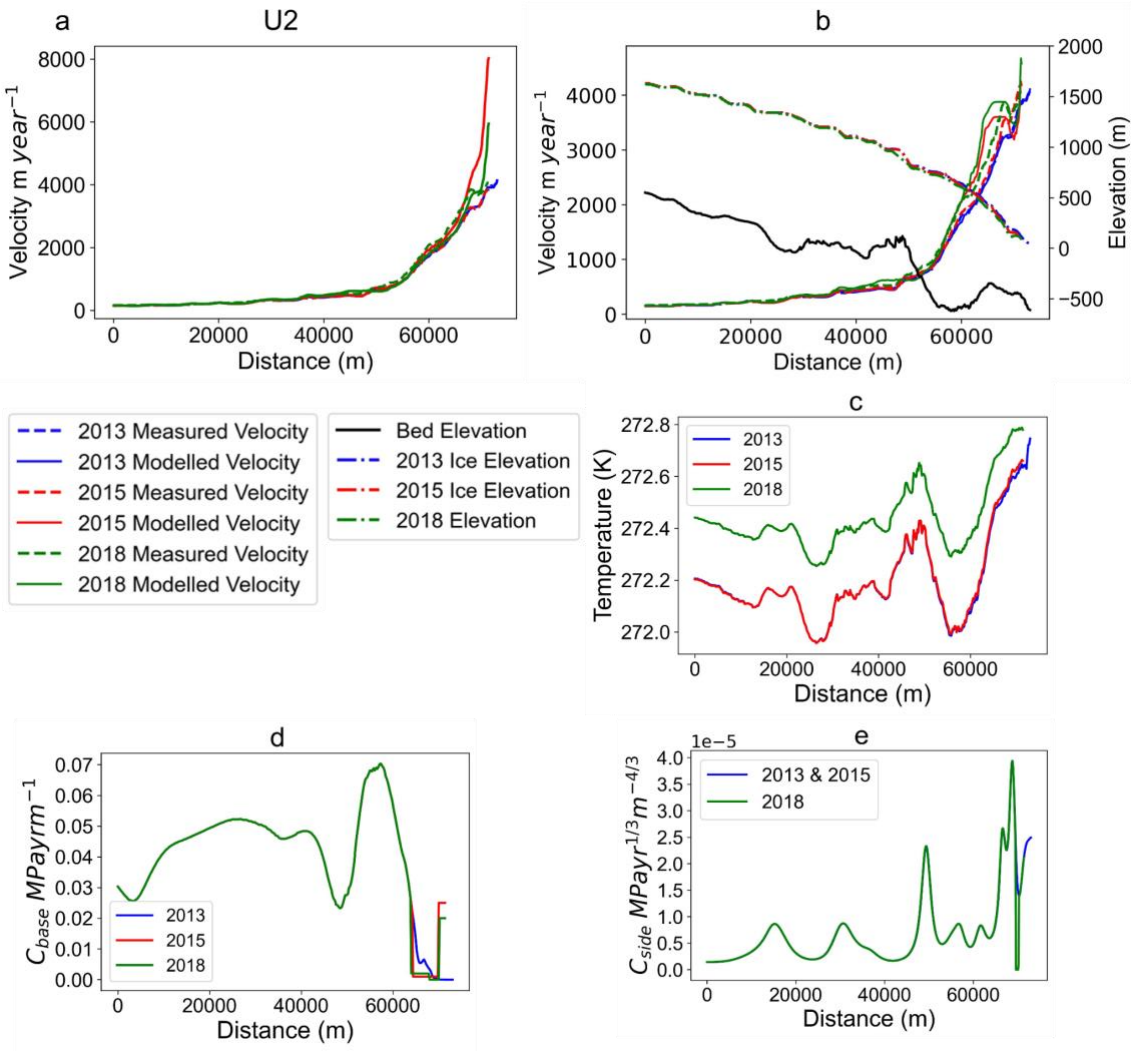

Figure 3.9: U2 model inputs and ice-flow speeds. (a) U2 measured and modelled velocity using the same drag coefficient inputs (C_{base}, C_{side}) over time. (b) U2 measured and modelled velocity in 2013, 2015, and 2018 using modified drag coefficient inputs, along with ice surface elevation and bed depth. (c) U2 basal temperature in 2013, 2015, and 2018. (d) U2 basal drag inversion output (C_{base}) in 2013 and the manipulated drag coefficient in 2015 and 2018. (e) U2 sidewall drag inversion output (C_{side}) in 2013 which was also used in 2015, and the

manipulated drag coefficient in 2018. The flowline at 0 m is the measured upper-glacier and as the flowline approaches 75000 m, this is the terminus section of the glacier.

U2 experienced more complex changes over time than U1, with terminus retreat from the loss of its floating ice tongue between 2013 and 2015, and then high thinning rates between 2015 and 2018. Following model initialization, we examined if the same basal drag coefficient and the 2013 sidewall drag output would yield accurate velocities in 2015 and 2018. Output terminus velocities increased almost 4000 m $year^{-1}$ from observed velocities in 2015 (Figure 3.9.a). In 2018, the ice-flow output was more accurate, with smaller deviations at the ice-front. Reduced driving stress as a result of thinning likely caused some slowdown by 2018, but did not completely explain the terminus velocity. For both 2015 and 2018, we investigated if adjusting the sidewall drag coefficient would give more accurate velocities (Appendix C: Figure 5.2, 5.3). For 2015, similar to U1, the sidewall drag coefficient had to increase by an unrealistic amount at the terminus over the 2-year period with little thinning (Appendix C: Figure 5.2). However, we noticed a weakened sidewall drag coefficient was required near the terminus in 2018 where thinning occurred (Figure 3.9.e). We then manipulated the basal drag coefficient using the same method as U1 and found the basal drag coefficient realistically explained ice-flow in 2015. We also observed the same upstream ice-flow response to basal drag coefficient adjustments as U1. We required higher friction at the terminus, which is more consistent with the basal drag coefficient profile for U1 in 2011. A similar basal drag coefficient profile was also necessary for 2018, but it required a zero-friction area near the terminus and lower basal drag at the terminus. However, similar to what we noticed in the sidewall drag investigation, the basal drag coefficient

alone did not correct the strong downturn in velocity before the terminus and thus, a weakened sidewall drag coefficient to zero was also required.

3.4 DISCUSSION

3.4.1 Floating Ice Tongue Evidence and Methods

Our methods for identifying floating ice tongue presence yielded mostly consistent results, and we had most confidence in floating ice tongue presence when multiple methods coincided. We found U1 to be floating from 2000 to 2007 and from 2013 onwards while U2 was floating from 2000 to 2014 and reached floatation again in 2017. Tabular icebergs appeared when both U1 and U2 were floating, which is consistent with iceberg records by Melton and others (2022) and Amundson and others (2010) when Helheim Glacier and Jakobshavn Isbræ were floating. Both hydrostatic elevation and ice-surface slope supported the tabular iceberg observations, indicating floating ice-tongue presence. When floatation occurred again for U1 and U2, tabular icebergs were not produced, yet hydrostatic elevation, a well defined slope-break, and thinning to a horizontal slope strongly indicated the presence of a floating ice tongue. U3 produced tabular icebergs throughout the record while not floating, including during 2017 when a short-lived floating ice tongue was evidenced by hydrostatic elevation and slope. This may indicate that tabular icebergs alone are not a reliable proxy for floatation.

Floating ice tongues may also have an impact on the channelization of subglacial outflow and the formation of plume polynyas (Melton and others, 2022). While Melton and others (2022) suggested observations of plume polynyas as a proxy for the floating

state of Helheim Glacier, we found contrasting observations at Upernavik. Out of available images, we observed plume polynyas both when there were and were not floating ice tongues for U1 and U2. These contrasting observations may be related to differing degrees of floatation at Helheim and Upernavik, contrasts in ice-tongue length, and/or differences in the strength of subglacial channelization. The variability in our results and contrasts with related literature highlight the importance of using a variety of evidence when investigating the floatation of marine-terminating glaciers, with the hydrostatic elevation and slope being the most reliable methods used in this study. When considering the floatation of glaciers, we suggest that assessing bed topography and bed depth is equally important. Tabular iceberg calving and plume-polynya presence may serve as secondary evidence, as the geometric characteristics of the grounding zone may dictate different types of calving and meltwater channelization.

While our observational results provided new insights into floatation and thinning for Upernavik's outlets, we were limited by available ice thickness data. The rapidly changing thicknesses and floatation conditions at the terminus of U1 and U2 are best constrained by ground-penetrating radar, highlighting the need for regular future collection of radar flightlines.

3.4.2 Causes of Complex Ice-Flow Changes at Upernavik's Outlets

3.4.2.1 Impacts of Floating Ice Tongue Changes on Ice-Flow

Changes in velocity did not correlate with changes in floating ice tongues at U1 and U2, contradicting the hypothesis that the changing floating conditions were responsible for changing ice flow. The loss of resistive buttressing as a result of the

disintegration of floating ice tongues or large calving events has been shown to be a driver of acceleration for many marine-terminating glaciers across Greenland (Joughin and others, 2004; Thomas, 2004; Howat and others, 2005, 2008). Larsen and others (2016) suggested the acceleration of U1 between 2008-09 was the result of the break-up of its floating ice tongue. Instead, we found the disintegration of the U1 and U2 floating ice tongues occurred after a sustained period of acceleration, including leading up to the partial retreat of the U2 floating ice tongue from 2009-10. We also measured deceleration for U1 following the disintegration of its floating ice tongue. This may indicate that the thinning and disintegration of both floating ice tongues was a response to acceleration, rather than its cause.

3.4.2.2 Impacts of Subglacial Hydrology on Ice Flow

The complex and fluctuating nature of Upernavik's ice-flow is likely due to subglacial hydrology. Moon and others (2014) categorized the seasonal velocity fluctuations of Greenland's outlet glaciers into three types depending on their sensitivity to ice-front-position or meltwater from 2009-13, followed by further classification by Vijay and others (2019, 2021). Type 1 glaciers display seasonal speed-up that corresponds with ice-front-position. Type 2 glaciers display patterns of early-summer speed-up and mid-summer slow-down to similar winter velocity speeds, indicating meltwater was lubricating the bed. Type 3 glaciers display late-summer velocity slow-downs lower than winter velocities; these changes were attributed to meltwater forming efficient drainage channels and reducing bed lubrication, increasing basal friction (Moon and others, 2014).

Glacier types at Upernavik varied between 2009 and 2019. U0 was classified by Vijay and others (2019, 2021) as Type 3 from 2015-19. During this time, U0 experienced higher summer velocities that took 13 weeks to slow down after the melt season (Vijay and others, 2021). U1 and U2 displayed continually changing patterns in seasonal speed-up and could not be sorted into one category between 2009 and 2013 by Moon and others (2014). In 2011, U1 and U2 displayed Type 2 behaviour, while in 2013, both glaciers displayed late-summer velocity slow-downs with speeds lower than winter velocities. Further classification by Vijay and others (2019, 2021) showed U1 as Type 2 only in 2017 and U2 as Type 1 from 2015 to 2017, in a study period spanning 2015-19. U3 was categorized as Type 2 from 2009-13 and was later categorized as Type 3 from 2015-19 with the exception of 2018, when it was Type 2 (Moon and others, 2014; Vijay and others, 2019, 2021). While U4 was not included in these studies, Larsen and others classified U4 as Type 3 from 2009 to 2013. Our seasonal velocity observations, extending published records through 2021, suggest that Upernavik's outlets are still Type 2 or 3.

The classifications that link Upernavik's velocity patterns to subglacial drainage are further supported by our model results, which suggest that ice-flow speeds are more sensitive to basal drag than sidewall drag for U1 and U2. Changes in basal drag can result from changes in subglacial water pressure over short timescales (Iken and others, 1981; Kamb, 1987; Paterson, 2000), which is a physically plausible mechanism for the observed velocity fluctuations. While shear-margin strengthening and weakening can also strongly impact ice-flow velocities (Cuffey and Paterson, 2010; Van Der Veen and others, 2011), the pace and direction of observed velocity changes between our model

years at Upernavik are not consistent with this mechanism. Increased basal drag applied over the shallow bed ridge and decreased basal drag while applying the same sidewall drag as 2011 explained the decline in U1's ice-flow from 2011 to 2014, consistent with meltwater classification of this outlet (Moon and others, 2014; Vijay and others, 2021). While U2 was more recently classified as having seasonal speed-up driven by ice-front-position (Vijay and others, 2019, 2021), retreat into shallower bed topography alone did not reasonably explain the flow speeds in 2015. Instead, increased basal drag near the terminus was required to achieve an accurate velocity. For 2018, the same drag as 2015 was too strong where thinning occurred and both a weakened basal and sidewall drag coefficient were required, which can be physically driven by crevassing or rifting in the margins (Cuffey and Paterson, 2010).

Numerical ice flow modelling by Rathmann and others (2017) found 79N glacier's floating ice tongue was unlikely to control its seasonal velocity and the contribution to the near-terminus stress budget was at most 34%. Only upstream basal slipperiness reductions yielded an accurate velocity rather than increased sliding along the sidewall margins, consistent with our results (Rathmann and others, 2017). In addition, the simplified results produced by our flow-line model are consistent with 2d, full-stokes modeling of Upernavik. The Ice-Sheet and Sea-Level System Model used by Downs and Johnson (2022) showed that U1 and U2 were highly sensitive to changes in basal drag from the terminus to 45 km upstream. Rapidly retreating glaciers at Upernavik were not less sensitive to basal drag coefficient reductions than non-rapidly retreating glaciers, and acceleration into the upper glacier rather than localized acceleration was observed as a result of reductions in the basal drag coefficient (Downs and Johnson,

2022). We found the surface velocities throughout the U2 glacier, during its rapid retreat, were sensitive to reductions in the basal drag coefficient. These results were consistent with the ice-flow outputs for U1, a non-rapidly retreating glacier.

We found that seasonal velocity fluctuations, which were on the order of ~100 m $year^{-1}$, were of a much lower magnitude than multi-year velocity fluctuations for all outlets, which were on the order of ~1000 m $year^{-1}$. This difference likely indicates that while surface melting affects seasonal velocity fluctuations, seasonal variability is not large enough to explain fluctuations over multi-year periods. While there is room for considerable future modelling and observational work to constrain the details of the controls on changes in subglacial hydrology and basal slipperiness, our results point to the glacier bed as the most plausible main control on Upernavik's velocity fluctuations.

Our flowline model for U1 and U2 enabled us to add additional understanding to the sensitivity of ice-flow to multiple parameters to establish possible reasons as to why we see such complex behaviour. While a flowline model makes significant simplifications to the complex stress state of a glacier like Upernavik, three-dimensional modelling was prevented by gaps in the input and validation data and was thus out of the scope for this study. Despite its limitations, the flowline model is able to capture some of the key controls on outlet-glacier flow, particularly terminus retreat, thinning, and basal and sidewall drag. Indeed, even these limited simulations give important insight for the subglacial hydrology of the two fastest flowing outlets, U1 and U2, which we hope will be explored in future studies.

3.4.3 Likely Future Changes at Upernavik's Outlets

Acceleration of U1, the fastest flowing outlet, is possible in the future if the glacier retreats past its shallow bed-ridge into the deepest bed of the flowline. Velocities at U2 have recently reached the same speed as U1, along with the beginning of new retreat, which poses the potential for further acceleration of this outlet. Our results indicate U1 and U2 still have floating ice tongues, making them more sensitive to ocean temperature as a result of the larger area in contact with the ocean (Straneo and Heimbach, 2013). Ocean-driven retreat of both glaciers could reach up to 11 km for U1 and 23 km for U2 by 2100 (Morlighem and others, 2019). We recommend further focus on these two outlets, as the depth of the glaciers could continue to be in contact with the warmest water mass in the fjord (Andresen and others, 2014; Muilwijk and others, 2022). Though U0, U3, and U4 glaciers have been decelerating, U3 has the potential to accelerate if it retreats into its long and deep bed. Increased subglacial discharge or thermal forcing could cause this glacier to retreat up to 29 km (Morlighem and others, 2019). There is the potential for continued thinning and retreat of U0 and U4 with increasing atmospheric temperatures as increased subglacial drainage interacting with the terminus can affect its stability (Holland and others, 2008; Rignot and others, 2010, Khan and others, 2013). Further retreat will lead U4 to become land-terminating.

3.5 CONCLUSION

Our results suggest that the observed complex velocity changes at Upernavik's largest outlets are likely to be primarily controlled by changes in basal slipperiness caused by evolving subglacial hydrologic conditions, rather than changes in floating ice tongue conditions. We therefore rejected our initial hypothesis regarding floating ice

tongues. The extended record of ice-tongue changes developed in this study show that ice-tongue changes are not coincident in time with large fluctuations observed in ice-flow speeds, suggesting that other physical mechanisms must be primary controls. This conclusion is supported by modelling work on the ice-flow response of the two largest outlets with the highest measured acceleration, U1 and U2, to changes in basal drag, sidewall drag, terminus retreat, and thinning. The sensitivity of the modelled ice flow to basal slipperiness was the most spatially consistent with the measured velocities of both outlets. This is consistent with recent ice-flow sensitivity modelling of Upernavik as well as other marine-terminating glaciers in Greenland with floating ice tongues (Rathmann and others, 2017; Downs and Johnson, 2022). Additionally, velocity observations on both seasonal and interannual timescales for all outlets indicated a fluctuating response characteristic of glaciers sensitive to meltwater availability at the bed (Moon and others, 2014).

While the flowline model used in this study, developed from Icepack's hybrid flow model (Shapero and others, 2021), is a highly simplified representation of glacier flow, it successfully captured essential dynamics to help us understand the forcings controlling Upernavik's velocities. We represented Upernavik's complex dynamics using the Icepack hybrid model with parameterizations for sidewall drag and basal slipperiness, and used it to determine the sensitivity to these parameters as ice-thickness and ice-front position changed over time. The consistency with other modeling literature demonstrates the utility of these simple model representations in understanding major controls on marine-terminating glacier dynamics.

Our results also illustrate the utility of multi-proxy records, including tabular iceberg calving, plume-polynya appearance, calculations of hydrostatic elevation, observations of slope break at the grounding line, and a horizontally sloped floating terminus, for identifying floating ice-tongue presence. When evaluating the terminus floatation of U1, U2, and U3, hydrostatic elevation and slope proved to be the most reliable and consistent methods compared to tabular icebergs and plume polynyas. During this investigation, we found evidence that U1 and U2, after losing their ice tongues in 2007 and 2014, both reached floatation again in 2013 and 2017 and were still floating in 2021 while U2 was recently accelerating.

We recommend further focus on both U1 and U2, the only two glaciers of the Upernavik Isstrøm in contact with Atlantic Water, if the ocean thermal forcing increases. The ice-flow results of all outlets also highlight the importance of further understanding the basal meltwater availability of the Upernavik Isstrøm, especially with increasing surface temperatures. Our findings show the complex nature of ice dynamics at Greenland's marine-terminating glaciers and the need for further work surrounding subglacial hydrology.

ACKNOWLEDGEMENTS

This work was supported by funding from NSERC grants CERC-2018-00002 and RGPIN-2021-02910.

References

Amundson, J. M., Fahnestock, M., Truffer, M., Brown, J., Lüthi, M. P., & Motyka, R. J. (2010). Ice mélange dynamics and implications for terminus stability, Jakobshavn Isbræ, Greenland. *Journal of Geophysical Research: Earth Surface*, *115*(F1).

Andersen, J. K., Fausto, R. S., Hansen, K., Box, J. E., Andersen, S. B., Ahlstrøm, A. P., ... & Vandecrux, B. (2019). Update of annual calving front lines for 47 marine terminating outlet glaciers in Greenland (1999–2018). *GEUS Bulletin*, *43*.

Andresen, C. S., Kjeldsen, K. K., Harden, B., Nørgaard-Pedersen, N., & Kjær, K. H. (2014). Outlet glacier dynamics and bathymetry at Upernavik Isstrøm and Upernavik Isfjord, north-west Greenland. *GEUS Bulletin*, *31*, 79-82.

Bentley, M. J., Smith, J. A., Jamieson, S. S., Lindeman, M., Rea, B. R., Humbert, A., ... & Roberts, D. H. (2022). Direct measurement of warm Atlantic Intermediate Water close to the grounding line of Nioghalvfjerdsfjorden (79N) Glacier, North-east Greenland. *The Cryosphere Discussions*, 1-25.

Bindschadler, R., Choi, H., Wichlacz, A., Bingham, R., Bohlander, J., Brunt, K., ... & Young, N. (2011). Getting around Antarctica: new high-resolution mappings of the grounded and freely-floating boundaries of the Antarctic ice sheet created for the International Polar Year. *The Cryosphere*, *5*(3), 569-588.

Blatter, H. (1995). Velocity and stress fields in grounded glaciers: a simple algorithm for including deviatoric stress gradients. *Journal of Glaciology*, *41*(138), 333-344.

Calvetti, D., Morigi, S., Reichel, L., & Sgallari, F. (2000). Tikhonov regularization and the L-curve for large discrete ill-posed problems. Journal of Computational and

Applied Mathematics, 123(1–2), 423–446. https://doi.org/10.1016/S0377-0427(00)00414-3

Chauché, N., Hubbard, A., Gascard, J. C., Box, J. E., Bates, R., Koppes, M., ... & Patton, H. (2014). Ice–ocean interaction and calving front morphology at two west Greenland tidewater outlet glaciers. *The Cryosphere*, *8*(4), 1457-1468.

Cuffey, K. M., & Paterson, W. S. B. (2010). *The physics of glaciers*. Academic Press.

Downs, J., & Johnson, J. V. (2022). A rapidly retreating, marine-terminating glacier's modeled response to perturbations in basal traction. *Journal of Glaciology*, 1-10.

Enderlin, E. M., Howat, I. M., & Vieli, A. (2013). High sensitivity of tidewater outlet glacier dynamics to shape. *The Cryosphere*, *7*(3), 1007-1015.

Fried, M. J., Catania, G. A., Bartholomaus, T. C., Duncan, D., Davis, M., Stearns, L. A., ... & Sutherland, D. (2015). Distributed subglacial discharge drives significant submarine melt at a Greenland tidewater glacier. *Geophysical Research Letters*, *42*(21), 9328-9336.

Gagliardini, O., Durand, G., Zwinger, T., Hindmarsh, R. C. A., & Le Meur, E. (2010). Coupling of ice-shelf melting and buttressing is a key process in ice-sheets dynamics. *Geophysical Research Letters*, *37*(14).

Gardner, A. S., M. A. Fahnestock, and T. A. Scambos, 2019 [update to time of data download]: ITS_LIVE Regional Glacier and Ice Sheet Surface Velocities. Data archived at National Snow and Ice Data Center; doi:10.5067/6II6VW8LLWJ7.

Holland, D. M., Thomas, R. H., De Young, B., Ribergaard, M. H., & Lyberth, B. (2008). Acceleration of Jakobshavn Isbræ triggered by warm subsurface ocean waters. *Nature geoscience*, *1*(10), 659-664.

Howat, I. M., Joughin, I., Tulaczyk, S., & Gogineni, S. (2005). Rapid retreat and acceleration of Helheim Glacier, east Greenland. *Geophysical Research Letters*, *32*(22).

Howat, I. M., Joughin, I., Fahnestock, M., Smith, B. E., & Scambos, T. A. (2008). Synchronous retreat and acceleration of southeast Greenland outlet glaciers 2000–06: ice dynamics and coupling to climate. *Journal of Glaciology*, *54*(187), 646-660.

Iken, A. (1981). The effect of the subglacial water pressure on the sliding velocity of a glacier in an idealized numerical model. *Journal of Glaciology*, *27*(97), 407-421.

Joughin, I., Tulaczyk, S., MacAYEAL, D. R., & Engelhardt, H. (2004). Melting and freezing beneath the Ross ice streams, Antarctica. *Journal of Glaciology*, *50*(168), 96-108.

Joughin, Ian, Sarah B. Das, Matt A. King, Ben E. Smith, Ian M. Howat, and Twila Moon. "Seasonal speedup along the western flank of the Greenland Ice Sheet." *Science* 320, no. 5877 (2008): 781-783.

Joughin, I., Smith, B. E., Howat, I. M., Scambos, T., & Moon, T. (2010). Greenland flow variability from ice-sheet-wide velocity mapping. *Journal of Glaciology*, *56*(197), 415-430.

Joughin, I., Smith, B. E., Howat, I. M., Floricioiu, D., Alley, R. B., Truffer, M., & Fahnestock, M. (2012). Seasonal to decadal scale variations in the surface velocity of Jakobshavn Isbrae, Greenland: Observation and model-based analysis. *Journal of Geophysical Research: Earth Surface*, *117*(F2).

Joughin, I. A. N., Smith, B. E., & Howat, I. M. (2018). A complete map of Greenland ice velocity derived from satellite data collected over 20 years. *Journal of Glaciology*, *64*(243), 1-11.

Joughin, I., I. Howat, B. Smith, and T. Scambos. 2011, updated 2019. *MEaSUREs Greenland Ice Velocity: Selected Glacier Site Velocity Maps from InSAR, Version 1.* [Indicate subset used]. Boulder, Colorado USA. NASA National Snow and Ice Data Center Distributed Active Archive Center. https://doi.org/10.5067/MEASURES/CRYOSPHERE/nsidc-0481.001.

Kamb, B. (1987). Glacier surge mechanism based on linked cavity configuration of the basal water conduit system. *Journal of Geophysical Research: Solid Earth*, *92*(B9), 9083-9100.

Kehrl, L. M., Joughin, I., Shean, D. E., Floricioiu, D., & Krieger, L. (2017). Seasonal and interannual variabilities in terminus position, glacier velocity, and surface elevation at Helheim and Kangerlussuaq Glaciers from 2008 to 2016. *Journal of Geophysical Research: Earth Surface*, *122*(9), 1635-1652.

Khan, S. A., Kjaer, K. H., Korsgaard, N. J., Wahr, J., Joughin, I. R., Timm, L. H., ... & Babonis, G. (2013). Recurring dynamically induced thinning during 1985 to 2010 on Upernavik Isstrøm, West Greenland. *Journal of Geophysical Research: Earth Surface*, *118*(1), 111-121.

Langen, P. L., Mottram, R. H., Christensen, J. H., Boberg, F., Rodehacke, C. B., Stendel, M., ... & Cappelen, J. (2015). Quantifying energy and mass fluxes controlling Godthåbsfjord freshwater input in a 5-km simulation (1991–2012). *Journal of Climate*, *28*(9), 3694-3713.

Larsen, S. H., Khan, S. A., Ahlstrøm, A. P., Hvidberg, C. S., Willis, M. J., & Andersen, S. B. (2016). Increased mass loss and asynchronous behavior of marine-terminating outlet glaciers at Upernavik Isstrøm, NW Greenland. *Journal of Geophysical Research: Earth Surface*, *121*(2), 241-256.

Li, T., Dawson, G. J., Chuter, S. J., & Bamber, J. L. (2022). A high-resolution Antarctic grounding zone product from ICESat-2 laser altimetry. *Earth System Science Data*, *14*(2), 535-557.

MacAyeal, D. R. (1993). A tutorial on the use of control methods in ice-sheet modeling. *Journal of Glaciology*, *39*(131), 91-98.

Melton, S. M., Alley, R. B., Anandakrishnan, S., Parizek, B. R., Shahin, M. G., Stearns, L. A., ... & Finnegan, D. C. (2022). Meltwater drainage and iceberg calving observed in high-spatiotemporal resolution at Helheim Glacier, Greenland. *Journal of Glaciology*, 1-17.

Moon, T., Joughin, I., Smith, B., & Howat, I. (2012). 21st-century evolution of Greenland outlet glacier velocities. *Science*, *336*(6081), 576-578.

Moon, T., Joughin, I., Smith, B., Van Den Broeke, M. R., Van De Berg, W. J., Noël, B., & Usher, M. (2014). Distinct patterns of seasonal Greenland glacier velocity. *Geophysical research letters*, *41*(20), 7209-7216.

Moon, T., Joughin, I., & Smith, B. (2015). Seasonal to multiyear variability of glacier surface velocity, terminus position, and sea ice/ice mélange in northwest Greenland. *Journal of Geophysical Research: Earth Surface*, *120*(5), 818-833.

Morlighem, M. et al. 2021, updated 2021. *IceBridge BedMachine Greenland, Version 4*. [Indicate subset used]. Boulder, Colorado USA. NASA National Snow and Ice

Data Center Distributed Active Archive Center. doi: https://doi.org/10.5067/VLJ5YXKCNGXO.

Mouginot, J., Rignot, E., Bjørk, A. A., Van den Broeke, M., Millan, R., Morlighem, M., ... & Wood, M. (2019). Forty-six years of Greenland Ice Sheet mass balance from 1972 to 2018. *Proceedings of the national academy of sciences*, *116*(19), 9239-9244.

Muilwijk, M., Straneo, F., Slater, D. A., Smedsrud, L. H., Holte, J., Wood, M., ... & Harden, B. (2022). Export of Ice Sheet Meltwater from Upernavik Fjord, West Greenland. *Journal of Physical Oceanography*, *52*(3), 363-382.

Nick, F. M., Vieli, A., Howat, I. M., & Joughin, I. (2009). Large-scale changes in Greenland outlet glacier dynamics triggered at the terminus. *Nature Geoscience*, *2*(2), 110-114.

Nick, F. M., Van der Veen, C. J., Vieli, A., & Benn, D. I. (2010). A physically based calving model applied to marine outlet glaciers and implications for the glacier dynamics. *Journal of Glaciology*, *56*(199), 781-794.

Paden, J., J. Li, C. Leuschen, F. Rodriguez-Morales, and R. Hale. 2010, updated 2019. *IceBridge MCoRDS L2 Ice Thickness, Version 1*. [Indicate subset used]. Boulder, Colorado USA. NASA National Snow and Ice Data Center Distributed Active Archive Center. doi: https://doi.org/10.5067/GDQ0CUCVTE2Q.

Paden, J., J. Li, C. Leuschen, F. Rodriguez-Morales, and R. Hale. 2014, updated 2019. *IceBridge MCoRDS L1B Geolocated Radar Echo Strength Profiles, Version 2*. [Indicate subset used]. Boulder, Colorado USA. NASA National Snow and Ice

Data Center Distributed Active Archive Center. doi: https://doi.org/10.5067/90S1XZRBAX5N.

Paterson, W. S. B. (2000). *Physics of glaciers*. Butterworth-Heinemann.

Pattyn, F. (2003). A new three-dimensional higher-order thermomechanical ice sheet model: Basic sensitivity, ice stream development, and ice flow across subglacial lakes. *Journal of Geophysical Research: Solid Earth*, *108*(B8).

Pfeffer, W. T. (2007). A simple mechanism for irreversible tidewater glacier retreat. *Journal of Geophysical Research: Earth Surface*, *112*(F3).

Porter, Claire, et al., 2022, *"ArcticDEM – Strips, Version 4.1",* https://doi.org/10.7910/DVN/C98DVS, Harvard Dataverse, V1, 2022.

Porter, Claire, et al., 2018, *"ArcticDEM, Version 3",* https://doi.org/10.7910/DVN/OHHUKH, Harvard Dataverse, V1, 2018.

Rathmann, N. M., Hvidberg, C. S., Solgaard, A. M., Grinsted, A., Gudmundsson, G. H., Langen, P. L., ... & Kusk, A. (2017). Highly temporally resolved response to seasonal surface melt of the Zachariae and 79N outlet glaciers in northeast Greenland. *Geophysical Research Letters*, *44*(19), 9805-9814.

Rignot, E., Koppes, M., & Velicogna, I. (2010). Rapid submarine melting of the calving faces of West Greenland glaciers. *Nature Geoscience*, *3*(3), 187-191.

Ridzal, D., Kouri, D. P., and von Winckel, G. J. (2017). Rapid Optimization Library., Sandia National Lab.(SNL-NM), Albuquerque, NM (United States). https://www.osti.gov/servlets/purl/1481491

Scambos, T., M. Fahnestock, T. Moon, A. Gardner, and M. Klinger. 2016. *Global Land Ice Velocity Extraction from Landsat 8 (GoLIVE), Version 1*. [Indicate subset

used]. Boulder, Colorado USA. NSIDC: National Snow and Ice Data Center. doi: https://doi.org/10.7265/N5ZP442B.

Shapero, D. R., Badgeley, J. A., Hoffman, A. O., & Joughin, I. R. (2021). icepack: A new glacier flow modeling package in Python, version 1.0. *Geoscientific Model Development*, *14*(7), 4593-4616.

Straneo, F., & Heimbach, P. (2013). North Atlantic warming and the retreat of Greenland's outlet glaciers. *Nature*, *504*(7478), 36-43.

Straneo, F., & Cenedese, C. (2015). The dynamics of Greenland's glacial fjords and their role in climate. *Annual review of marine science*, *7*, 89-112.

Thomas, R. H. (2004). Force-perturbation analysis of recent thinning and acceleration of Jakobshavn Isbræ, Greenland. *Journal of Glaciology*, *50*(168), 57-66.

Van Der Veen, C. J., Plummer, J. C., & Stearns, L. A. (2011). Controls on the recent speed-up of Jakobshavn Isbræ, West Greenland. *Journal of Glaciology*, *57*(204), 770-782.

Vermassen, F., Andreasen, N., Wangner, D. J., Thibault, N., Seidenkrantz, M. S., Jackson, R., ... & Andresen, C. S. (2019). A reconstruction of warm-water inflow to Upernavik Isstrøm since 1925 CE and its relation to glacier retreat. *Climate of the Past*, *15*(3), 1171-1186.

Vieli, A., & Nick, F. M. (2011). Understanding and modelling rapid dynamic changes of tidewater outlet glaciers: issues and implications. *Surveys in geophysics*, *32*(4), 437-458.

Vijay, S., Khan, S. A., Kusk, A., Solgaard, A. M., Moon, T., & Bjørk, A. A. (2019). Resolving seasonal ice velocity of 45 Greenlandic glaciers with very high temporal details. *Geophysical Research Letters*, *46*(3), 1485-1495.

Vijay, S., King, M. D., Howat, I. M., Solgaard, A. M., Khan, S. A., & Noël, B. (2021). Greenland ice-sheet wide glacier classification based on two distinct seasonal ice velocity behaviors. *Journal of Glaciology*, *67*(266), 1241-1248.

Wild, C. T., Alley, K. E., Muto, A., Truffer, M., Scambos, T. A., & Pettit, E. C. (2022). Weakening of the pinning point buttressing Thwaites Glacier, West Antarctica. *The Cryosphere*, *16*(2), 397-417.

Wood, M., Rignot, E., Fenty, I., An, L., Bjørk, A., van den Broeke, M., ... & Zhang, H. (2021). Ocean forcing drives glacier retreat in Greenland. *Science advances*, *7*(1), eaba7282.

Zwally, H. J., Abdalati, W., Herring, T., Larson, K., Saba, J., & Steffen, K. (2002). Surface melt-induced acceleration of Greenland ice-sheet flow. *Science*, *297*(5579), 218-222.

CHAPTER 4.0: SUMMARY AND CONCLUSIONS

4.1 Summary of Changes at Upernavik's Five Outlets from 2000-2021

4.1.1 U0

U0 is Upernavik's smallest and most northerly outlet. It has a current stable terminus position and terminus bed depth of 150 m, where it is likely pinned. It was in a deep bed of up to 367 m when it was connected to U1's floating ice tongue between 2000 and 2007. The glacier is likely no longer in contact with Atlantic Water (between 250 m and 450 m in depth) due to thinning and retreat (Andresen and others, 2014; Muilwijk and others, 2022). Velocities declined in the early 2000's.

When retreat occurred as a result of the breakup of U1's ice tongue and the two glaciers separated in 2007, the glacier retreated into a wider but shallower fjord. Terminus acceleration was seen from 2005 to 2011 as the glacier was retreating, with two velocity peaks in 2008 of 1248 m $year^{-1}$ and 2011 of 1276 m $year^{-1}$. Winter terminus velocities peaked higher, to 1512 m $year^{-1}$ in 2009-10. Lower-middle glacier acceleration in U0 was also high as the velocities were almost as high as terminus velocities between 2006 and 2007. Since 2011, deceleration has been seen with a 2021 summer terminus velocity of 478 m $year^{-1}$.

We frequently observed plume polynyas at this outlet, with most occurring from 2008 onwards, including multiple large drainage events. The glacier likely developed an efficient drainage system that in turn allows for higher basal friction, impacting the interannual velocity (Vijay and others, 2019, 2021). A thinning rate of 5.43 m $year^{-1}$ between 2011 and 2021 was significant for its size when compared to the thinning

measurements of the larger glacier U2. The maximum thinning along the flowline was 54.27 m at the terminus, higher than the maximum measured at U1.

4.1.2 U1

U1 is the second most northerly outlet and one of the largest trunks of the Upernavik Isstrøm, with a currently stable terminus position and a terminus bed depth of 576 m. It had a floating ice tongue until 2007 and the depth of the fjord below the ice tongue calving front was 516 m. The bed has been deep enough over our record for the glacier to interact with warm Atlantic Water (Andresen and others, 2014; Muilwijk and others, 2022).

Like U0, terminus velocities declined until 2003 with a velocity of 3042 m $year^{-1}$, then rapidly increased to a velocity peak in 2008 of 6240 m $year^{-1}$. The ice tongue disintegrated quickly after 2007, as evidenced by the observed switch from tabular to non-tabular calving. The glacier experienced a large retreat into a wider and deeper fjord, with depths up to 652 m along the flowline, before stabilizing its terminus position in a narrower trough. The glacier terminus velocities declined after 2008 to a low of 5043 m $year^{-1}$ in 2010 but then peaked again at its high in 2011 of 6648 m $year^{-1}$, after major retreat. Sustained acceleration was observed leading up to the floating ice tongue collapse.

Velocities slowly declined at the beginning in 2013 until 2021 with lower winter velocities, with a slight summer peak in 2015 of 5945 m $year^{-1}$. Strong summer peaks indicate basal lubrication from increased meltwater (Moon and others, 2014; Vijay and others, 2019, 2021). In our numerical ice-flow model, the glacier was sensitive to changes in the basal drag coefficient, and basal drag changes can explain the

decreased velocities between 2011 and 2014 in our model. U1 ice flow was more likely driven by subglacial hydrology than changes in its floatation. U1's terminus thinned steadily before reaching floatation again in 2013, and a floating ice tongue has likely been maintained through 2021. The thinning of 3.03 m $year^{-1}$ between 2011 and 2021 was not as high as U2. The maximum thinning along the flowline was 46.23 m in the lower-middle glacier. The terminus velocity in 2021 was measured to be 4928 m $year^{-1}$.

4.1.3 U2

U2 is the central outlet of Upernavik and, like U1, is situated in a deep bed with a current terminus bed depth of 455 m. U2 had a long floating ice tongue in the early 2000's, with a deeper bed of up to 645 m, based on its large tabular iceberg calving and previous elevation analysis by Larsen and others (2016). Throughout the entire study period, while U2 retreated into a shallower bed, all bed-depths were deep enough to be in contact with Atlantic Water (Andresen and others, 2014; Muilwijk and others, 2022).

This outlet underwent two large periods of retreat followed by ice-flow acceleration, both when its floating ice tongue partially or fully disintegrated, and new retreat observed in 2021. U2 did not lose its floating ice tongue as U1 did during a period of higher ocean temperatures around 2007, though it partially disintegrated at this time. The shift from stable velocities to rapid acceleration was seen in 2008, with velocities at 2855 m $year^{-1}$ until reaching a velocity peak in 2011 of 3856 m $year^{-1}$. A short decline followed in 2012 with a velocity of 3689 m $year^{-1}$ before acceleration continued from from 2013 to 2016 with a velocity peak in 2016 of 4284 of m $year^{-1}$. The outlet continued producing tabular icebergs until 2014 and was at hydrostatic elevation in 2013. Our calving and elevation evidence suggest that U2 lost its floating ice tongue

after 2014. Sustained acceleration occurred for several years before the break up of its ice tongue in 2014, indicating this outlet's velocities were not driven by its changing floating ice tongue. The glacier retreated into a shallower and slightly wider fjord following 2014 before the new terminus thinned to hydrostatic elevation again in 2017. Rapid deceleration occurred from 2017 to 2019, with a terminus velocity of 3581 m year^{-1}, followed by acceleration until 2021 with a terminus velocity of 4063 m year^{-1}. Surface slope suggests that the new floating ice tongue continues to be present all the way through 2021.

Plume polynyas were spotted through to 2008 and also from 2010 to 2011 (including a large supraglacial lake drainage event) and in 2014 and 2016. Seasonal variation was not as extreme as U0 or U1, but higher winter velocities were observed from 2009 to 2013. Our modelled ice-flow sensitivity to basal slipperiness is consistent with ice-flow speed driven by meltwater availability at the bed (Moon and others, 2014). The retreat in our model of U2 between 2013 and 2015 did not explain the change in velocity, which contrasts with categorization by Vijay and others (2019, 2021) that seasonal velocities at this outlet were driven by terminus position rather than meltwater. U2 thinned the most out of all other outlets, with a thinning rate of 5.99 m year^{-1} from 2011 to 2021 and a maximum thinning of 103.16 m in the lower glacier near the terminus. U2 is clearly still accelerating at the conclusion of the study period.

4.1.4 U3

U3 sits on a shallow shoal in the southern region of the Upernavik Fjord. It has a current terminus bed depth of 302 m, which has been mostly constant throughout the time period as the terminus position has remained relatively stable. The glacier front sits

above the depths of Atlantic Water observed in the fjord (Andresen and others, 2014; Muilwijk and others, 2022). The shallow bed topography likely pins the terminus in place.

U3 experienced deceleration throughout the entire time period. The terminus velocity peak in 2000 at 3051 m year^{-1}, while the terminus velocity in 2021 was 2207 m year^{-1}. Its thin ice at the terminus and long, low slope is likely what allows large tabular icebergs to form from 2000 to 2021, which often get caught on the bed topography, although other proxies do not suggest floating ice-tongue presence. There was a general cycle in ice flow, with 2-6 year increases followed by 1-2 year decreases throughout the record. Increases occurred from 2005 to 2011, 2012 to 2014, and 2015 to 2018. For example, the terminus velocity increased to 2671 m year^{-1} in 2005, to 2957 m year^{-1} in 2011, and then declined to 2586 m year^{-1} in 2012. A short terminus section of U3 reached hydrostatic elevation in 2017 but this was likely a result of the shallow bed as the elevation profile did not suggest a fully floating ice tongue.

Subglacial drainage was fairly prominent at this glacier, with plume-polynyas spotted over the entire time period but most occurring after 2014. The slightly higher to similar winter velocities as summer velocities that were observed over the record. This is likely characteristic of a glacier with meltwater lubricating the bed, where an early-summer velocity increase is followed by a mid-summer decline and averages the summer velocities closer to or lower than the winter velocities (Moon and others, 2014). This is consistent with what was observed and classified by Moon and others (2014) and Vijay and others (2019, 2021) for this outlet. U3 experienced almost no thinning

over time and has advanced in recent years. Its shallow bed topography likely plays a role in its terminus position and deceleration.

4.1.5 U4

U4 is the small southern outlet that resides in the shallowest bed at Upernavik, which is currently grounded at a depth of 212 m. In the fjord near the terminus of U4 there is a shallow sill with a depth of ~130 m measured in our flowline. The shallow bed and sill allows no Atlantic Water contact at the ice front (Andresen and others, 2014; Muilwijk and others, 2022).

The glacier retreated approximately 2 km over the study period. U4 had the lowest measured velocities out of all other outlets and declined over the entire time period, with the exception of two peaks. U4 had its highest terminus velocities in 2001 of 1111 m $year^{-1}$, before observed retreat, and a second velocity peak in 2008 of 923 m $year^{-1}$ with acceleration starting in 2006.

A few plume polynyas were observed at the terminus, mostly after 2014. Higher winter velocities were seen at U4 from 2008 onwards. This strong seasonality compared to the other outlets indicates an efficient drainage system that outputs meltwater over the summer, reducing meltwater lubrication at the bed and increasing basal friction so that summer velocities decline well below winter velocities (Moon and others, 2014; Larsen and others, 2016). The terminus velocity in 2021 along the flowline was measured to be 327 m $year^{-1}$, the lowest out of all outlets. The thinning rates of U4 were comparable to U1 and U2. This may be due to terminus destabilization from the efficient meltwater channelization (Holland and others, 2008; Rignot and others, 2010, Khan and others, 2013). U4 had a measured thinning rate of 2.62 m $year^{-1}$ from 2011 to 2021 and

a maximum thinning of 44.46 m near the terminus. The asynchronous results of all outlets is summarized in Figure 4.1.

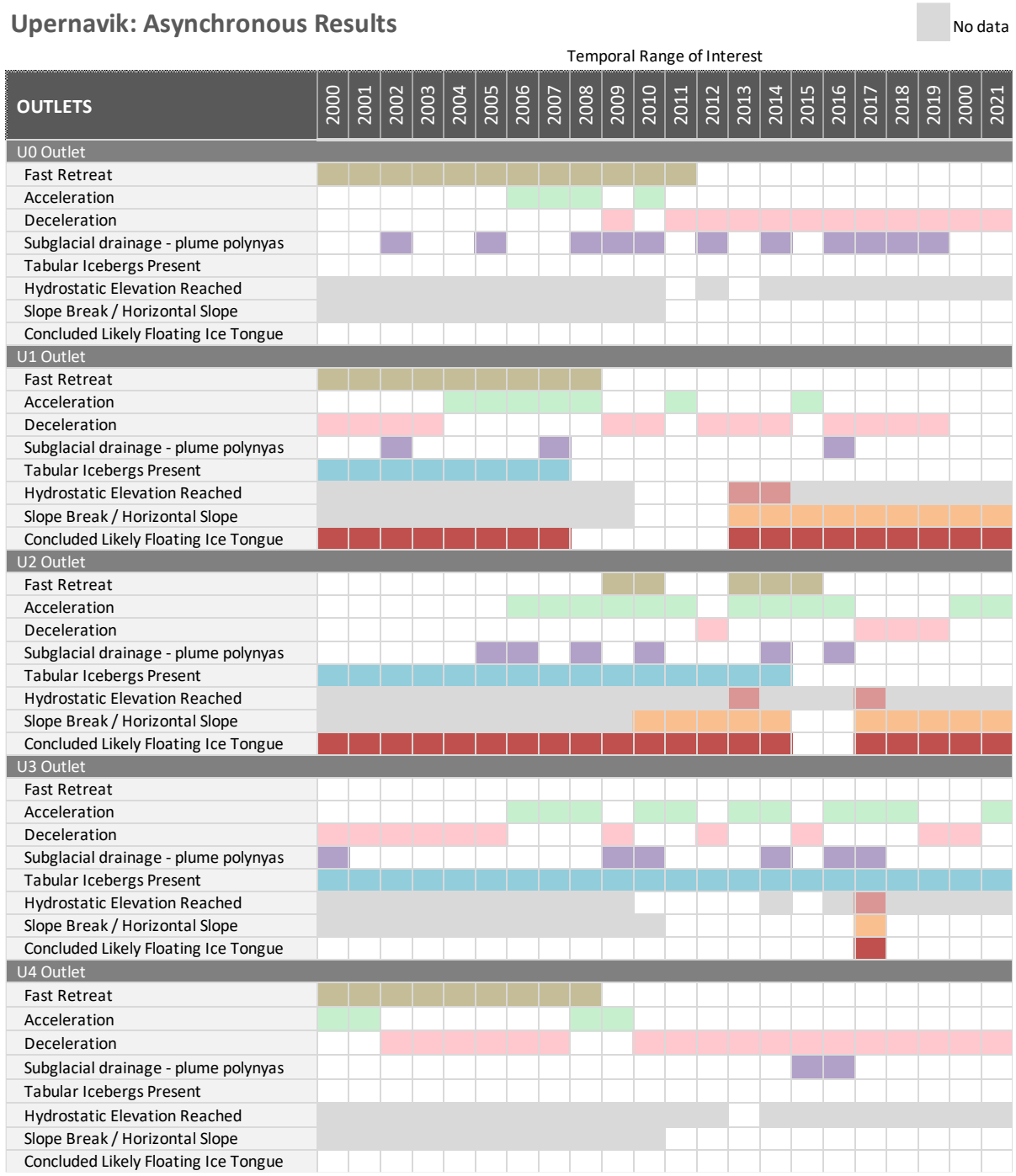

Figure 4.1: Asynchronous Results of Upernavik. A visual representation of the varying patterns of behaviour for each outlet, regarding retreat, velocities, floating ice tongues, and subglacial drainage. Floating ice tongue presence was determined by plume polynyas, tabular icebergs, hydrostatic elevation, and slope.

4.1.6 Contrasting and Comparable Behaviours Between Outlets

Many contrasting and complex dynamics were observed at Upernavik. Calving was mostly seen from the three main trunks of Upernavik (U1, U2, and U3). The northern outlets (U0, U1, and U2) retreated the most, with U4 also retreating a significant amount despite its southern location and shallow bed. The currently stable termini of U0, U1, and U3 (compared to the faster retreat of U2 and U4) are located in both shallow and deep beds. U1 and U2 are the only outlets likely currently in contact with Atlantic Water (Andresen and others, 2014; Muilwijk and others, 2022). All outlets accelerated during warmer atmosphere and ocean temperatures in the 2000's. U1 and U2, the outlets with the highest terminus velocities, continued accelerating into the 2010's, with U2 being the only outlet accelerating presently. U1 and U2 were the only two outlets with clear evidence of floating ice tongues and likely have new floating ice tongues at present. U0, U3, and U4 had the most observations of plume polynyas at the terminus. These three outlets have been decelerating over time, mostly since 2008. While the deeper outlets (U1 and U2) were hypothesized to be more sensitive to ocean forcing than the shallower outlets (U0, U3, and U4), multiple factors involving the asynchronous behaviour are likely responsible other than bed depth. Subglacial hydrology likely drives seasonal and interannual velocity patterns at Upernavik's outlets. These results are consistent with newer ice-flow modelling of Upernavik's sensitivity to subaqueous melting and basal slipperiness (Downs and Johnson, 2022) as well as basal slipperiness modelling at other marine-terminating glaciers (Rathmann and others, 2017).

4.2 Error Analysis and Limitations

4.2.1 Available Data and Data Quality

Observations of plume polynya and tabular iceberg appearances were limited by the availability of cloudless Landsat imagery. In addition, a Scan Line Corrector failure on Landsat 7 after May 31st, 2003, greatly lowered the quality of available images. Ultimately, we were able to collect ~75 usable images for Landsat 7 and ~50 for Landsat 8. Clusters of images in specific years enabled us to see changes in drainage events, but this was not available for every year. Shadows at the jagged terminus of U3 and the lack of ice melange at U3 and U4 made plume polynya detection more difficult. Clouds also greatly reduced the Landsat coverage around the time of U1's floating ice tongue disintegration in 2007, but we were able to constrain the changes with images in 2006 and 2008.

We did not have along-flow IceBridge flightines available for every year for each outlet. Between the available flightlines, some of the automated radar processing did not always work, mainly because the L2 MCoRDS radar was unable to determine ice thicknesses near the terminus when L1B echograms were unavailable (Paden and others, 2010, 2014). In some cases, our own echogram picks by manually selecting the strongest reflector representing the ice bottom enabled us to fill in this data, but in some years the ice base could not be confidently determined, including during 2011 when successful data collection could have illuminated important changes on U2. We had to rely on our additional methods for identifying floating ice during this time period. For U0, four flow-parallel IceBridge flightlines were available in 2010, 2011, and 2013. We obtained hydrostatic results for U0 in 2011 and 2013, as the ice base in the 2010

echogram could not be clearly identified. U1 had seven IceBridge flightlines available across 2010, 2011, 2012, 2013, 2014, and 2015. We obtained hydrostatic results for each year except 2015 and the additional flightline in 2011. U2 had three IceBridge flightlines available in 2011, 2013, and 2017. The 2011 echogram was unclear and this flightline only covered a small area on the southern portion of the outlet's terminus. There were six flightlines available for U3 in 2010, 2011, 2012, 2013, 2015, and 2017, and we were able to conduct the hydrostatic analysis for each of these years. U4 only had one IceBridge flightline available, in 2013. We stress the importance of using ice thickness data to identify likely floating ice tongues on rapidly accelerating glaciers, highlighting the need for clear and readily available thickness data in Greenland. While other methods can be used as evidence for floatation, the hydrostatic analysis proved the most reliable.

We assessed error in the ArcticDEM strip products by measuring the variation in rock outcrop elevations compared to the averaged ArcticDEM mosaic for Greenland (Porter, Claire, and others, 2019, 2022). Errors were generally well below the observed thinning signals. Our elevation analysis mainly focussed on the terminus of each outlet, all of which were constrained by rock outcrops. However, the upper glacier elevations may have a higher error, and this may prove problematic for analysis of other marine-terminating glaciers in Greenland. We incorporated this error in our plots and also only used data that fell within two standard deviations of the average elevation across all years. Some years had more coverage than others for Upernavik and we lacked data in 2010. The recent addition of 2019, 2020, and 2021 strip data greatly improved our analysis

For our velocity data, ITS_LIVE Greenland velocity mosaics have not yet been released for 2019, 2020, and 2021 (Gardner and others, 2019). Instead, we created mosaics from GoLIVE image pairs to fill in these years in our plots and Hovmöller diagrams. We also had to manually input coordinates for each glacier point and extract ITS_LIVE point data (Gardner and others, 2022). We used the standard deviation of the pixel stacks as an estimate for error in these mosaics and point measurements. Because ITS_LIVE and GoLIVE use a similar methodology for deriving ice-flow velocity, and because the methods have been shown to yield accurate results (Gardner and others, 2019), we do not believe the absence of ITS_LIVE mosaics during the last three years of the record has any impact on our final results.

4.2.2 Comparison Methods and Software Limitations

The flowlines that underpin most of our velocity analysis were produced using averaged ITS_LIVE data from the available mosaics from 2000-2018. Mosaics were not yet available for 2019-2021 at the time of analysis, and many of the mosaics from the Landsat-7 era (2000-2013) had sparse measurements. These flowlines are therefore reasonably representative of our time period. Regardless of the flowlines chosen, they provide a consistent framework for comparing velocity changes at each outlet throughout the record. . For U0, we had to combine two flowlines as the glacier separated from U1 early on and this affected the available velocity mosaics. The averaged data from 2000 to 2018 would not account for its original connection to U1 due to the retreat and separation of these two outlets. We generated the first flowline for U0 using the 2000 to 2018 mosaics and then added on its flowline extension into the fjord using stacked and averaged data from 2000 to 2003. Though approximately

flowlines follow the line of maximum ice-flow speed, which tends to be along the centre of the glacier, this is not exact and we acknowledge that our surface flowline velocities do not capture all dimensions of glacier change. Bed topography likely varies laterally, and it is possible we do not capture the deepest parts of the bed. Ideally, we would use three-dimensional models of every outlet. However, flowline data allowed for successful comparison between outlets in this study, and we were able to build off multiple studies that did more in-depth analysis of individual outlets.

We faced many challenges while incorporating the flowline model into this study. We determined which years to model based on interesting events as well as available ArcticDEM and ITS_LIVE data. As there were always data gaps along our model flowlines, we had to interpolate short sections of data. We tested the use of Icepack to be able to model a complex ice stream and if it could reasonably handle the fast ice-flow with our input data (Shapero and others, 2021). Though our model was heavily simplified to two dimensions over a few years, we were able to run the model during interesting years for two important outlets, which allowed for detailed comparison when evaluating subglacial hydrology. We confirmed that Icepack is a very useful model for a complex case and the results coincided with extensive modelling of Upernavik by Downs and Johnson (2022). More modelling is needed at Upernavik to further understand its ice flow, especially with the recent acceleration and retreat of U2, but we are confident that by having this model available in our results, we can provide a detailed enough direction for future studies to investigate subglacial hydrology.

4.3 Future Recommendations and Considerations

A detailed evaluation of the proxies used for floating ice tongues in this study proved the reliability and usefulness of hydrostatic elevation and ice-surface slope. These proxies conclude contrasting results for tabular icebergs, which were observed when Helheim Glacier was floating (Amundson and others, 2010; Melton and others, 2022). We observed tabular icebergs both when U1, U2, and U3 were floating and when they were not; similarly, plume polynyas, a proxy used by Melton and others (2022), were also observed during times when hydrostatic elevation indicated floatation, and times where it did not. As floatation is complex and can vary based on bed and fjord geometry, we recommend using a variety of evidence to investigate the floatation of a marine-terminating glacier terminus, with focus on the most reliable proxies: hydrostatic elevation and ice-surface slope. We suggest tabular icebergs and plume polynyas are not reliable proxies on their own. This also highlights the need for continued ice thickness data in the Upernavik area as well as other marine-terminating glaciers in Greenland. With newly released data, future work can monitor the recent floating ice tongues observed at U1 and U2.

We rejected our initial hypothesis that the complex and fluctuating ice flow was due to changes in floating ice tongues. Our results suggest subglacial hydrology the likely cause of the complex nature of Upernavik's ice flow, highlighting the need for future modelling and analysis. Subglacial hydrology will likely continue to play an important role in controlling the changing seasonal and interannual velocity nature of Upernavik's outlets. With two floating ice tongues still present at U1 and U2, future studies should continue to monitor ocean warming. While subglacial hydrology is the

primary control on acceleration at U1 and U2 based on our modelled ice-flow sensitivity, the response of these glaciers to increased ocean thermal forcing should not be ignored as the loss of resistive back-stress from the loss of floating ice tongues and large calving events from the disintegration of floating ice tongues can still contribute to the acceleration (Nick and others, 2009; Vieli and Nick, 2011). With increasing atmosphere and ocean temperatures as a consequence of anthropogenic climate change, we recommend monitoring these two glaciers as well as other glaciers across Greenland that fit similar patterns. Understanding and quantifying mass loss from the Greenland Ice Sheet and sea-level rise from marine-terminating glaciers is becoming increasingly important.

References

Amundson, J. M., Fahnestock, M., Truffer, M., Brown, J., Lüthi, M. P., & Motyka, R. J. (2010). Ice mélange dynamics and implications for terminus stability, Jakobshavn Isbræ, Greenland. *Journal of Geophysical Research: Earth Surface*, *115*(F1).

Andresen, C. S., Kjeldsen, K. K., Harden, B., Nørgaard-Pedersen, N., & Kjær, K. H. (2014). Outlet glacier dynamics and bathymetry at Upernavik Isstrøm and Upernavik Isfjord, north-west Greenland. *GEUS Bulletin*, *31*, 79-82.

Cuffey, K. M., & Paterson, W. S. B. (2010). *The physics of glaciers*. Academic Press.

Downs, J., & Johnson, J. V. (2022). A rapidly retreating, marine-terminating glacier's modeled response to perturbations in basal traction. *Journal of Glaciology*, 1-10.

Gardner, A. S., M. A. Fahnestock, and T. A. Scambos, 2019 [update to time of data download]: ITS_LIVE Regional Glacier and Ice Sheet Surface Velocities. Data archived at National Snow and Ice Data Center; doi:10.5067/6II6VW8LLWJ7.

Holland, D. M., Thomas, R. H., De Young, B., Ribergaard, M. H., & Lyberth, B. (2008). Acceleration of Jakobshavn Isbræ triggered by warm subsurface ocean waters. *Nature geoscience*, *1*(10), 659-664.

Khan, S. A., Kjaer, K. H., Korsgaard, N. J., Wahr, J., Joughin, I. R., Timm, L. H., ... & Babonis, G. (2013). Recurring dynamically induced thinning during 1985 to 2010 on Upernavik Isstrøm, West Greenland. *Journal of Geophysical Research: Earth Surface*, *118*(1), 111-121.

Larsen, S. H., Khan, S. A., Ahlstrøm, A. P., Hvidberg, C. S., Willis, M. J., & Andersen, S. B. (2016). Increased mass loss and asynchronous behavior of marine-terminating outlet glaciers at Upernavik Isstrøm, NW Greenland. *Journal of Geophysical Research: Earth Surface*, *121*(2), 241-256.

Melton, S. M., Alley, R. B., Anandakrishnan, S., Parizek, B. R., Shahin, M. G., Stearns, L. A., ... & Finnegan, D. C. (2022). Meltwater drainage and iceberg calving observed in high-spatiotemporal resolution at Helheim Glacier, Greenland. *Journal of Glaciology*, 1-17.

Moon, T., Joughin, I., Smith, B., Van Den Broeke, M. R., Van De Berg, W. J., Noël, B., & Usher, M. (2014). Distinct patterns of seasonal Greenland glacier velocity. *Geophysical research letters*, *41*(20), 7209-7216.

Muilwijk, M., Straneo, F., Slater, D. A., Smedsrud, L. H., Holte, J., Wood, M., ... & Harden, B. (2022). Export of Ice Sheet Meltwater from Upernavik Fjord, West Greenland. *Journal of Physical Oceanography*, *52*(3), 363-382.

Nick, F. M., Vieli, A., Howat, I. M., & Joughin, I. (2009). Large-scale changes in Greenland outlet glacier dynamics triggered at the terminus. *Nature Geoscience*, *2*(2), 110-114.

Paden, J., J. Li, C. Leuschen, F. Rodriguez-Morales, and R. Hale. 2010, updated 2019. *IceBridge MCoRDS L2 Ice Thickness, Version 1*. [Indicate subset used]. Boulder, Colorado USA. NASA National Snow and Ice Data Center Distributed Active Archive Center. doi: https://doi.org/10.5067/GDQ0CUCVTE2Q.

Paden, J., J. Li, C. Leuschen, F. Rodriguez-Morales, and R. Hale. 2014, updated 2019. *IceBridge MCoRDS L1B Geolocated Radar Echo Strength Profiles, Version 2*. [Indicate subset used]. Boulder, Colorado USA. NASA National Snow and Ice Data Center Distributed Active Archive Center. doi: https://doi.org/10.5067/90S1XZRBAX5N.

Porter, Claire, et al., 2022, *"ArcticDEM – Strips, Version 4.1",* https://doi.org/10.7910/DVN/C98DVS, Harvard Dataverse, V1.

Porter, Claire, et al., 2018, *"ArcticDEM, Version 3",* https://doi.org/10.7910/DVN/OHHUKH, Harvard Dataverse, V1, 2018.

Rathmann, N. M., Hvidberg, C. S., Solgaard, A. M., Grinsted, A., Gudmundsson, G. H., Langen, P. L., ... & Kusk, A. (2017). Highly temporally resolved response to seasonal surface melt of the Zachariae and 79N outlet glaciers in northeast Greenland. *Geophysical Research Letters*, *44*(19), 9805-9814.

Rignot, E., Koppes, M., & Velicogna, I. (2010). Rapid submarine melting of the calving faces of West Greenland glaciers. *Nature Geoscience*, *3*(3), 187-191.

Shapero, D. R., Badgeley, J. A., Hoffman, A. O., & Joughin, I. R. (2021). icepack: A new glacier flow modeling package in Python, version 1.0. *Geoscientific Model Development*, *14*(7), 4593-4616.

Van Der Veen, C. J., Plummer, J. C., & Stearns, L. A. (2011). Controls on the recent speed-up of Jakobshavn Isbræ, West Greenland. *Journal of Glaciology*, *57*(204), 770-782.

Vieli, A., & Nick, F. M. (2011). Understanding and modelling rapid dynamic changes of tidewater outlet glaciers: issues and implications. *Surveys in geophysics*, *32*(4), 437-458.

Vijay, S., Khan, S. A., Kusk, A., Solgaard, A. M., Moon, T., & Bjørk, A. A. (2019). Resolving seasonal ice velocity of 45 Greenlandic glaciers with very high temporal details. *Geophysical Research Letters*, *46*(3), 1485-1495.

Vijay, S., King, M. D., Howat, I. M., Solgaard, A. M., Khan, S. A., & Noël, B. (2021). Greenland ice-sheet wide glacier classification based on two distinct seasonal ice velocity behaviors. *Journal of Glaciology*, *67*(266), 1241-1248.

CHAPTER 5.0 APPENDICES

5.1 Appendix A: Additional Hydrostatic Figures

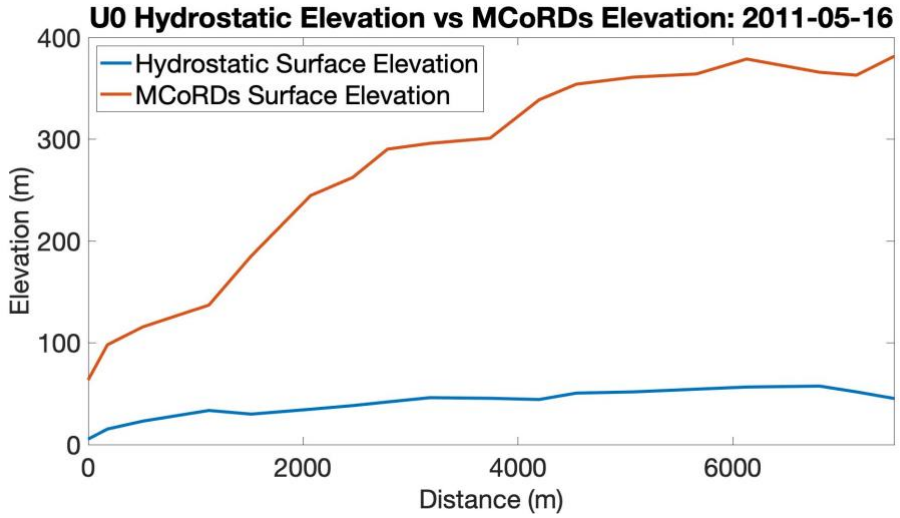

Figure 5.1: U0 2011 Hydrostatic Profile. U0 hydrostatic elevation compared to the actual elevation in 20110516. The hydrostatic elevation, calculated using the hydrostatic equilibrium equation with MCoRDS data (Paden and others, 2010, 2014).

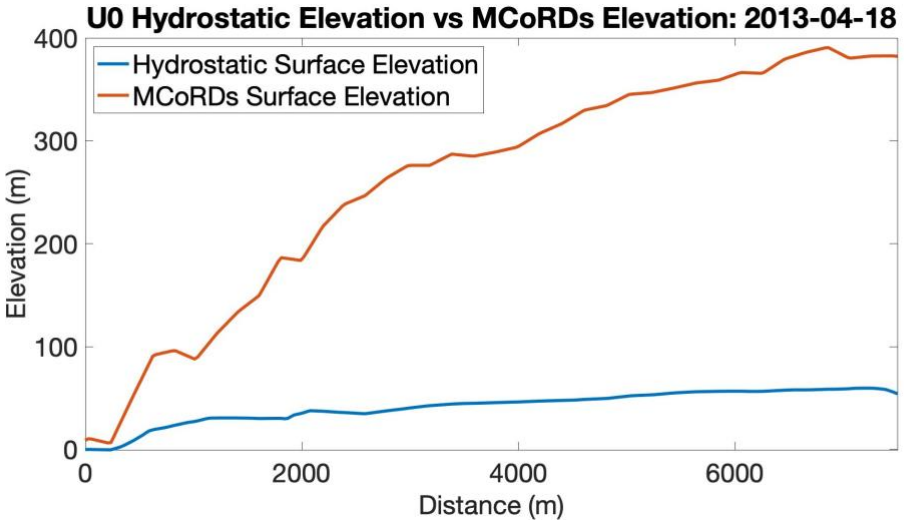

Figure 5.2: U0 2013 Hydrostatic Profile. U0 hydrostatic elevation compared to the actual elevation in 20130418. The hydrostatic elevation, calculated using the hydrostatic equilibrium equation with MCoRDS data (Paden and others, 2010, 2014).

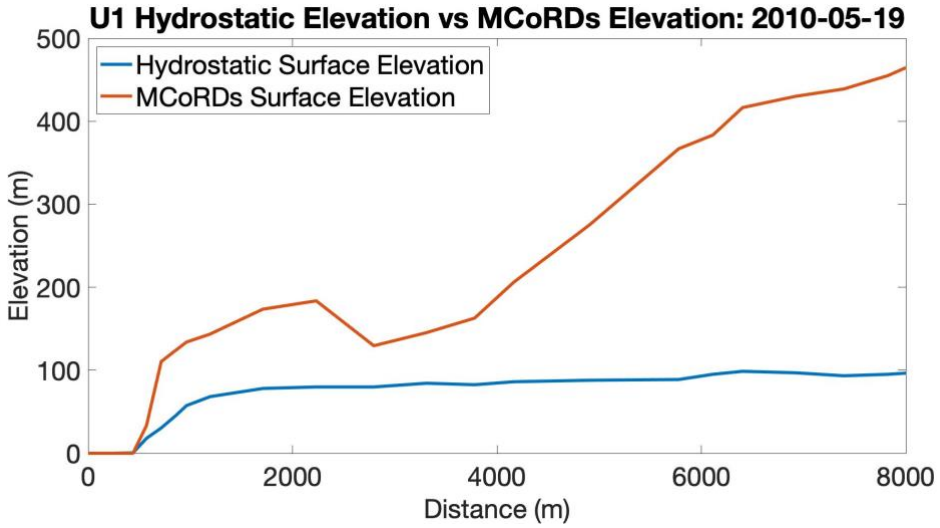

Figure 5.3: U1 2010 Hydrostatic Profile. U1 hydrostatic elevation compared to the actual elevation in 20100519. The hydrostatic elevation, calculated using the hydrostatic equilibrium equation with MCoRDS data (Paden and others, 2010, 2014).

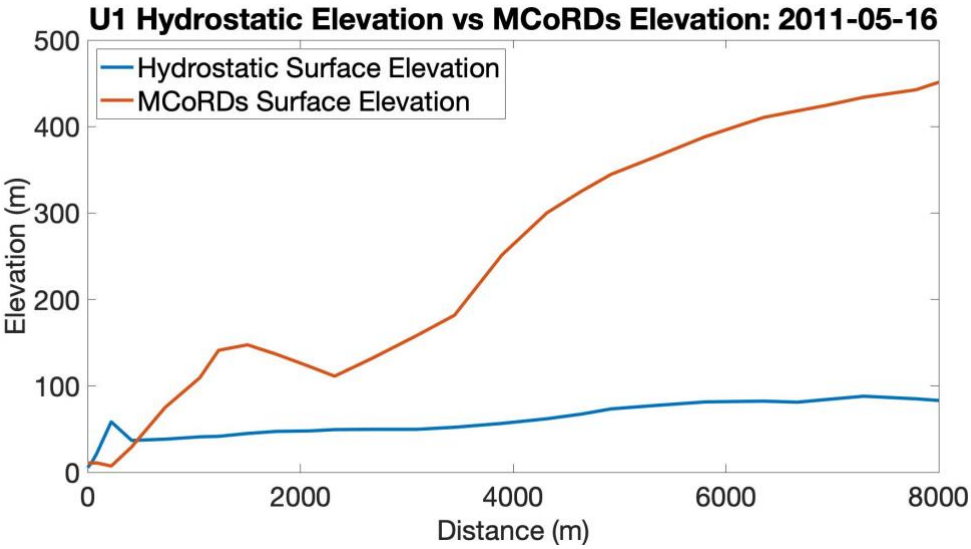

Figure 5.4: U1 2011 Hydrostatic Profile. U1 hydrostatic elevation compared to the actual elevation in 20110516. The hydrostatic elevation, calculated using the hydrostatic equilibrium equation with MCoRDS data (Paden and others, 2010, 2014).

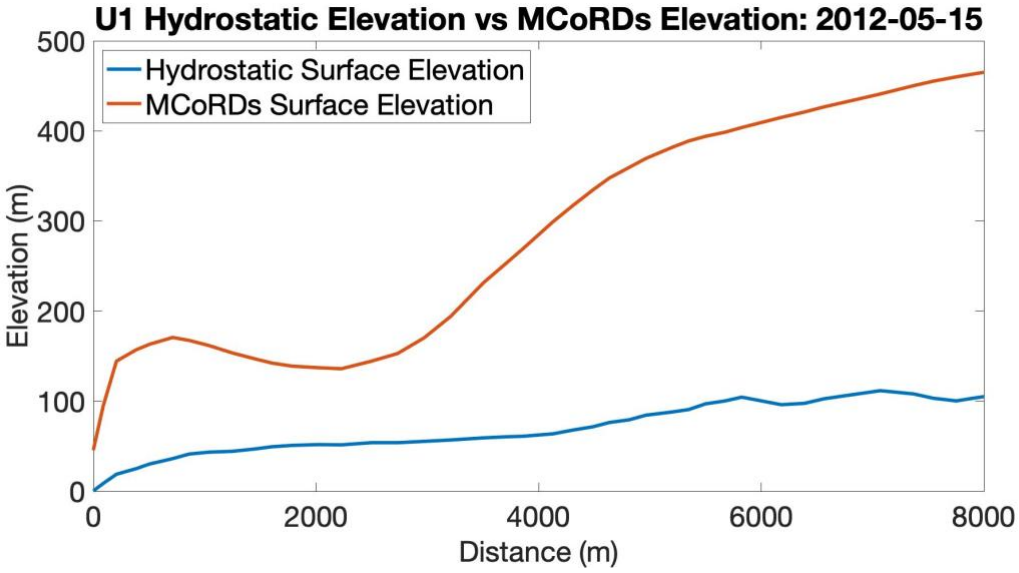

Figure 5.4: U1 2012 Hydrostatic Profile. U1 hydrostatic elevation compared to the actual elevation in 20120516. The hydrostatic elevation, calculated using the hydrostatic equilibrium equation with MCoRDS data (Paden and others, 2010, 2014).

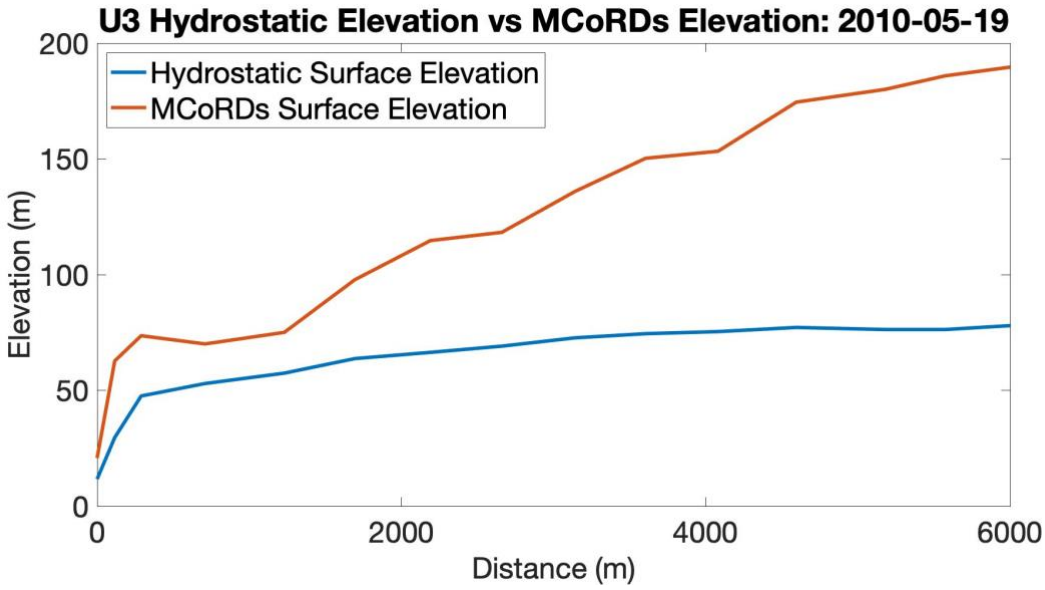

Figure 5.5: U3 2010 Hydrostatic Profile. U3 hydrostatic elevation compared to the actual elevation in 20100519. The hydrostatic elevation, calculated using the hydrostatic equilibrium equation with MCoRDS data (Paden and others, 2010, 2014).

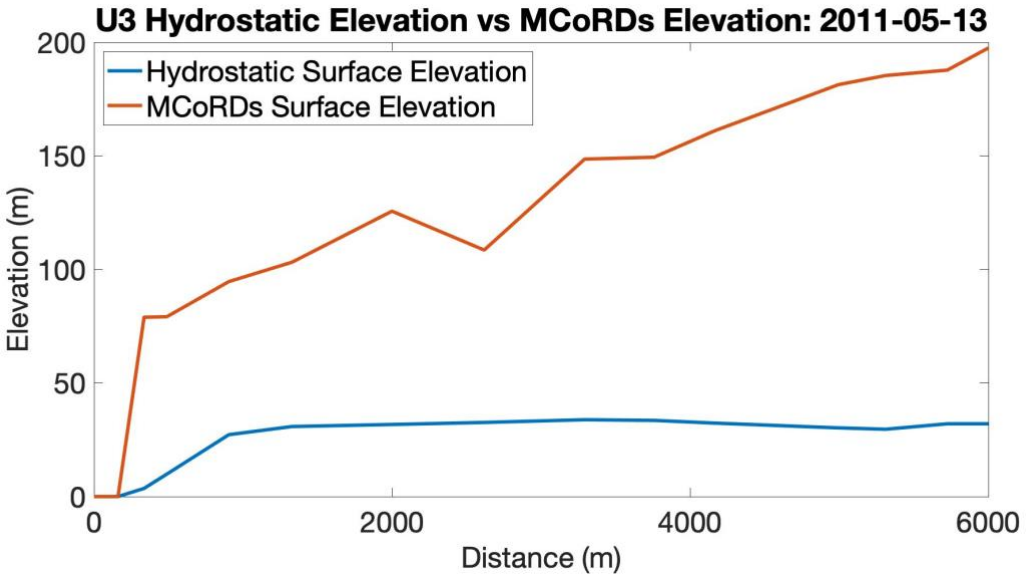

Figure 5.6: U3 2011 Hydrostatic Profile. U3 hydrostatic elevation compared to the actual elevation in 20110513. The hydrostatic elevation, calculated using the hydrostatic equilibrium equation with MCoRDS data (Paden and others, 2010, 2014).

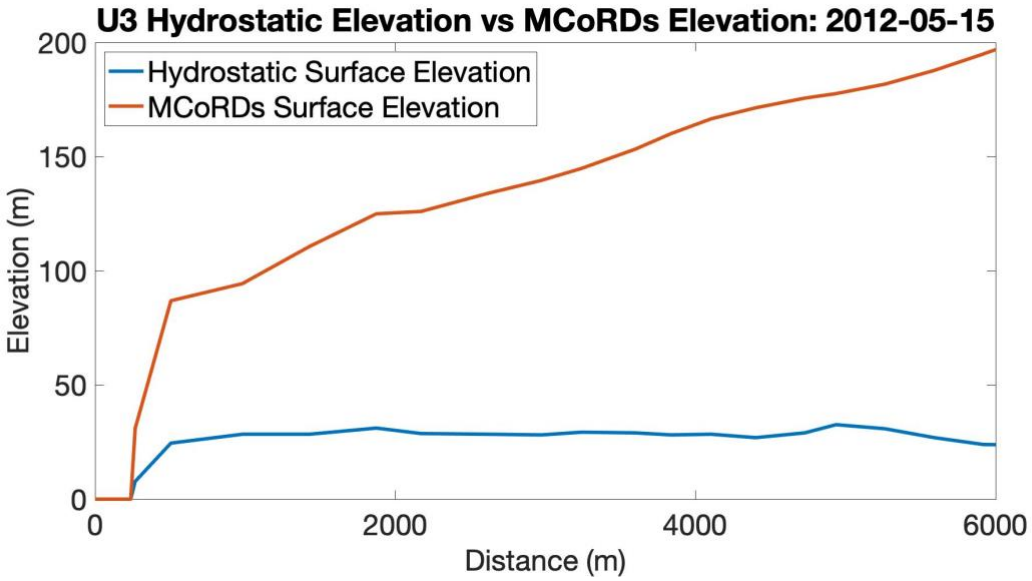

Figure 5.7: U3 2012 Hydrostatic Profile. U3 hydrostatic elevation compared to the actual elevation in 20120515. The hydrostatic elevation, calculated using the hydrostatic equilibrium equation with MCoRDS data (Paden and others, 2010, 2014).

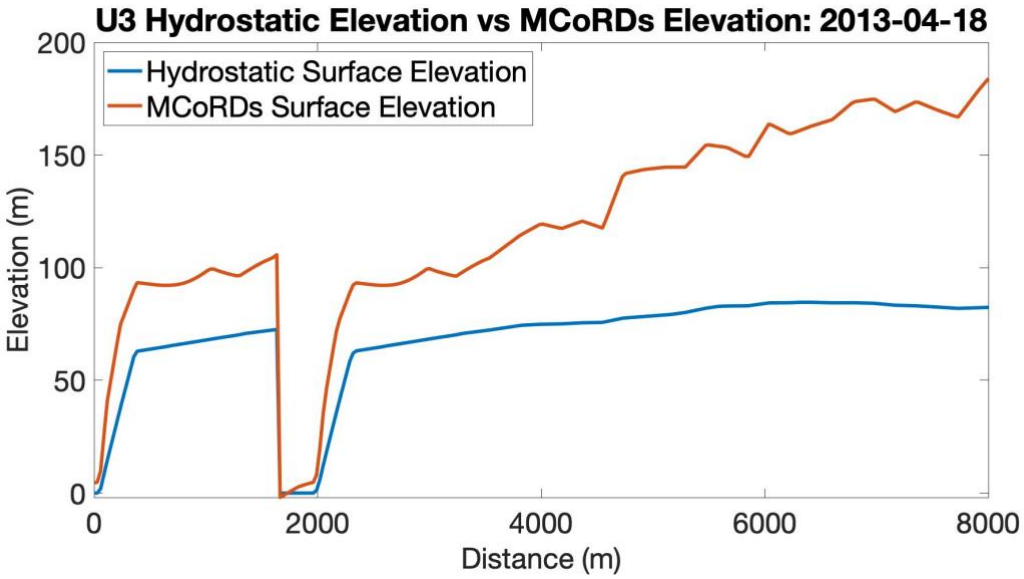

Figure 5.8: U3 2013 Hydrostatic Profile. U3 hydrostatic elevation compared to the actual elevation in 20130418. The hydrostatic elevation, calculated using the hydrostatic equilibrium equation with MCoRDS data (Paden and others, 2010, 2014).

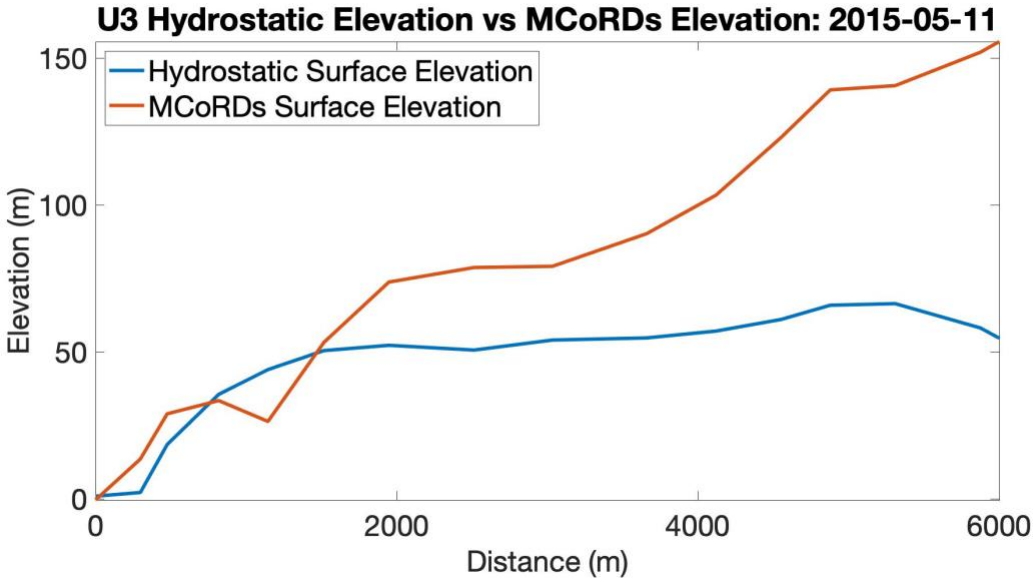

Figure 5.9: U3 2015 Hydrostatic Profile. U3 hydrostatic elevation compared to the actual elevation in 20150411. The hydrostatic elevation, calculated using the hydrostatic equilibrium equation with MCoRDS data (Paden and others, 2010, 2014).

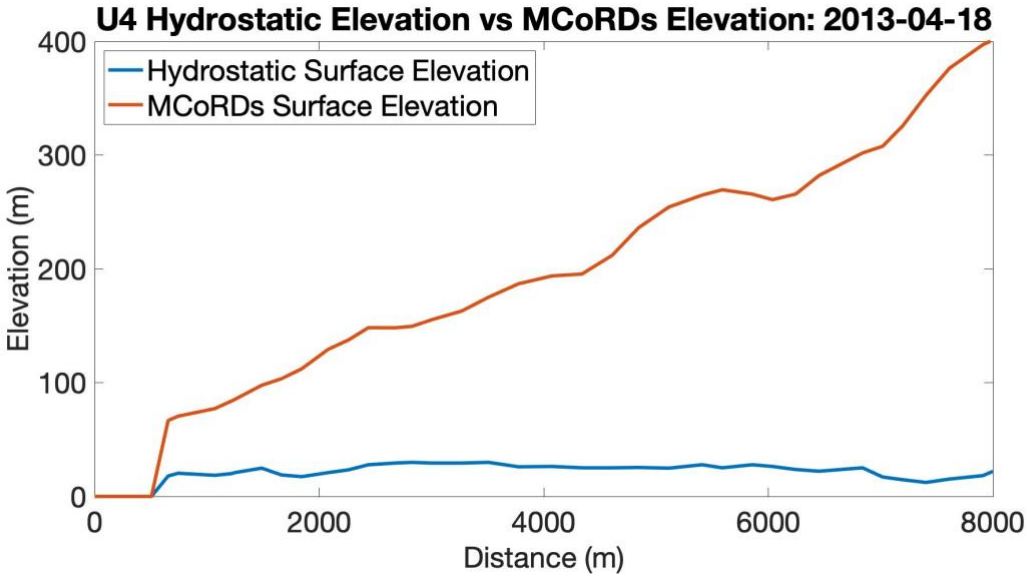

Figure 5.10: U4 2013 Hydrostatic Profile. U4 hydrostatic elevation compared to the actual elevation in 20130418. The hydrostatic elevation, calculated using the hydrostatic equilibrium equation with MCoRDS data (Paden and others, 2010, 2014).

5.2 Appendix B: Subglacial Drainage and Tabular Iceberg Images

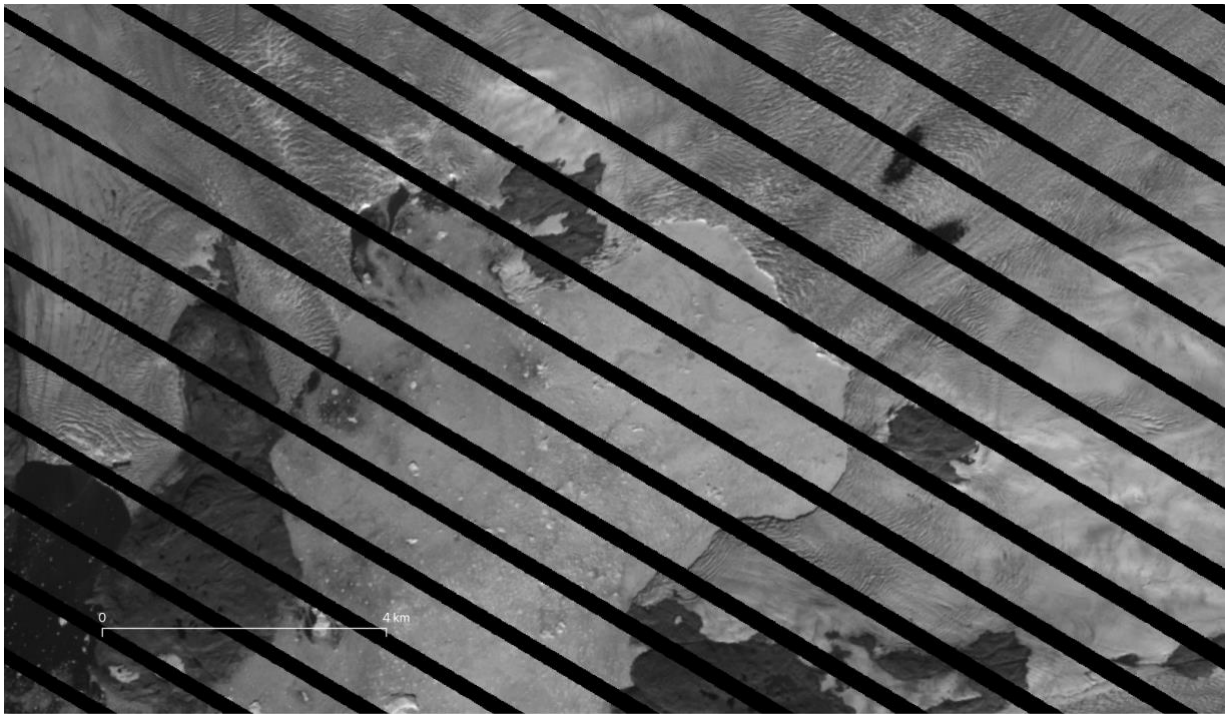

Figure 5.1: U0 drainage event example. An example of a drainage event that occurred for U0, represented as a larger than average plume polynya at the northern terminus as shown in the Landsat 7 image from July 8, 2010, courtesy of the U.S. Geological Survey. This event was also shared with the drainage event that occurred for U2 in Figure 2 around the same time.

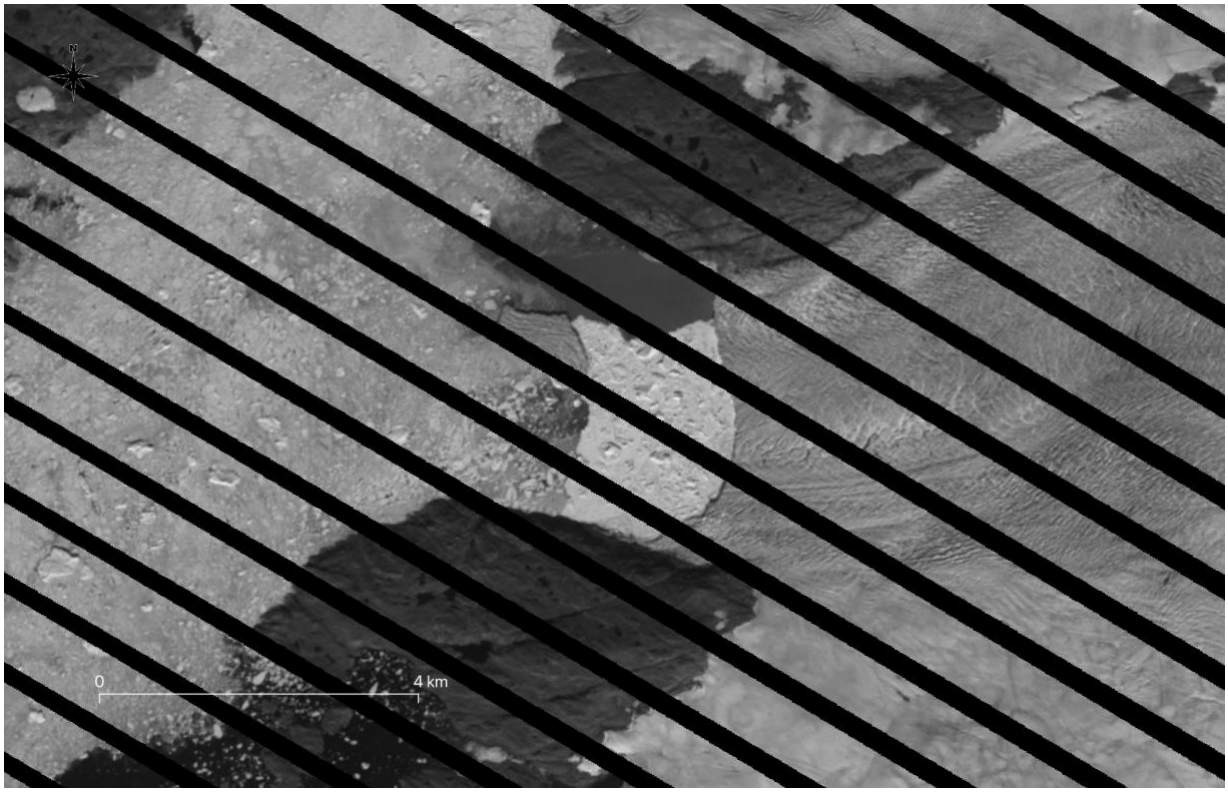

Figure 5.2: U2 drainage event example. An example of a drainage event that occurred for U2, represented as a larger than average plume polynya at the northern terminus as shown in the Landsat 7 image from June 22, 2010, courtesy of the U.S. Geological Survey. This event was also shared with the drainage event that occurred for U0 around the same time.

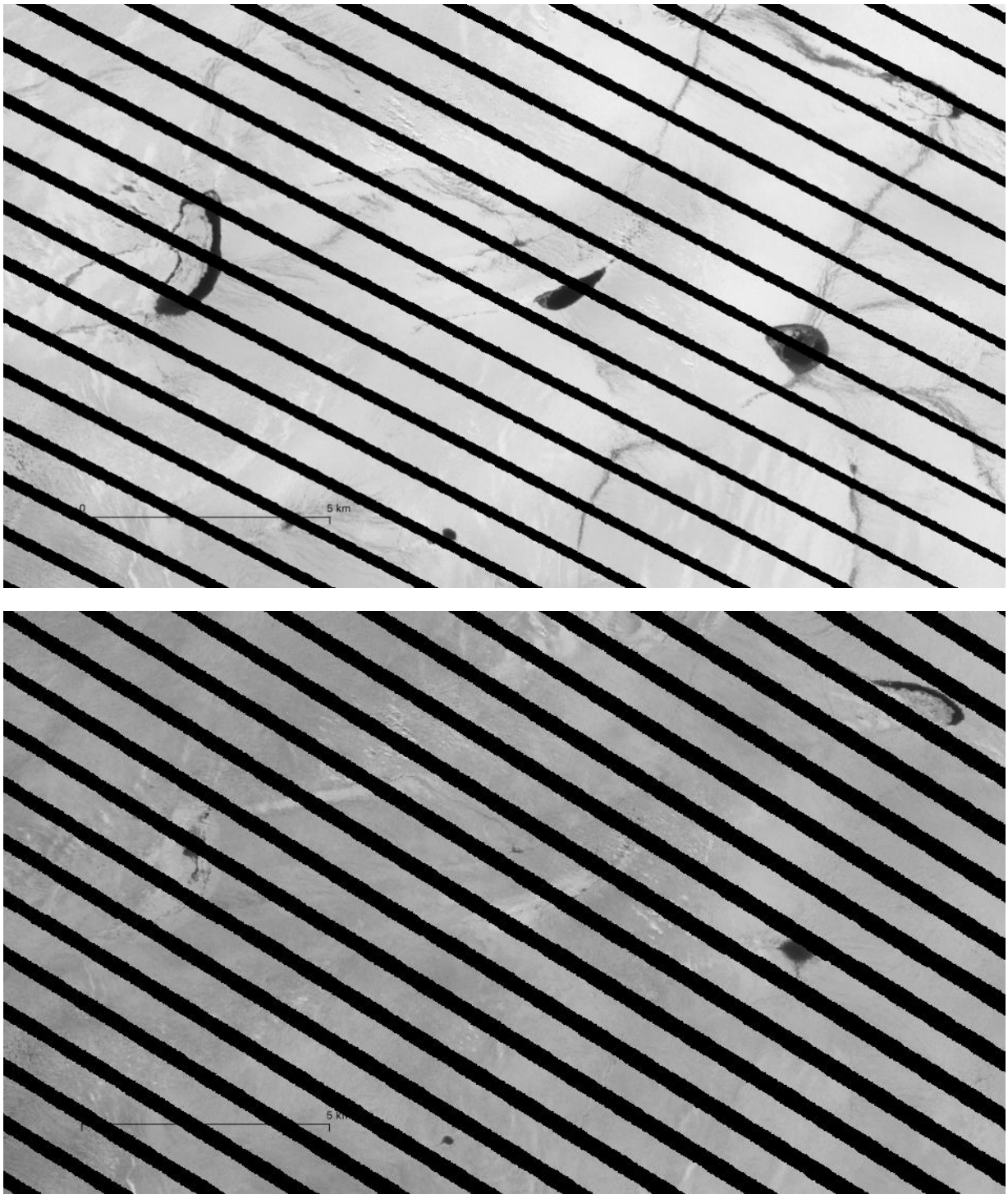

Figure 5.3: U2 lake drainage event. An example of a drainage event that occurred for U2 in the upstream lakes. Above: three supraglacial lakes, as shown in the Landsat 7 image from June 17, 2010, courtesy of the U.S. Geological Survey. Below: three supraglacial lakes that have drained, as shown in the Landsat 7 image from July 8, 2010, courtesy of the U.S. Geological Survey.

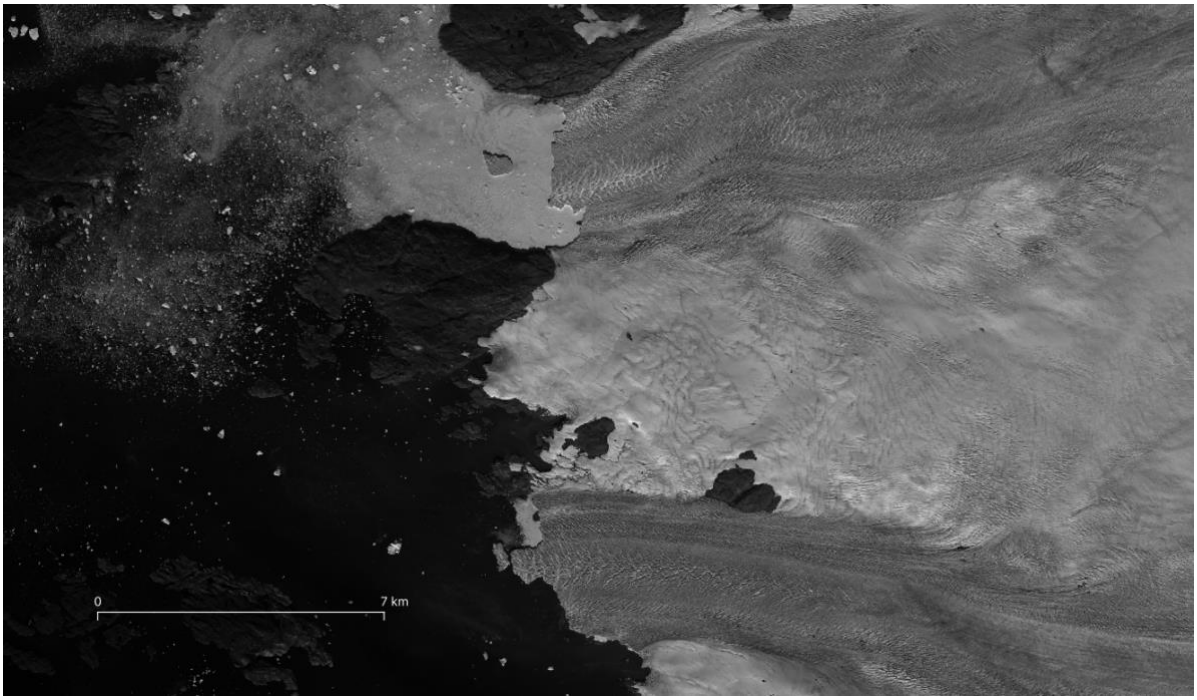

Figure 5.4: Tabular icebergs and plume polynyas. An example of two tabular icebergs from U2 and U3, along with two plume polynyas at the south terminus of U2 and the north terminus of U3 visible in the Landsat 8 image from August 5, 2014, courtesy of the U.S. Geological Survey. This event was also shared with the drainage event that occurred for U0 around the same time.

5.3 Appendix C: Modelling Figures

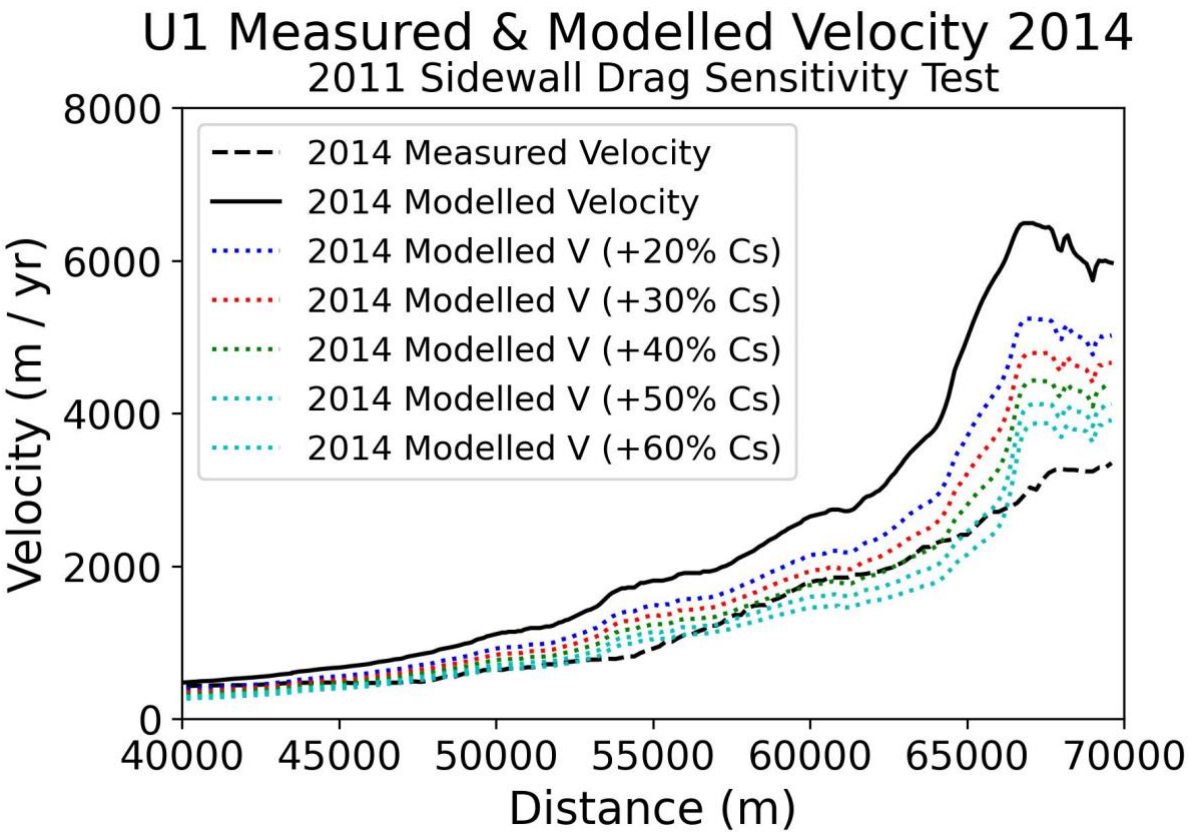

Figure 5.1: U1 2014 modelled velocity and C_{side} sensitivity. This plot displays the U1 2014 measured and modelled velocity using the same drag inputs (C_{base}, C_{side}) as 2011, and the adjusted C_{side} required to output more realistic velocities.

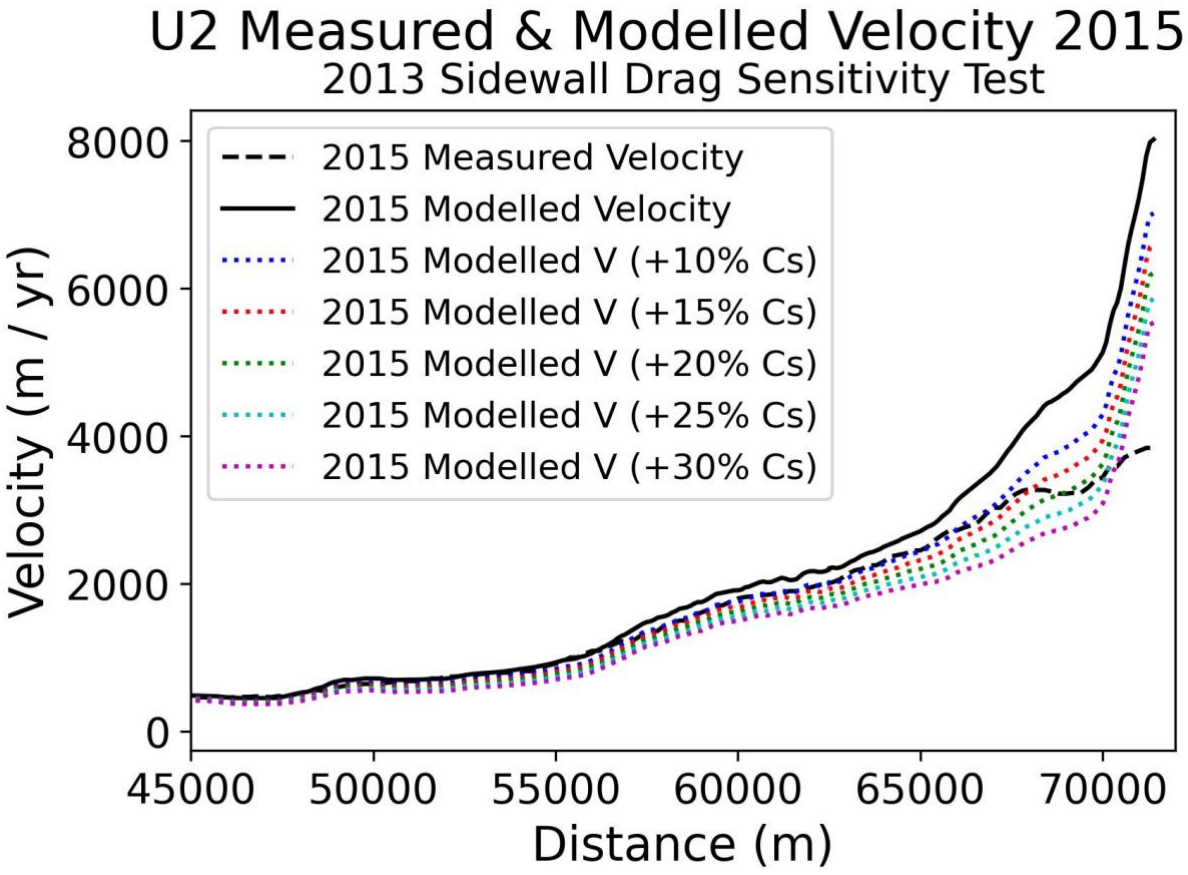

Figure 5.2: U2 2015 modelled velocity and C_{side} sensitivity. This plot displays the U2 2015 measured and modelled velocity using the same drag inputs (C_{base}, C_{side}) as 2013, and the adjusted C_{side} required to output more realistic velocities.

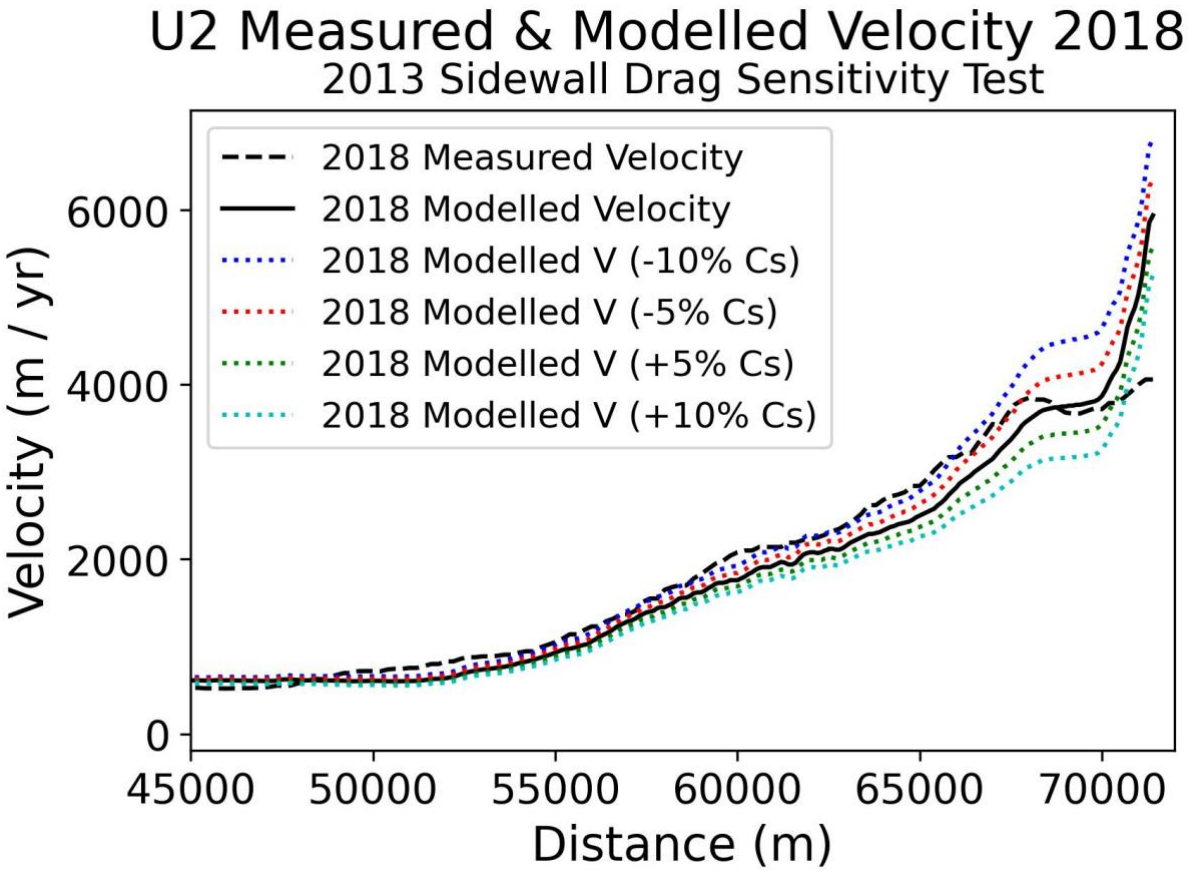

Figure 5.3: U2 2018 modelled velocity and C_{side} sensitivity. This plot displays the U2 2018 measured and modelled velocity using the same drag inputs (C_{base}, C_{side}) as 2013, and the adjusted C_{side} required to output more realistic velocities.